PATTERN RECOGNITION BASED MICROSIMULATION CALIBRATION AND INNOVATIVE TRAFFIC REPRESENTATIONS

A Dissertation

presented to

the Faculty of the Graduate School

at the University of Missouri-Columbia

In Partial Fulfillment

of the Requirements for the Degree

Doctor of Philosophy

---

by

SANDEEP MENNENI

Dr. Carlos Sun, Dissertation Supervisor

December 2008

The undersigned, appointed by the dean of the Graduate School, have examined the [thesis or dissertation] entitled

PATTERN RECOGNITION BASED MICROSIMULATION CALIBRATION

AND INNOVATIVE TRAFFIC REPRESENTATIONS

presented by Sandeep Menneni,

a candidate for the degree of doctor of philosophy,

and hereby certify that, in their opinion, it is worthy of acceptance.

1. Dr. Carlos Sun

2. Dr. Mark Virkler

3. Mr. Charles Nemmers

4. Dr. Wooseung Jang

5. Dr. Praveen Edara

I dedicate this document to my Mom, Dad, and Sister.

And, to my guitars for stopping me from going crazy...

ACKNOWLEDGEMENTS

I would like to thank my professor and doctoral advisor Dr. Carlos Sun for the person that he is; helping others, including me, is just a part of his nature. In no small measure I would also like to thank my professors, advisors, and committee members Dr. Mark Virkler, Mr. Charles Nemmers, Dr. Wooseung Jang, and Dr. Praveen Edara for their invaluable help, encouragement and support.

I would like to thank the Department of Civil Engineering and the University of Missouri Columbia for providing the opportunity and support in making this doctoral dissertation possible.

I would like to thank Thomas Bauer, PTV America and Peter Vortisch, PTV AG for sponsoring part of this research. I would like to thank Blake Ingerslew and James Rice for their invaluable help all through the research.

I would like to thank my friends Nagendra Patta, Venkata Chilukuri, Samir Parab, Ronnie Matthews, Ajay Toshniwal, Shailesh lopes, Derek Vap, Siddharth Sharma, Indrajit Chatterjee, Thirulokesh Krishnan, Robert Rescot, and others

Finally, I thank my family for being there all the time.

TABLE OF CONTENTS

LIST OF FIGURES

LIST OF TABLES

PATTERN RECOGNITION BASED MICROSIMULATION CALIBRATION AND INNOVATIVE TRAFFIC REPRESENTATIONS

Sandeep Menneni

Dr. Carlos Sun, Dissertation Supervisor

ABSTRACT

Even though calibration techniques for traffic simulation abound, this dissertation presents the first mathematical formalization using representations and invariants. The calibration is defined succinctly over three levels of representation: traffic, dissimilarity, and search. The methodology encompasses the currently used calibration procedures while improving the calibration process. The theoretical formulation of calibration lays the foundation for several improvements in calibration such as improvement in traffic relationships employed in calibration, new pattern recognition methods for accurate measurement of the differences in complex relationships, and seamless integration into direct search methods. These new methods are demonstrated in the microsimulation of a freeway network in California. In the first case study, speed-flow graphs were shown to replicate field data better than methods based on either capacity or sustained flow. The study also demonstrates the usefulness of pattern recognition in automatically measuring the degree-of-closeness of traffic relationships based on graphs. In the second case study, the calibration process is improved by integrating a microscopic traffic representation (action points) and a macroscopic representation (speed-flow graphs). The microscopic traffic representations are developed by analyzing several leader-follower vehicle pairs from real-world vehicle trajectories.

1 | Introduction

"Ring the bells that still can ring
Forget your perfect offering
There is a crack in everything
That's how the light gets in"

-"ANTHEM", Leonard Cohen

1.1 | SIMULATION

Traffic simulation models have proven to be beneficial in analyzing complex traffic situation that exist beyond the scope of traditional analytical methods. Traffic simulation models have also found application in transportation planning process, due to their flexibility and feasibility in testing different alternatives that do not currently exist in the real-world. For the benefit of the reader, a brief definition of simulation is provided below; a detailed explanation of traffic simulation models is provided in the next chapter.

A simulation is a representation by imitation of behavior, characteristics, and relationships of distinct elements of a system or a process. Simulation is not necessarily a true representation of a system or a process, rather a simplification. In addition, an exact representation is only possible if the system or process is deterministic; however in real-world, there but a few systems or processes that satisfy such a condition. A

representation can be achieved in a variety of mediums like computer, mathematical, logical, electrical, or fluid.

Development of traffic simulation models has inherently led to a deeper comprehension of behavior, characteristics, and relationships of driver, vehicles, and other traffic elements. Traffic simulation models vary in complexity from simple deterministic queuing models to complex microscopic stochastic models. They also vary in detail from a single isolated intersection to a large-scale traffic networks. Since no single simulation model can be expected to replicate the range of traffic conditions that exist in the real-world, parameters are provided to tweak the simulation model to suit local traffic behavior or conditions. The process of tweaking the parameters is called calibration, and the parameters are known as calibration parameters. Without calibration, a traffic simulation model cannot provide accurate predictions of measures of effectiveness (MOE), which are paramount in transportation decision making process.

Traditional traffic analysis has roots in three basic traffic variables: flow, speed, and density. These variables continue to play a very important role in decision making. Researchers, over the decades, have studied these variables and their inter-relationships.

1.2 | RESEARCH MOTIVATION AND GOALS

This dissertation concerns itself with calibration. The motivation for this research stems from various aspects of calibration of simulation models. Over the years, there have been many methodologies presented for calibration of simulation models. It is the intent of this study to develop a comprehensive generic formulation of calibration. There is a need to develop efficient calibration methodologies which result in accurate results. It is also important to include traffic flow considerations during calibration methodology

development process. Majority of this work is based on traffic microsimulation models[1], but much of the results and methodologies need to be applicable to other types of simulation models in general, not just traffic simulation models. Original contribution is sought in use of theory or tools from non-traffic fields in the area of calibration. Generic tools and methodologies are desired for application in calibration with a great deal of consideration towards data type and availability. This consideration helps in developing methodologies and tools that can be implemented by practitioners. Further discussions on research motivations are provided in a context-based manner.

1.3 | BRIEF OVERVIEW OF RESEARCH

This research concerns itself with the improvement of calibration procedures in traffic simulation models. Even though calibration techniques for traffic simulation abound, this dissertation presents the first mathematical formalization using representations and invariants. The generic formulation of calibration definition and accompanying procedures provides a deeper understanding of the nature of the problem. The calibration objective is defined over three levels of representation: traffic, dissimilarity, and search (see Figure 1.1). These three levels of representation succinctly encompass all of the currently used calibration procedures, while presenting a new methodology that improves the quality of calibration by utilizing several traffic flow processes. Each of the levels of representation results in a certain loss of information, but such representations are ultimately necessary in solving the complex calibration problem. The theoretical formulation of calibration lays the foundation for several improvements in calibration. First, the traffic representations (or relationships) employed in calibration are improved to

[1] Definition provided in the next chapter

account for several traffic flow processes. Second, new pattern recognition based dissimilarity measures are developed for accurately measuring the differences in complex traffic representations. Third, the dissimilarity measures are then seamlessly integrated into direct search methods. The representations also provide a better insight into the information flow in a calibration process. The invariance concept improves the calibration process by developing traffic representations that are robust to input or measurement errors and reduces the calibration parameter set to the most important parameters.

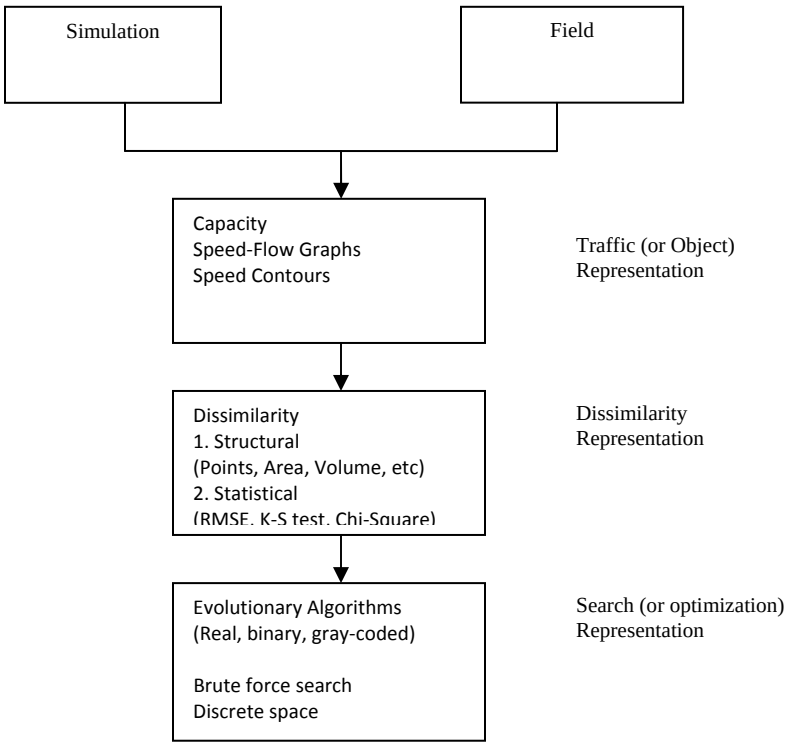

Figure 1.1 Representation based formulation of calibration.

These new methods are demonstrated in the microsimulation of a freeway network in California. The new calibration method based on speed-flow graphs was shown to replicate field data better than the methods based on either capacity or sustained flow. The study also demonstrates the usefulness of a pattern recognition based dissimilarity representation for automatically measuring the degree-of-closeness of traffic relationships based on graphs, contours, or histograms. The automated pattern recognition is essential for application using direct search methods such as Evolutionary Algorithms. It solves various consistency problems that occur in visual inspection techniques previously applied. The automated graph matching concepts are extended to higher dimensions such as n-dimensional point sets. The pattern recognition methods in the case study are simple, flexible, efficient, extendable and robust. The simplicity of the model helps practitioners develop and deploy pattern recognition based calibration that requires no human intervention. The main advantage of dissimilarity measures is that there are no specific assumptions being made about the system, data, population, or the model.

In the second case study, the calibration process is improved by integrating a microscopic traffic representation (action points) and a macroscopic representation (speed-flow graphs). Several leader-follower vehicle pairs from NGSIM vehicle trajectories are analyzed to develop microscopic traffic representation. The data is then utilized to accurately estimate the values of calibration parameter set. Both case studies demonstrate simpler methods that will help practitioners calibrate their simulation models accurately and efficiently

1.4 | ORGANIZATION OF DOCUMENT

Chapter 1 provides a brief introduction to the subject of the document. It provides preliminary information about concepts discussed in the document. It also provides brief overview of the research. Organization and brief summaries of all chapters in the document are also provided.

Chapter 2 defines and describes traffic simulation models. Brief descriptions of the inner workings of the model followed by a detailed review of car-following models are presented. Car following model of VISSIM, microsimulation software utilized all through this research, is described in detail.

Chapter 3 concentrates on laying the ground work for this research. It provides a very comprehensive review of calibration methodologies for simulation models. The literature review is structured in a chronological order to emphasize the change in methodologies over the years. Chapter 3 also provides a categorization of the methods presented in the literature review.

Chapter 4 describes in detail the theoretical formulation of calibration. This chapter lays the ground work for all the concepts discussed in detail in the following chapters. The chapter defines a formal calibration definition, objective and procedure.

Chapter 5 details the traffic representations in calibration. Several traffic representations based on relationships of traffic variables are analyzed for their applicability in calibration. The concept of information in traffic representation is emphasized.

Chapter 6 takes a deeper look at dissimilarity representation in calibration. Applications of pattern recognition in microsimulation calibration are detailed and

discussed. The methods developed in this chapter are capable of producing robust quantifiable measures for measuring the degree of closeness of traffic representations presented in chapter 4.

Chapter 7 details search representation in calibration. Evolutionary algorithms are introduced for application in microsimulation calibration. Details about implementation of evolutionary algorithms in this research are also presented.

Chapter 8 describes a generalized hierarchical calibration methodology. This chapter integrates the various concepts introduced in the previous chapters. Descriptions of sensitivity analysis model, range definition model, generalized calibration model, and generalized hierarchical calibration model have been provided.

Chapter 9 describes a case study effort that describes the benefits of using traffic, dissimilarity representation, and search representation in microsimulation calibration by comparing to existing methodologies.

Chapter 10 describes in the detail the integration of microscopic and macroscopic traffic representations in calibration. This chapter extends on the case study presented in chapter 9 to address several unanswered questions.

Finally, chapter 11 delineates the conclusions and unanswered questions in the research, and future direction

2 | Traffic Simulation Models

"…for distinction sake, a deceiving by words, is commonly called a lie, and a deceiving by actions, gestures, or behavior, is called simulation…"

-South, Robert (1643 – 1716)

2.1 | SIMULATION

There have been a variety of definitions proposed for traffic simulation models. May (1991) defines simulation models as mathematical computer-based models that describe behavior of transportation systems over time. Drew (1968) defines simulation as a dynamic representation of parts of real-world that can be used to study complex traffic situations in a laboratory. Gerlough and Huber (1975) define simulation as an experiment performed on an artificial model of a real system. Wohl and Martin (1967) define simulation as an imitation that assumes the appearance without reality. Liebermann and Rathi (2005) define simulation as an abstraction of real-world systems. Each of these definitions brings to light a different concept and characteristic of traffic simulation models.

Traffic simulation models have found growing use in traffic and transportation analysis for analyzing complex traffic situations that exist beyond the scope of traditional

analytical or deterministic traffic analysis methods such as Highway Capacity Manual (HCM).

2.2 | CLASSIFICATION OF TRAFFIC SIMULATION MODELS

Traffic simulation models can be divided into different categories based on classification type (FHWA, 2004).

2.2.1 | TRAFFIC STREAM REPRESENTATION

Microscopic simulation models simulate the movement of individual vehicles in a traffic stream based on car-following and lane-changing theories; e. g. VISSIM, PARAMICS, AIMSUN, MITSIM, CORSIM.

Macroscopic simulation models simulate on a section-by-section basis in a transportation network rather than by tracking individual vehicles. Macroscopic simulation models are based on deterministic relationships of flow, speed, and density of a traffic stream; e. g. TRANSYT-7F, PASSER, NETCELL.

Mesoscopic simulation models combine the properties of microscopic and macroscopic simulation models, wherein movement of individual vehicles in traffic stream is governed by macroscopic relationships; For example, lane changing can be based on lane densities and average lane speeds rather than interaction of individual vehicles as in microscopic simulation models; e. g. DYNAMIT, DYNASMART.

2.2.2 | SYSTEM UPDATE MECHANISM

Continuous Simulation Models describe how the elements of a system change continuously over time in response to continuous stimuli.

Discrete Simulation Models

1. **Discrete Time Models** segment time into a succession of known time intervals. Within each such interval, the simulation model computes the activities which change the states of selected system elements; e. g., VISSIM, PARAMICS, CORSIM.
2. **Discrete Event Models** are usually used to represent entities whose states change infrequently. For example, a green traffic signal indication state does not change for a certain amount of time; therefore, instead of updating the state every time step, the model updates the state after a designated amount of time. This type of modeling can save significant amount of computing requirements; e. g., NETFLO1

2.2.3 | RANDOMNESS IN TRAFFIC FLOW

Deterministic Models include no random variables with all entity interactions are defined by exact relationships; e. g., DYNASMART

Stochastic Models include probability functions and random variables. e. g., reaction time can be a constant or a random variable; e. g., VISSIM, PARAMICS, CORSIM, and AIMSUN

The work presented here is for the most extent based on traffic microsimulation models, but discussions about other traffic simulation models have been provided when appropriate. Since most of microsimulation models currently used by practitioners in transportation engineering are discrete-time stochastic models, much emphasis has been placed on such models.

2.3 | TRAFFIC MICROSIMULATION MODELS

Traffic microsimulation models have seen a surge in application partly due to increase in affordability and computing power of modern computers. Traffic microsimulation models represent traffic in greater detail than macroscopic or mesoscopic traffic simulation models; therefore, requiring significantly higher computing power. Traffic microsimulation (henceforth referred to as microsimulation) due to greater detail is classified as a high-fidelity model, whereas macroscopic is classified as a low-fidelity and mesoscopic as a mixed-fidelity model (Liebermann and Rathi, 2005). Microscopic models due to a greater level of detail can produce more accurate results. They also can be used to study a larger number of measures of traffic performance than macroscopic or mesoscopic models. But due to increased detail, simulation models carry a lot more number of parameters that require user input and calibration, and hence prone to significant error. In microsimulation, calibration is needed to achieve accurate results that surpass their counterparts. Microsimulation models have their own share of advantageous and disadvantages. For advantages and disadvantages, please find a comprehensive list in May (1991), Liebermann and Rathi (2005), and FHWA (2004).

2.3.1 | CORE MODULES IN A GENERIC MICROSIMULATION MODEL

Traffic microsimulation models differ significantly in their architecture, algorithms, and information flow. But, some of the core algorithms and functions remain the same. In a prototypical microsimulation model there are seven distinct core algorithms or modules. A brief description of the core modules is provided below. Car following model, primary model in microsimulation, is addressed in greater detail in a subsequent section. A more detailed review of other modules is provided when appropriate.

Random-number generation model: generates random number for application in various other models

Vehicle and driver attributes model: defines attributes of vehicles and drivers entering the network.

Vehicle generation model: defines where and when a vehicle enters the network.

Car following model: defines how a car accelerates, decelerates, and follows another.

Lane changing model: defines how and when a car changes lane.

Traffic signal controller model: controls the traffic signals in the network.

Animation model: displays animation of vehicles in the network.

2.3.2 | TRAFFIC MICROSIMULATION MODEL DEVELOPMENT AND APPLICATION PROCESS

A typical simulation based traffic analysis process includes: project definition; data collection; simulation model development; calibration; validation; and, application. Figure 2.1 describes a flow chart of the above process. An alternate flow chart is provided in Federal Highway Administration's (FHWA) microsimulation application guidelines. (FHWA, 2004)

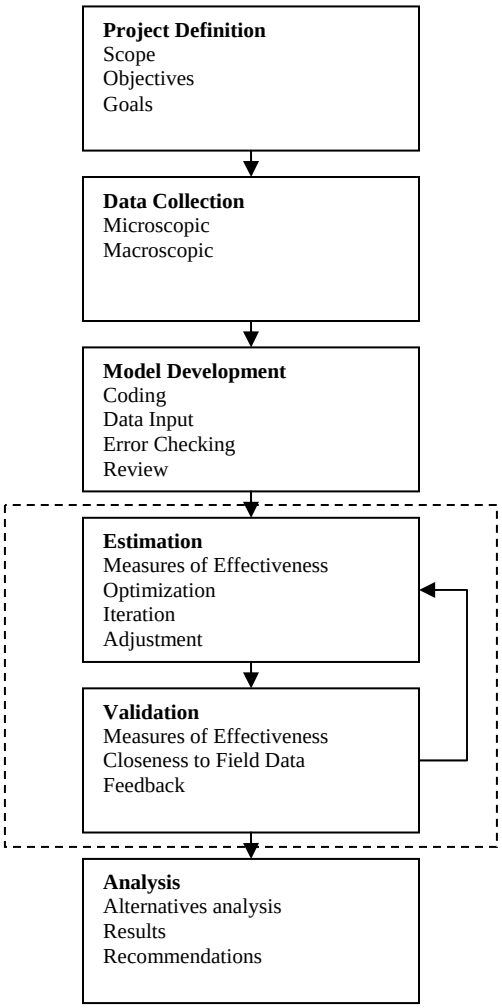

Figure 2.1 Typical microsimulation model development and application process.

2.4 | CAR FOLLOWING MODELS

Car following models, as the name suggests, describe how one car follows another car on a road. This model forms the core of most of the current microsimulation models. Research on car following models started in early 1950s by Reuschel (1950) and Pipes (1953). Car following models were later extended by Kometani and Saski (1958), Forbes (1958), and various papers by Herman, Rothery and associates (1958 -1963). The collective works of many researchers at General Motors from late 1950s through early

1960s are usually referred to as General Motors' car following models. Mathematically, car following models describe the position of a vehicle following another over time. In this literature review, it is intent to expose the reader to a brief variety of car following models, which form the core of microsimulation model. For ease in explanation of various car following models a widely used notation is described first.

Car Following Models: Notations and Definitions

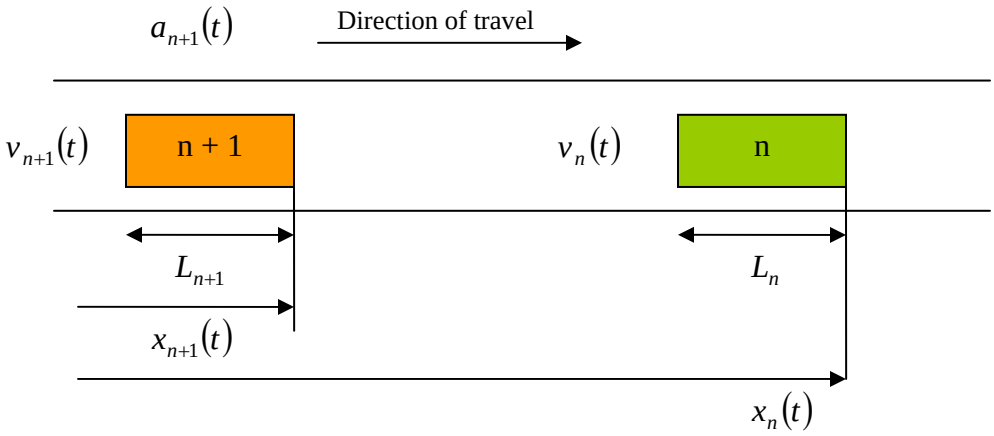

Figure 2.2 Car Following Model Notation

Where,

n is the vehicle index
t is the time
Δt is the time interval
$a_{n+1}(t)$ is the length of vehicle n
$x_n(t)$ is the position of vehicle n at time t
$v_n(t)$ is the velocity of vehicle n at time t
$a_n(t)$ is the acceleration of vehicle n at time t

2.4.1 | PIPES', AND FORBES' CAR FOLLOWING MODELS

Some of the earliest car-following models were based on simple driving rules. Pipes (1953) developed models based on the following vehicle maintaining a safe distance from

the leading vehicle. The car following model can be mathematically expressed as follows:

$$d_{\min} = \min\left[x_n(t) - x_{n+1}(t)\right] = L_n\left[1 + k * v_n(t)\right]$$

Forbes (1958, 1963, 1968) car following model is based on a slightly different theory. In Pipes' car following model the following vehicle tries to maintain a time gap (from rear of the lead vehicle to the front of the following vehicle) greater than or equal to the reaction time of the following vehicle.

$$h_{\min} = \Delta t + \frac{L_n}{v_n(t)}$$

2.4.2 | STIMULUS-BASED MODELS: GENERAL MOTORS' CAR FOLLOWING MODELS

Researchers at General Motors (GM) developed car following models that were more extensive. The experiments at GM were also followed by extensive field evaluations. The GM car following models can also be classified as stimulus-based models. Over the period of many years, researchers at GM developed five different car following models. All of these models were based on a similar form, where response of the following vehicle is a function of its sensitivity and stimuli.

Response = Function (Sensitivity, Stimuli)

The response of the following vehicle in all the models is represented by acceleration or deceleration, and the stimuli were represented by relative velocity of following and leading vehicle. The difference in the five generation of GM models was due to different terms for sensitivity.

The first generation or linear car following model was based on a constant sensitivity parameter. Mathematically, the model took the form represented in the following

equation. Where, Δt is the reaction time of the following vehicle. Field experiments revealed reaction times varied from 1 to 2.2 seconds and sensitivity parameter, α, varied from 0.17 to 0.74.

$$a_{n+1}(t+\Delta t) = \alpha[v_n(t) - v_{n+1}(t)]$$

Due to a significant variation in the sensitivity parameter in the first generation of car following model, researchers suggested a two-regime sensitivity parameter. A high sensitivity parameter was suggested for close following situations and a low sensitivity parameter for larger following distances. The formulation was slightly altered to account for two-regime sensitivity parameter.

$$a_{n+1}(t+\Delta t) = \begin{matrix} \alpha_1 \\ or \\ \alpha_2 \end{matrix} [v_n(t) - v_{n+1}(t)]$$

Upon further investigation, the researchers found the sensitivity parameter, α, was directly proportional to the inverse of the following distance. The third generation GM car following model was formulated as presented in the following equation.

$$a_{n+1}(t+\Delta t) = \frac{\alpha_0}{[x_n(t) - x_{n+1}(t)]}[v_n(t) - v_{n+1}(t)]$$

In the fourth generation of the models, the researchers argued that as the speed of traffic stream increased, drivers are more sensitive to speed difference. The formulation of the fourth generation car following model is presented below.

$$a_{n+1}(t+\Delta t) = \frac{\alpha'(v_{n+1}(t))}{[x_n(t) - x_{n+1}(t)]}[v_n(t) - v_{n+1}(t)]$$

Through continued effort, researchers introduced a more generalized form for the sensitivity term. Two new generalized exponents, *m* and *l*, were introduced into the fifth

generation. The consequence of such would make it possible to derive the previous four generations of models from the fifth generation model.

$$a_{n+1}(t+\Delta t)=\frac{\alpha_{m,l}\left(v_{n+1}(t)\right)^{m}}{\left[x_n(t)-x_{n+1}(t)\right]^{l}}\left[v_n(t)-v_{n+1}(t)\right]$$

By varying exponents, *m* and *l*, the fifth generation model morphs into previous generations of GM car following models. The sensitivity parameter constant, $\alpha_{m,l}$, and exponents, m and l, are considered as calibration parameters. These parameters have no obvious relationship with the driver or the vehicle. The main critique towards GM car following models has been its inability to models desired speed of drivers. In GM car following models, the following vehicle is always trying to match the speed of the leading vehicle. For this reason they are often referred to as follow-the-leader models. The inability to model desired speed of following driver adversely affects applicability in multi-lane conditions. And coupling of vehicles reduces headways even if the desired speed of the following vehicle is lower than lead vehicle speed. This can result in lower headways on the highway, thereby increasing the flow. There have been some modifications to GM car following models in order to account for such a behavior. MITSIM microsimulation uses the GM car following model, but accounts for free flow regime at large headways.

2.4.3 | STOPPING DISTANCE BASED MODEL: GIPPS' CAR FOLLOWING MODEL

Stopping distance based car following models, also known as collision avoidance models, are formulated such that the following vehicle maintains a safe following distance in order to avoid a collision. A typical example for these models is the Gipps' car following model. The Gipps' car following model, unlike GM car following models, accounts for

the desired speed of the vehicle. In free flow conditions, vehicles accelerate to reach their desired speed, but do not exceed desired speed. And during following condition, the driver maintains a safe following distance that would avoid collisions even if the leading vehicle stops at its highest deceleration rate. The maximum acceleration and deceleration are modeled in order to rule out physically impossible acceleration and deceleration rates. It also differs from stimulus-based model, due to asymmetrical vehicle acceleration and deceleration modeling. The exact formulation of vehicle following behavior is beyond the scope of this introduction, and will be presented in detail if required. The Gipps' car following model is used in AIMSUN microsimulation software.

2.4.4 | PSYCHO-PHYSICAL CAR FOLLOWING MODELS

Psycho-physical models or action-point models are car following models based on human perception and reaction research. Todosiev (1963) and Michaels (1963) are among the first to research human perception and reaction thresholds in car following. Wiedemann (1974, 1991) later extended the research to develop the traffic simulation model MISSION, that incorporated perception thresholds for modeling car following behavior. VISSIM microsimulation model is based on two implementations of the Wiedemann (1974, 1991) MISSION model. VISSIM defines two different driver behavior models: Wiedemann 74, and Wiedemann 99; the former suited for urban traffic and later for freeway traffic. In the MISSION model, Wiedemann defines four different car following regimes.

1. **Free-Flow:** The vehicle is not influenced by any other vehicle; the vehicle tries to keep its desired speed, but fluctuates around its desired speed due to imperfect throttle control.

2. **Approaching:** Once the vehicle realizes it is approaching another vehicle, it decelerates to match lead vehicle's speed as it reaches its desired safety distance
3. **Following:** In this driving condition, the following vehicle unconsciously follows the lead vehicle to keep speed differences and acceleration low.
4. **Emergency:** If the vehicles following distance falls below desired following distance, the vehicle reacts by applying maximum deceleration (within vehicular capabilities) to avoid collision.

The calibration methodology presented in this research is demonstrated using the VISSIM microsimulation software. However, the calibration methodology is equally applicable to other similar microsimulation models. Calibrating psycho-physical car following models is still a work in progress. Research is required in developing calibration methodologies for psycho-physical car following models; however, the methodologies need to be generic enough to be applicable to other car following models. The other reason is that VISSIM and other psycho-physical car following models (e.g. PARAMICS) are currently among the most widely used models in microsimulation. Any research in calibrating such models will greatly help the practitioners. For this reason, a more detailed review of the Wiedemann 74 and 99 driving models is presented in the next section.

2.5 | VISSIM CAR FOLLOWING MODELS: WIEDEMANN 74 AND 99

The VISSIM microsimulation software has two different implementations of the car following model: Wiedemann 74, and Wiedemann 99. Wiedemann 74 model is suggested for use in urban conditions, whereas Wiedemann 99 model is suggested for use in freeway conditions. Both of the models are similar in that both are based on human

perception thresholds. The difference lies in how the perception thresholds are implemented. Wiedemann 74 and Wiedemann 99 were both developed by Wiedemann (1974, 1991). Wiedemann 74 and 99 models have four driving regimes: free-flow, approaching, following, and emergency; as described in section 2.3.4. Descriptions of Wiedemann 74 and 99 models are provided in the following sub-sections.

2.5.1 | WIEDEMANN 74 CAR FOLLOWING MODEL

The Wiedemann 74 car following model is one of the two implementations of car following models available in VISSIM. This model is suggested for use in urban traffic. The driver behavior modeling in car following is based on perception thresholds. The formulation is best explained using a relative velocity vs. relative distance graphs. Many of the thresholds can be represented in these dimensions. Figure 2.3 describes a typical goal-seeking behavior in a car following process. A brief explanation of different perception thresholds is presented below.

1. **AX:** is the minimum distance headway (front-bumper to front-bumper distance) in a standstill condition
2. **ABX:** is the minimum desired following distance
3. **SDX:** is the maximum desired following distance
4. **SDV:** the threshold at which driver recognizes that he is approaching a slower vehicle
5. **OPDV:** is the threshold for speed difference in an opening process during a following condition
6. **CLDV:** is the threshold for speed difference in a closing process during a following condition

The minimum desired following distance for a vehicle in following condition is proportional to the square root of the slower vehicle's speed. The slower vehicle can be either the leading vehicle or the following vehicle. In addition, in some cases the following vehicle behavior is also controlled by the next vehicle downstream.

$$ABX = AX + (bx\_add + bx\_mult * N[0.5,0.15]) * \sqrt{v_{slower}}$$

As it can be seen, the calibration parameters for car following are *bx_add* and *bx_mult*. Driving behavior can be altered by changing these parameters.

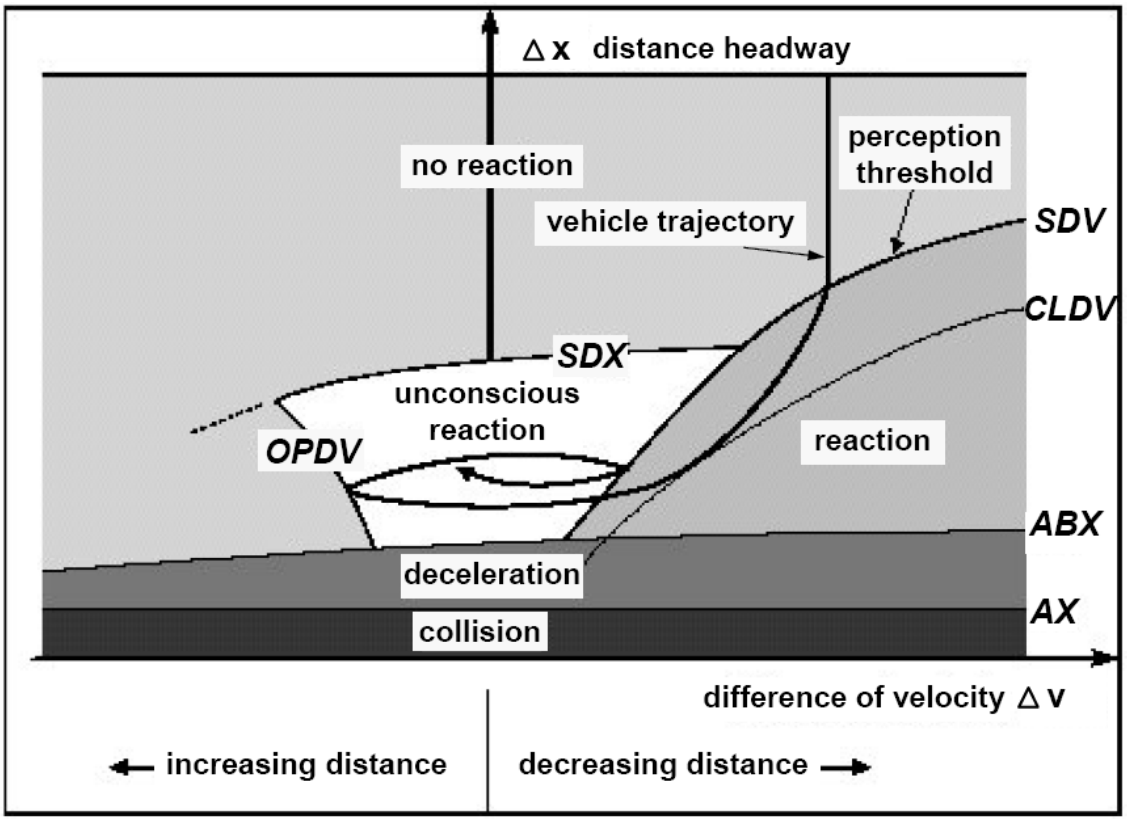

Figure 2.3 Wiedemann 74 car following model thresholds

2.5.2 | WIEDEMANN 99 CAR FOLLOWING MODEL

The second implementation of the VISSIM car following model is the Wiedemann 99 model. This model is very similar in relation to the Wiedemann 74 model. The core execution or logic in Wiedemann 99 remained the same; however, some of the thresholds

are calculated differently from Wiedemann 74 model. The thresholds described in the Wiedemann 74 model have the same meaning in the Wiedemann 99 model, but are calculated in a different way. In order to explain the difference, ten Wiedemann 99 calibration parameters are defined in the next section.

CC0: defines the desired rear bumper-to-front bumper distance between stopped cars. This parameter has no variation.

$$AX = CC0$$

CC1: defines the time (in seconds) the following driver wishes to keep. The VISSIM manual reports this as headway time, which is wrong, because it doesn't define front bumper-to-front bumper time differences, rather a totally different parameter.

$$ABX = L_{n-1} + CC0 + CC1 * v_{slower}$$

CC2: defines, rather restricts the longitudinal oscillation during following condition. In other words, it defines how much more distance than the desired safety distance (**ABX**) before the driver intentionally moves closer.

$$SDX = ABX + CC2$$

CC3: defines the start (in seconds) of the deceleration process; i.e., the time in seconds, when the driver recognizes a slower moving preceding vehicle, and starts to decelerate.

$$SDV = CC3$$

CC4 and CC5: define the speed difference (in m/s) during the following process. CC4 controls speed differences during closing process, and CC5 controls speed differences in an opening process.

CC6: defines the influence of distance on speed oscillation during following condition.

CC7: defines actual acceleration during oscillation in a following process.

CC8: defines the desired acceleration when starting from a standstill.

CC9: defines the desired acceleration when at 80km/hr. However, it is limited by maximum acceleration for the vehicle type.

The ten parameters defined in above are the Wiedemann 99 calibration parameters. Some of them define perception thresholds, while others define desired driver behavior parameters.

3 | Literature Review: Calibration

"At the source of every error which is blamed on the computer you will find at least two human errors including the error of blaming it on the computer"

-Anonymous

3.1 | CALIBRATION

Calibration is arguably one of the most important steps in traffic simulation model development process. Calibration has always been an important issue since the advent of traffic simulation models. The validity of measurements and decisions made using simulation models are often directly proportional to the time and effort devoted to calibration. Development of traffic simulation model that can replicate a variety of driving behaviors that exist in the real-world is practically impossible. Instead, traffic simulation models have parameters that can be tweaked to reproduce such a variation in driving behavior. Calibration is the process of varying such parameters to match local driving behavior. Without calibration, traffic simulation models cannot be expected to provide accurate results. In this chapter, a review of current state of the art of literature on calibration is presented.

3.2 | LITERATURE REVIEW ON CALIBRATION

The development of calibration started with the start of microsimulation models in the early 1950s. Various methodologies have been proposed for calibration of microsimulation models. There has been much literature published in the field of calibration. Research efforts vary from "strategies" or logical steps to perform calibration to optimizations methods employed in the calibration process. But the goals of all such research efforts remain the same; i.e., achieving efficiently calibrated models that reasonably replicate local traffic behavior or conditions. This reasonable replication is achieved when calibrated simulation models meet desired constraints or "targets". The methodology for calibration of simulation models is constantly altered to suit research goals or organizational goals. In addition, there has also been research effort directed towards developing universal calibration methodologies.

Calibration of microsimulation process involves varying a wide variety of parameters to match local traffic behavior. Calibration by itself can be a very time consuming task, due to the large number of parameters involved. Since parameters can have effects that go beyond a single measure of performance, calibration requires an iterative process to help effectively reach an optimal solution. A variety of methods have been used to calibrate simulation models. These methods were largely dependent on research objectives and simulation models. In many cases, the type of calibration parameter and specific nature of the simulation model determined the calibration methodology. In the consecutive sections, a review of selected calibration literature is presented in a chronological order. In the authors view, the calibration can be divided into following sections, each time period representing a different focus.

3.2.1 | CALIBRATION (1950-1980)

In the initial years of research in traffic simulation, most of the calibration efforts were directed towards estimation of parameters for car following models. Various car following models were calibrated to field conditions based on experimental data. The experimental data varied from test track data (Chandler et al. 1998) to vehicular tunnel experiments (Edie et al. 1963). A common theme among such experiments is the use of relative velocity, relative distances, speeds, and accelerations of the leading and following vehicles. General Motors, and New York Port Authority's experiments were based on two cars connected to each other with cable on a pulley. The experiments were used to determine ranges for the GM car following model sensitivity parameters. But most of these results were limited to certain scenarios, due to the unavailability of large data sets. Hoefs and Leutzbach (1972) and Hoefs(1972) collected relative speed, relative velocity, and speed data that was used to calibrate perception thresholds in psycho-physical car following models of Michaels (1965) and Todosiev (1963).

Many of the experiments were based on matching the car following model to the test track data. Relationships from macroscopic data such as speed-flow, speed-density, etc were also utilized in estimating parameters of models (Edie et al. 1963). Since standard integrated simulation models were in development, calibration techniques were tailored on modifying a few of the parameters of individual models. In addition, microscopic vehicle trajectory data used by many of the authors did not model whole range of driver behavior and traffic conditions. One common theme among such early methodologies was the use and importance of relationships to calibrate simulation models; e.g. volume-speed, volume density, volume vs. number of lane changes, etc.

Much of the calibration methodologies in use today are largely borrowed from these early studies.

3.2.2 | CALIBRATION (1980-1998)

In the years following the studies mentioned in the previous paragraph, some standard simulation models which integrated individual car following model such as car following and lane changing (e.g. FREQ) were subject of calibration studies; for instance, Stokes and Mounce (1984) and Alperen and Gersten (1987) used FREQ models and capacity as a primary traffic variable in their calibration efforts. Researchers developed "strategies" for calibration (e.g. Cheu et al., 1994). However, many of the calibration objectives were based on reducing the difference between observed and field capacities. Many of the researchers (e.g. Aycin and Benekohal, 1998; Payne et al., 1997; Radwan et al., 1991) calibrated their simulation models based on single or averages values of traffic variables, this kind of representation results in significant loss of information. However, use of better goodness-of-fit measures such as Kolmogrov-Smirnov tests helped in acurate measurement of differences (Dixon 1997; Zarean and Nameth, 1998). Cheu et al. (1994) matched volume and occupancy plots without performing OD calibration, which has a significant effect on volume and occupancy registered at loop detectors. A calibration methodology based on matching volume over time at loop detectors would result in a much better calibrated model (e.g. Rakha et al., 1998). The research in these years still lacked a systematic calibration effort. In addition, many of calibration techniques were based on trial error that lacked mathematical or statistical basis.

3.2.3 | CALIBRATION (1998-2002)

In these years of calibration, the researchers started employing robust optimization techniques like genetic algorithms (Cheu et al., 1998; Ma and Abdulhai, 2002). But, many of the calibration methods lacked a systematic approach, thereby resulting in a poorly calibrated simulation model. The methods were mostly based on volume and speed time-series. Ma and Abdulhai (2002) also reported using a variety of goodness-of-fit measures such as Point Mean Absolute Error (PMAE), Global relative Error (GRE), Theil's Inequality Coefficient, and Point Mean Relative Error (PMRE)

Rakha and Crowther (2002) proposed a unique calibration methodology based on steady-state car following behavior. In this methodology the steady-state behavior of various car following models such as CORSIM, VISSIM, and Van-Aerde is used to develop a macroscopic traffic stream model. Then the car following sensitivity parameters are proposed as solution to such macroscopic relationships. In the study, the Pipes' car following model sensitivity factor can be derived from roadway capacity, jam density, and free speed. Solutions have also been proposed for steady-state car following models equivalent to Greenshields and Van Aerde traffic stream models.

Gardes et al. (2002) describe a general calibration methodology that involves both qualitative and quantitative aspects of simulation. Qualitative assessment such as visual analysis of vehicle movements is used in calibration. The quantitative aspects involve network-wide measures such as total travel time, total distance traveled, and average speed; link or intersection measures such as travel times, traffic flow levels, etc. Calibration parameters that required changes include link speeds, speed memory, mean target headway, mean reaction time, etc.

3.2.4 | CALIBRATION (2003-2007)

Toledo at al. (2003) described a two step calibration procedure as part of their calibration framework. The calibration framework is replicated in Figure 3.1. The calibration procedure is divided into two levels: disaggregate and aggregate. In the first step, parameters in individual models such as driver behavior and route-choice models are statistically estimated from disaggregate data or microscopic data such as vehicle trajectory data. In the second step, the general parameters are calibrated using aggregate data such as speed, flow, time headways, etc. The aggregate calibration is formulated as an optimization or search problem. The authors stress the importance of inter-relationships between O-D matrices, route-choice parameters, and driver behavior parameters and their effect on calibration. The authors propose using an iterative approach to calibrate route choice parameters and estimate O-D matrix, and an overall iteration with driver behavior parameter until convergence as shown in figure 3.2

Hourdakis et al. (2003) described a generic calibration methodology for freeway simulation models. Initially, the parameters are divided into two categories: global parameters such as desired speeds, vehicle characteristics, maximum acceleration and deceleration, and minimum headway; local parameters such as speed limits, and other link specific parameters. The calibration process is then divided into mainly two stages: volume, and speed-based calibration. In addition, an optional third stage involving a research objective-based calibration for fine tuning of the simulation model is also suggested. Between the first two stages, the authors suggest volume-based calibration followed by speed-based calibration.

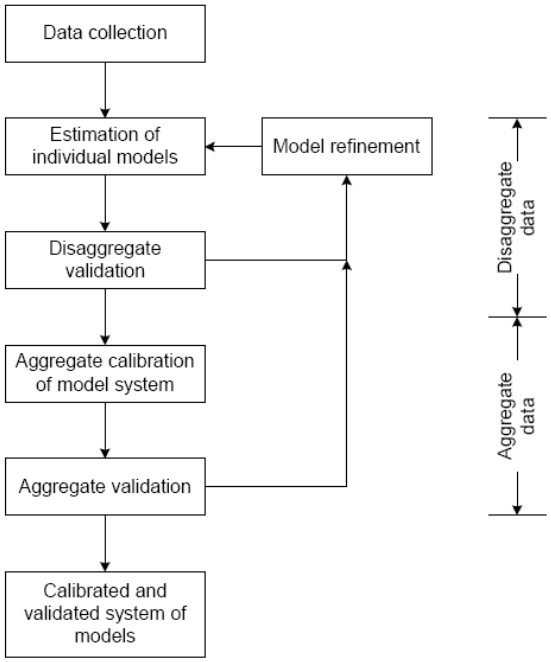

Figure 3.1 Calibration Framework [Toledo et al, 2003]

Dowling et al. (2004) describe a generic calibration framework for simulation models (figure 3.3). The authors suggest dividing the calibration parameters into two categories. One category includes parameters where the user is reasonably certain and not willing to adjust, and second category of parameters the user is uncertain and willing to adjust. The authors then suggest dividing the adjustable parameters into parameters that directly impact capacity and parameters that directly impact route choice. It is also suggested that each of the parameters be classified into global or link specific parameters. The authors then propose the use of three-step methodology: capacity calibration, route choice calibration, and system performance calibration. In addition, the authors propose that calibration of the model to field capacity be one of the first steps in microsimulation calibration. It is also suggested that queue discharge flow rate be used to estimate a numerical value for capacity. The calibration procedure is performed until calibration

targets are met, since calibration can be a time consuming task. These calibration targets are usually based on organizational and research goals (Figure 3.4)

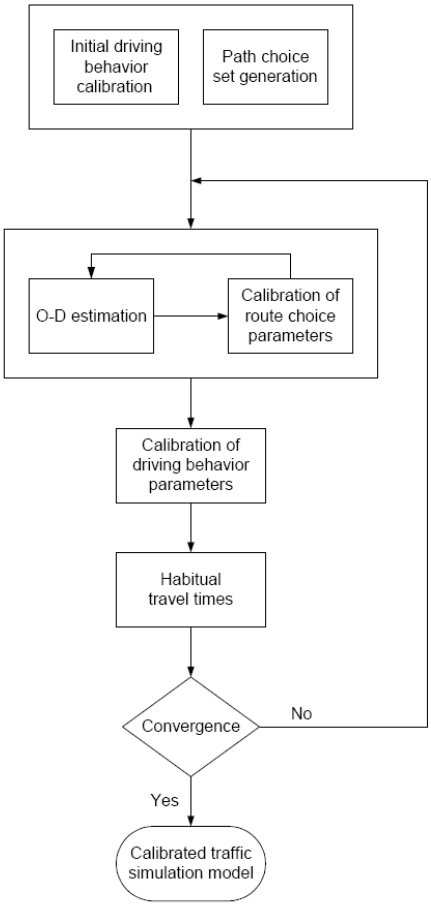

Figure 3.2 Methodology for aggregate calibration of simulation models. [Toledo et al, 2003]

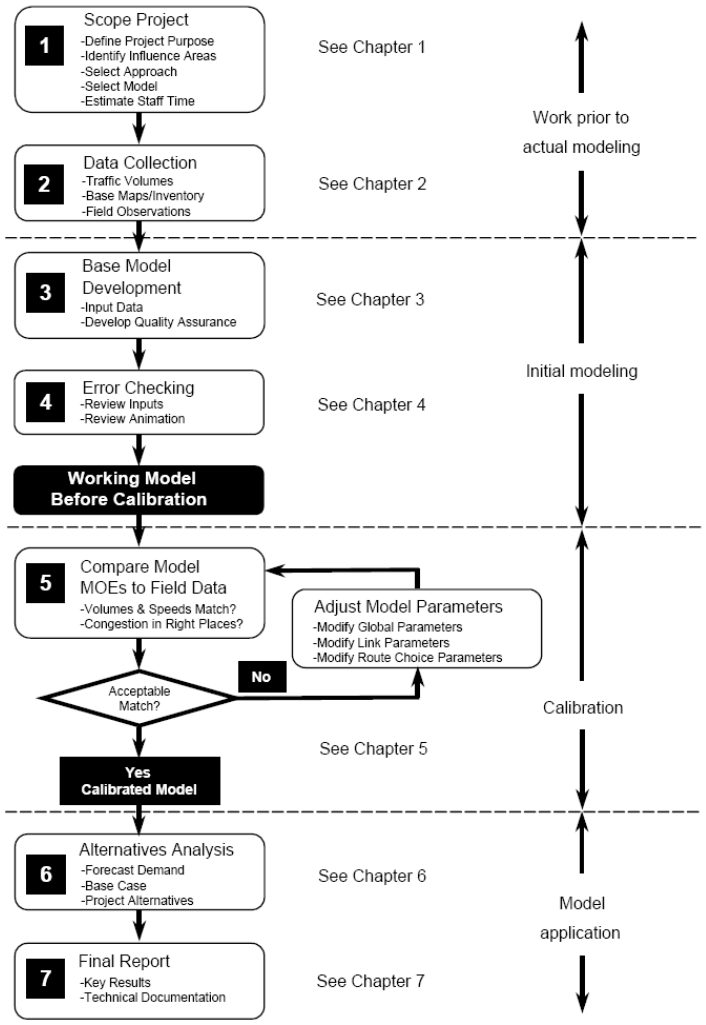

Figure 3.3 Prototypical microsimulation analysis tasks adapted from *The Advanced CORSIM Training Manual*, Minnesota department of Transportation

Criteria and Measures	Calibration Acceptance Targets
Hourly Flows, Model Versus Observed	
Individual link flows	
Within 15%, for 700 vph < flow < 2700 vph	>85% of cases
Within 100 vph, for flow < 700 vph	>85% of cases
Within 400 vph, for flow > 2700 vph	>85% of cases
Sum of all link flows	within 5% of sum of all link counts
GEH statistic < 5 for individual link flows[a]	>85% of cases
GEH statistic for sum of all link flows	GEH < 4 for sum of all link counts
Travel Times, Model Versus Observed	
Journey times network within 15% (or one minute, if higher)	>85% of cases
Visual Audits	
Individual link speeds	
Visually acceptable speed-flow relationship	to analyst's satisfaction
Bottlenecks	
Visually acceptable queuing	to analyst's satisfaction

[a] The GEH statistic is computed as follows:

$$GEH = \sqrt{\frac{(V-E)^2}{(E+V)/2}}$$

where E is the model estimated volume and V is the count.

Figure 3.4 Wisconsin Department of Transportation calibration targets [Dowling et al, 2004]

Toledo et al. (2004) describe a calibration methodology which is based on slight modification to a previous methodology presented in Toledo et al. (2003). The proposed methodology is presented in figure 3.5.

Brockfield et al. (2004) describes calibration of car following models based on data obtained from test track in Japan. The calibration of the car following models was based on reducing the percentage absolute error in gaps measured in simulated vs. the field data.

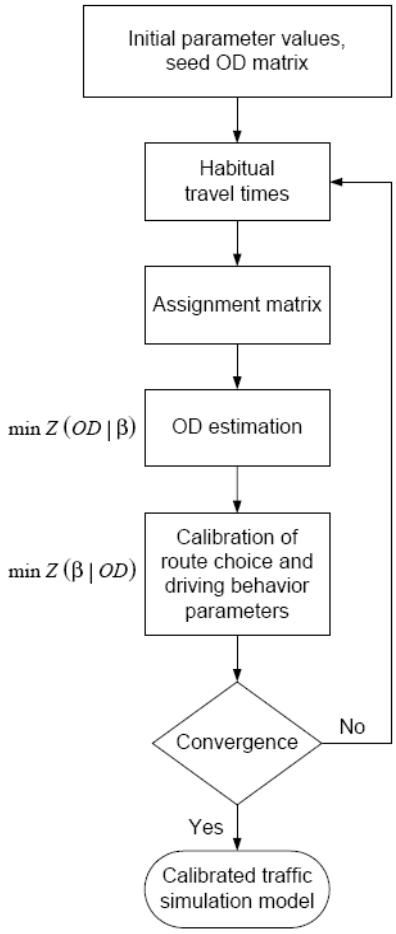

Figure 3.5 Solution to steady state calibration approach [Toledo et al., 2004]

Bayarri et al. (2004) describe a unique calibration methodology based on Bayesian analysis techniques. The authors suggest dividing calibration parameters into three categories: parameters than can be estimate form field data (vehicle mix, arrival rate, turning percentages); parameters that are not measurable or based on choice (discharge headway distribution); parameters that are not "real" but required for tuning by the simulation model (free-flow speed). The authors dedicated much of the effort to demonstrating their Bayesian methodology for demand and turning probabilities.

Gomes et al. (2004) describes a unique calibration methodology of matching the location of bottlenecks, queue lengths, and HOV lane utilization for congested freeway

simulation model in VISSIM. The calibration methodology was based on qualitative as well as quantitative measures of differences in simulation and field data.

Ranjitkar et al. (2004) described a research effort comparing different car following model with microscopic test track data. The authors made conclusions about the performance of various car following models based on calibration to speed and headway data.

Kim et al. (2005) used a non-parametric statistical method for calibration of VISSIM simulation model. The authors used a genetic algorithm as an optimization tool in the objective function. The method is a distribution free method where the simulation output is compared to field data using Moses' distribution free rank-like test and Wicoxon rank-sum test. The possible solutions that pass these two tests are selected to the next generation in the genetic algorithm. The comparative fitness values of possible solutions are evaluated using a Kolmogrov-Smirnov test.

Park and Qi (2005) describe a multi-stage calibration methodology for simulation models. In the first step, an initial evaluation of default parameters is performed by comparing field and simulation outputs, and default parameters are accepted if it is a close match. In the second stage, an initial calibration parameter set is identified, followed by Latin Hypercude Design (LHD) is used to develop multiple parameter sets that reasonably cover parameter surface while keep the set size to manageable numbers. Within the second stage additional feasibility test and Analysis of variance (ANOVA) tests are performed to identify key parameters and ranges. This stage followed by the third stage involving parameter calibration using genetic algorithms. And finally, the

genetic algorithm recommended parameter set is evaluated using statistical techniques. A flow chart summarizing the following methodology is provided in figure 3.6.

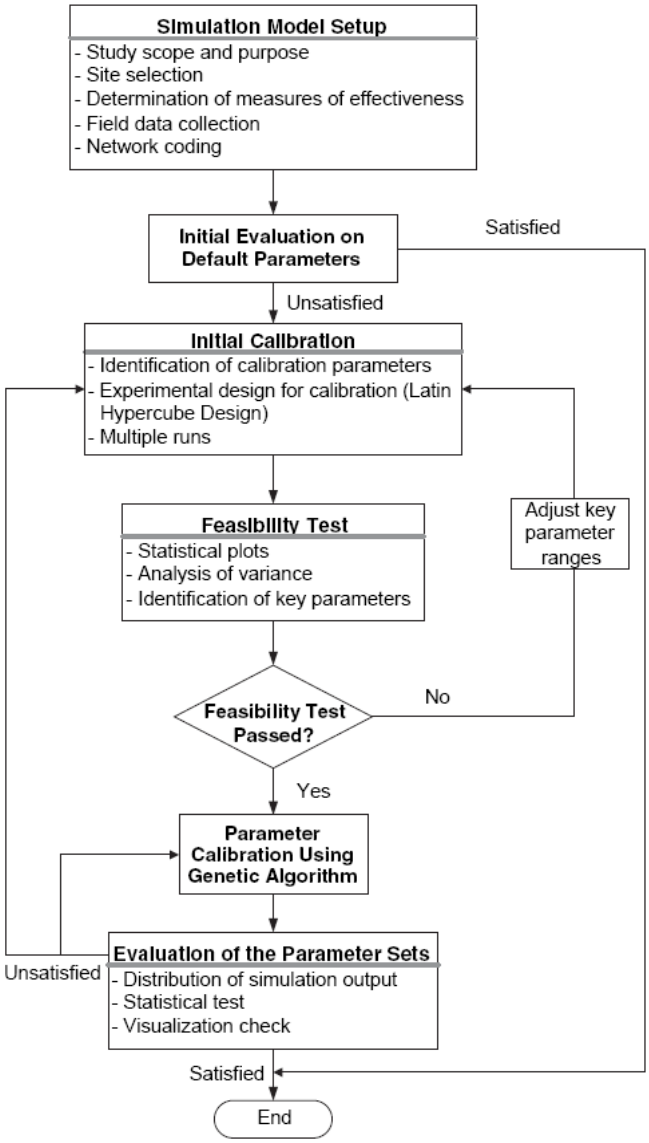

Figure 3.6 Latin Hypercube Design (LHD) based calibration methodology [Park and Qi, 2005]

In summary, over the recent years researchers started developing systematic calibration frameworks for application in microsimulation calibration (e.g. Dowling et al., 2004; Toledo et al., 2003, 2004). The concept of calibration targets were also introduced

to assist in optimization process. Most of the objective functions for measuring the difference between field and measured discharge flows are based on different statistical goodness-of-fit measures (Dowling et al., 2004; Toledo et al., 2003, 2004; Schultz et al., 2004, Gomes et al. (2004) described qualitative efforts based on eye-balling the difference in field and simulated graphs. However, these methods lacked a quantifiable or mathematical basis for accessing the differences). Kim et al. (2005) reported the use of non-parametric statistical methods for comparison of distributions, but such methods are not applicable in measuring the degree of closeness of graphs. Much of the research still suffers from poor traffic flow representation of the model. And in cases where a good representation is used, no quantifiable methods are proposed to measure the differences. Unfortunately, in many cases, there was no definition for calibration qualification. In other words, researchers were focused on the action (calibration), but did not address the qualification (i.e., what is model calibration?).

3.3 | CLASSIFICATION OF OBJECTIVES IN CALIBRATION

After an extensive review of literature on calibration methodologies and frameworks proposed by many researchers over the decades, the objectives in calibration methodologies can be broadly classified into two different categories: Qualitative, and Quantitative. Each of the categories can be classified further into various subcategories.

3.3.1 | QUALITATIVE METHODS

These methods, as the name suggests, are methods that lack mathematical or statistical foundation. Not that such methods cannot be expressed in mathematical or statistical form, rather such representation is often complex, or more appropriately beyond the

scope of the study. In qualitative methods, authors usually rely on their perception of reality to decide if the simulation model is performing close to reality. For example, in testing car following models, authors subject a lead vehicle in the platoon to speed disturbances that range from moderate to extreme, and observations are made on the stability of the car following process of the platoon, and compared to author's perception of reality; e.g., Zarean and Nemeth (1988). A similar example relates to Gardes et al. (2002), and several other studies, is the use of visual analysis of vehicle movements in a traffic network to calibrate simulation models. Such methods are usually undertaken to rule out "bad" calibration parameter values form possible parameter solutions. A very good example of qualitative measures in calibration is Gomes at al. (2004), wherein the authors matched speed-contour graphs obtained from field and simulation. This method is similar to matching extent of congestion in the traffic network. In the process, the authors' primary intent was to vary certain calibration parameters to replicate bottleneck locations, and extent of queues in the network. These types of qualitative methods are applied all through the calibration process to tweak the model.

3.3.2 | QUANTITATIVE METHODS

Quantitative methods are methods that are based on mathematical or statistical foundation. Due to a wide variety of quantitative methods in calibration, sub categorization of these methods is necessary to gain a better understanding of the differences. The categorization is loosely based on different concepts like parameters and their representation, and procedural techniques.

Single Parameter Methods are based on measuring the difference between field and simulated parameter values. There are many statistical goodness-of-fit measures for

measuring the difference between field and simulated values. Examples of parameters that are typically used in calibration include capacity, average or maximum queue lengths, average travel time, total travel time, many others. Much of the studies in the current state-of-the-art utilize such simple measures of difference to calibrate their simulation models. Typical examples of statistical goodness-of-fit measures for single parameter values include the following:

1. Mean Error (ME)
2. Mean Absolute Error (MAE)
3. Mean Absolute Error Ratio (MAER)
4. Mean Square Error (MSE)
5. Root Mean Squared Error (RMSE)
6. Mean Percentage Error (MPE)
7. Mean Absolute Percentage Error (MAPE)
8. Root Mean Squared Percentage Error (RMSPE)
9. Root Relative Square Error (RRSE)
10. Relative Absolute Error (RAE)

For a detailed explanation about these statistical goodness-of-fit measures, the reader is directed to any standard statistical reference. Each of the error has its own advantages and disadvantages. Selection among these measures is usually based on research objectives, goals, and nature of the problem. Discussions about “noise”, outliers, weights for the errors, etc is important to select the appropriate measure.

Multiple Parameter Methods are similar in nature to single parameters methods. In multiple parameter methods the errors from different parameters should be weighted

according the units and importance. The objective can include penalties to include different constraints. A typical example is calibrating of simulation models with respect to volume and speed.

Time-Series Methods include error accrual of multiple parameters over time. Various multiple parameters methods like weights, penalties are also applicable to these methods. Examples of such methods include calibration of simulation models to microscopic vehicle trajectory data, volumes over time, speeds over time, etc.

Statistical Parametric Methods are based on comparing distributions of parameters, where it is assumed that the population is assumed to fit a parameterized distribution. Some of the typical assumptions include either a normal or a uniform distribution. Common methods employ measures based on mean and variance. Some of the popular tests include the z-test, t-test, F-test, ANOVA, etc.

Distribution-Free or Non-Parametric Statistical Methods, unlike parametric measures, do not have an underlying assumption about the nature of the distribution of the population. Typical examples of non-parametric statistical methods include Kolmogrov-Smirnov test, chi-square test, etc.(Zarean and Nemeth, 1998; Dixon 1997)

Other Methods there are methods that are different from the one described above. Some of the methods are heuristic in nature and specific to the problem at hand. Some examples of these calibration methods include methodologies wherein a simultaneous or iterative approach is used. Bayesian inference techniques have also found use in some of the calibration methods.

3.4 | DATA CONSIDERATION IN MICROSIMULATION CALIBRATION

Data considerations are important in development of calibration procedures for simulation models. It is paramount to incorporate data considerations and requirements into the development process. It is the intent of the study to develop a generic calibration methodology based on such considerations. A brief description of data collection efforts and types of data is provided in this section. Comprehensive efforts were directed towards data collection to obtain a variety of microscopic and macroscopic real-world data. Data was obtained from a variety of sources including Federal Highway Administration (FHWA), state departments of transportation (DOTs), and Traffic Management Centers (TMC). The advent of Intelligent Transportation Systems (ITS) has made collection of a variety of traffic data possible. Data collected for this project is divided into two main categories: microscopic and macroscopic.

3.4.1 | MICROSCOPIC DATA

Microscopic Data includes detailed sub-second information about vehicle trajectories over time. The main source for microscopic data for this research is provided by Federal Highway Administration. FHWA collected detailed sub-second vehicle trajectory information as part of Next Generation Simulation (NGSIM) program. The data is available free to the research community through the World Wide Web (WWW). Microscopic data available from the NGSIM effort includes sub-second vehicle position, speed, acceleration, headway, and spacing information. The data also includes information about following and leading vehicles for each of the vehicles. The data collected from this source include detailed vehicle trajectory information from two freeway sections and one arterial section. The two freeway sections include I-80 and

US101 freeway sections. NGSIM has put forth data sets from three different locations: I-80, US101, and New Lankershim Boulevard. The length of each of the data sets is approximately two to three 15 minute periods.

3.4.2 | MACROSCOPIC DATA

Macroscopic Data includes aggregated vehicle information. This data is typically obtained from state DOTs and TMCs. The aggregation level varies from 20 seconds to 15 minutes. There four different sources were identified for this research.

1. Performance Management Systems, California Department of Transportation (CalTrans)
2. Traffic.com, St. Louis, Missouri
3. Portland Traffic Management Center, Oregon Department of Transportation
4. NAVIGATOR, Atlanta Traffic Management Center, Georgia.

Macroscopic data available from the sources mentioned above are based on loop detectors or microwave detectors placed on freeways. The information available ranges from 20-second to 15 minute aggregate volume, speed, and occupancy counts. All detectors do not have speed information, since most of the detectors are single loop detectors. Any speed information from single loop detectors is biased information. But, there are some detectors with speed information coming from dual loops, and microwave detectors. And as mentioned before the aggregation interval varies from 20-second raw data to 15-min aggregated data.

4 | A Methodological Formulation of Calibration Based on Representations and Invariants

"We build our computer (systems) the way we build our cities: over time, without a plan, on top of ruins"

-Ullman, Ellen

4.1 | INTRODUCTION

The importance of calibration of traffic simulation models is well appreciated in the literature. After several years of research in traffic simulation models, many of the existing formulations of calibration objective are still ad-hoc or incomplete. In many cases, the definition of calibration is informal. For instance, one of the most common methods is to reduce the difference in capacity or link volume counts from the field and the simulation model. In this informal method the definition is that if capacity and link-counts of simulation model match, the simulation model is considered calibrated to the field. And in many cases, the choice of these traffic variables varies widely. However, a variety of traffic variables that are not part of the calibration process are still collected and analyzed in simulation model, and thereafter used in the decision making process.

A simple example that illustrates this is if a user calibrates the length of queues of the simulation model to match the field queue lengths, the traffic simulation model can only

serve as a queuing model. The model cannot be expected to replicate flow process that exist beyond queuing; for instance, freeway weaving analysis.

A traffic simulation model, by definition, needs to replicate all of the traffic flow processes observed in the real world. A formal calibration would define a calibration definition based on all such traffic flow processes. The following needs exist for defining a formal system for calibration. First, a formal definition of calibration in terms of qualification; in other words, what does it mean when a model is calibrated? Second, a formal definition of calibration procedure; also of interest is when can a model be qualified as calibrated; "when" may be formally stated as the stopping criteria or convergence criteria.

It is the intent of this research to develop a generic formulation of calibration based on representations and invariants. A generic formulation of calibration will help the researchers and users understand calibration and the importance of various steps and assumptions involved; for instance, the choice of traffic variables, relationships, and goodness-of-fit measures in calibration.

Unfortunately, there exists little known literature with a formal formulation of calibration definition; however, in many instances in the literature authors have presented various views of calibration and validation. In most cases, calibration is loosely defined as an act of changing parameters to match local site conditions. For instance, Lieberman and Rathi (2000) define calibration as follows:

> *"Calibration is the activity of specifying data describing traffic operations and other features that are site-specific."*

This particular explanation defines the action (adjusting) and not the qualification or definition (What does it mean when a model is calibrated to the field scenario?) Many of the calibration procedures in use today are largely borrowed from initial studies from 1960s and 1970s. Initially, the calibration procedures were focused on estimating parameters for individual core models such as car following, lane changing, gap acceptance, etc. The authors in many cases used controlled experiments to collect a variety of microscopic data. This microscopic calibration was in most cases followed up with a validation of the model using macroscopic data

In the following years, few works have described methods that extend the methodologies in use in the early years. The focus instead shifted to a secondary but accompanying action of finding the solution. Significant research was addressed towards employing robust optimization techniques such as genetic algorithms in calibration of simulation models. However, the traffic variables, relationships, and methodologies employed were simpler and less rigorous than in the initial years. In the recent years, researchers started developing systematic calibration frameworks for application in microsimulation calibration. The concept of calibration targets was also introduced to reach a “good enough” calibration solution. In addition, most of the objective functions for measuring the difference between field and measured variables were still based on different statistical goodness-of-fit measures. In some cases, the simple goodness-of-fit measures restricted the use to simple relationships of traffic variables. Qualitative measures are often employed for complex relationships. Although, few use cases exist of non-parametric statistical methods for comparison of distributions, but such methods are

not applicable in measuring the degree of closeness of complex relationships such as n-dimensional point sets.

In this chapter, a high level look at calibration is presented initially. The discussions are tied together and presented in a formal mathematical fashion. The formulation is followed by examples to assist in understanding the concepts. The generic formulation of calibration definition and accompanying objective will provide a deeper understanding of the nature of the problem.

4.2 | WHAT IS THE IDEA?

In this discussion, a calibration objective defined as a function that always seeks to minimize the difference between two objects; the simulation model: S; and the real-world (field) scenario: F. It can be defined as follows:

Objective: **Z** = **Minimize (F difference S)** given a finite vector of calibration parameter set: P, where elements of P may be linearly or non-linearly constrained.

The assumption is that minimizing the difference between field and simulation objects would result in a calibrated simulation model. Although trivial, such an assumption is necessary for logical consistency. Measuring the difference between two objects is often not possible; especially, when one of the objects is the real-world. Therefore, an object representation is required to reduce the complexity of the problem. In which case, the difference in objects is measured in object representation "space". In other words, the objects that cannot be directly compared are done so by what they represent, i.e., features such as speed, flow, density, etc.

The previous paragraph defined the first-level of representation in this discussion. This representation is based on common measurable features of the two objects such as

volume, speed, density, time, headway, etc. Since the object in reference is traffic, this representation is named *traffic representation.* The inherent consequence of object representation is the loss of information about the object itself. The amount of information loss can be minimized partly by increasing the size of the measured feature set.

The next logical question is: how do we measure the difference between feature sets (representations) of objects? This question defines the second level of representation in this discussion: Dissimilarity Representation. Measuring differences in feature sets is often a complex task due to the variety of variables and relationships involved in the feature set. Dissimilarity representation of feature sets reduces the complexity of measuring such differences. For instance, the most commonly used statistical error measures such as root-mean-square error, absolute error are essentially measures in dissimilarity space. A dissimilarity measure provides a value to measure the degree of commonality (or lack thereof) between objects or its features. A dissimilarity measure can be defined in many forms. The two principal directions of dissimilarity measures include structural and statistical (Pekalska and Duin, 2005). Structural (or syntactical) measures are qualitative intuitive measures that are appealing to human cognition or perception. Statistical measures are quantitative and based on well developed mathematical theories on vector spaces Measures of difference in objects, sets, and data are referred to as dissimilarity measures, whereas measures of closeness are referred to as similarity measures.

Finally, a third level of representation: search (or optimization) representation is needed. In this level, the calibration parameter sets are represented in search space to

find solutions[2] to the calibration objective. The most pertinent example of such a search representation is seen in Genetic or Evolutionary Algorithms, where the calibration parameter sets are represented commonly in binary, real, or gray-coded search spaces. Therefore, the dissimilarity measures are essentially used to define the search path in this search space.

The three levels of representations in formulation of generic calibration objective are presented in Figure 4.1.

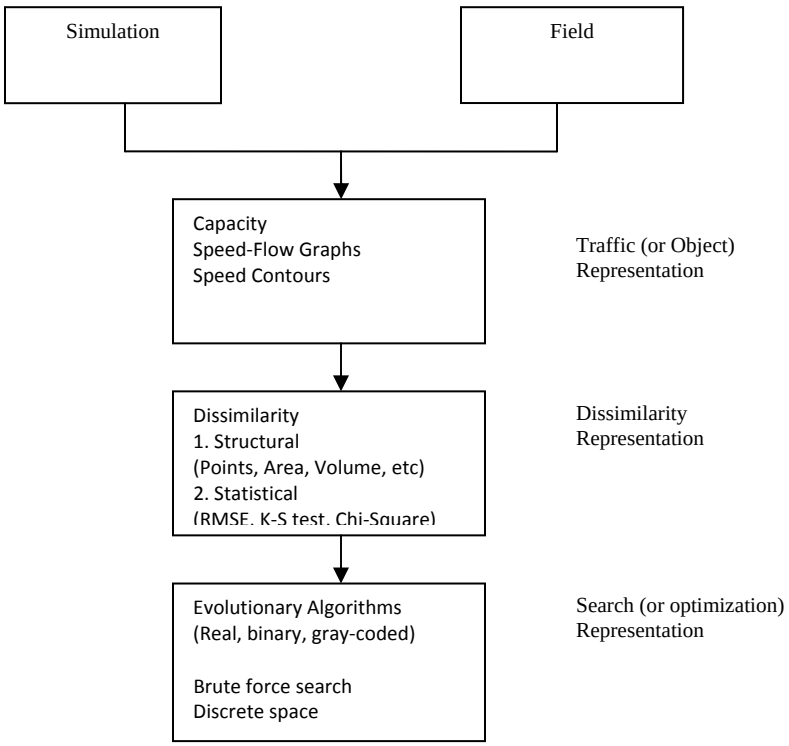

Figure 4.1 Representation based formulation of calibration.

In summary, a calibration procedure can be stated in general as a function which measures the dissimilarity between simulated and field conditions. An objective function

[2] A unique solution is not expected, because the calibration objective is always under defined.

is one of the most important parts of the calibration process. First, the better the variables represent the simulation and the field (traffic representation), the better is the calibration process. Second, the better the representation of variables (dissimilarity representation), the better is the calibration process. Finally, the better the representation of the parameters in search space (search representation) the better is the accuracy of suggested solutions. In combination they form an objective function and are valuable to the calibration process. The objective function can range from a simple function based on a single parameter to complex function based on multiple parameters. The arguments in this section were two fold. In this three level representation of the calibration objective, each of the representations results in a certain loss of information. But such representations are ultimately required to solve a complex problem

In this discussion on high-level generic formulation of calibration, the calibration procedure was defined. However, a very crucial assumption was made in the process. It was assumed that reducing the dissimilarity of traffic representations meant the model was calibrated. In the next section, a formal definition of calibration is presented and the objective is then derived of such a definition.

4.3 | WHAT IS CALIBRATION?

In this section a detailed mathematical formulation of calibration is presented based on concepts and discussions presented in the previous section.

4.3.1 | MATHEMATICAL FORMULATION OF CALIBRATION

Notation

$\exists$: There exists

$\forall$: For all

$\in$: Belongs to

$\wedge$: And

$\Rightarrow$: Implies

\ : Set difference operator

$\subset$: Subset of

':': Such that

$\{\ \}$: Empty set

P(X) : power set of X

Definition 1.1: The simulation model and the field scenario are defined as two different objects. The simulation model is defined as object S. The field scenario is defined as object F.

Definition 1.2: $X_A = \{x_1, x_2, ..., x_a\}$ is defined as a set of all independent measurable variables or features of an object A.

In traffic engineering terms, X is defined as all possible independent measurable variables, micro and macroscopic, such as headway, speed, density, flow, etc.

Representation

Definition 1.3: A representation set $R_{X,A}$ of an object A is defined as a power set of all possible object measurements (features) $X_A = \{x_1, x_2, ..., x_a\}$; i.e. $R = \mathrm{P}(X)$ or 2^X. In addition, each element $r \in R$ and $r \neq \{\ \}$ is defined as a representation.

A power set of set S is defined as set of all subset of S. A representation $r \in R$ describes a relationship of variables or features describing traffic. For instance, representation: $r_a = \{speed, flow\}$ describes the relationship between two variables speed

and flow. Therefore, a power set of a set of all measurable variables describes all the relationships that exist between such variables.

Therefore encompassing all traffic relationships that exist between variables, formal definition of calibration can be proposed based on representation set: R

Calibration Definition 1

A formal definition of calibration is presented as follows

Definition 1.4: An object S is considered calibrated (and validated) to an object F, iff

$R_{X,S} = R_{X,F} \; \forall I \mid X = X_s \cap X_F \; \& \; X \neq \{\;\}.$

Where,

I is the input to the objects

X is a non-empty set of common independent measurements between the objects: S and F

In other words, the simulation model is considered calibrated to the field scenario, if and only if, the representation sets of simulation and field based on common independent measurements are equal.

If object S is calibrated to F, a calibration relation '=' is defined, and used as follows: $S = F$. The calibration relation is conditional based on representation set: R_X . Hereafter, for simplicity, the conditional relation is assumed to be implicit but is still very important.

X is defined as the common set of possible measurements between the simulation model and the field. Only common set of measurements are utilized, since all measurement possible in simulation are not often possible in the field. Since a calibration

procedure based on variables that cannot be measured field do not hold any value, since no inference can be made of the variable.

The calibration relation is not an equivalence relation, because it is not transitive; ($A = F, B = F$ does not imply $A = B$). The transitive property may only satisfied in the special case where the representations of measurement set are the same (i.e. $X = X_A \cap X_F = X_B \cap X_F$). However the relation is both reflexive and symmetric. Since the input I to a real-world object F is often of high cardinality (i.e., number of elements in a set), a common input I to both objects is often not possible or realistic. In addition, accurate measurement of quantities is not possible due to measurement errors, and various simplifications and assumptions. For this reason, the following estimate is defined

Definition 1.5: An estimate $\hat{I}$ of I is defined as input to the simulation object S.

Since no single simulation model is expected to be applicable universally, a set of calibration parameters are defined as an input to the simulation object S to match local conditions.

Definition 1.6: A set of calibration parameters $P = \{p_1, p_2 \ldots p_n\}$ is defined as an input to the simulation object S.

Calibration Definition 2

Definition 1.7: Redefining the calibration definition, an object S is considered calibrated (and validated) to an object F, iff.

$$\exists P.\, R_{X,S} = R_{X,F}\ \forall I \mid X = X_s \cap X_F, X \neq \{\ \}, S\left(P, \hat{I}\right), F\left(I\right).$$

In other words, there exists a P , within its constraints, such that the representation set, R , of the objects S and F are equal for all physically possible inputs I .

Definition 1.8: For two given objects: O_A and O_B, a representation R defined over the two objects is defined as definite iff. $R_A = R_B \Leftrightarrow O_A = O_B$. In addition, a representation $\overline{R}$ is defined as indefinite if $O_A = O_B \Rightarrow \overline{R}_A = \overline{R}_B$, but not otherwise.

Since it is not possible to measure all possible variables of each of the simulation model and the field, it is often that researchers work with partial representations of objects. Also due to errors in measurements and randomness (or stochasticity), and inability of calibration parameter set, attaining equality of representation sets is also a difficult task; therefore, a calibration threshold is defined

In addition, the cardinality of R is 2^n, since R is power set of X, which has a cardinality of n. The cardinality of representation set R can be inordinately high; thereby, computation cost of such representation set is prohibitively large. Also every representation $r \in R$ might not be of engineering or physical interest, some representations are of more interest than the other. To capture the fewer sets employed in real-world calibration to reduce computation cost, a new representation set is defined.

Definition 1.9: A representation set $R' \subset R$ is defined

However, such reduction in cardinality of representation set results in significant loss of information. If $R = \mathrm{P}(X)$, then by definition, R is a definite representation. In addition R' is an indefinite representation, since it is a subset of R. Therefore, partial calibration equality is needed to redefine the calibration definition.

Calibration Definition 3

Definition 2.0: Redefining the calibration definition, S is partially calibrated or $S \approx F$, iff. $\exists P.\left(R'_{X',S} - R'_{X',F}\right) < \delta \ \forall I \mid R' \subset R, X = X_s \cap X_F, X \neq \{\ \}, S\left(P, \hat{I}\right), F\left(I\right)$

Where,

P satisfies its constraints, and

δ is the calibration target or threshold.

Therefore, as the cardinality of R' approaches the cardinality of R (2^n), the simulation model approaches a fully calibrated relation:'='. In other words, the higher the cardinality of R', the closer it the objects are to a fully calibrated relation.

Invariance:

One of the important concepts of representations is the property of invariance, especially when they are used to measure differences. Invariance is property of being constant under a set of transformations. Invariant properties that satisfy these concepts play an important role in understanding the underlying importance of the system. A good representation is invariant to data measurement errors, input errors, and randomness (or stochasticity).

Further, until now the relation between calibration parameter set P and representation R was not explored. It is important to only expose parameters that significantly affect the representations. It is captured in the consequent re-definition of calibration.

Calibration Definition 4

Definition 2.1: Redefining the calibration definition using partial representation set, S is partially calibrated or $S \approx F$, iff.

$$\exists \overline{P}.\left(R'_{X',S} - R'_{X',F}\right) < \delta \ \forall I \mid R' \subset R, X = X_s \cap X_F, X \neq \{\ \}, S\left(P, \hat{I}\right), F\left(I\right),$$

where, $\overline{P} = P - P'$ or $P \setminus P'$ and $P' = \left\{ p \in P : \frac{\partial R'_{x,s}}{\partial p} < \alpha \right\}$,

δ is the calibration threshold, and

α is the invariance threshold.

First, the partial calibration relationship is based on partial representation set R'; therefore, no inference can be made of the elements not included from the power set, which is the difference set: $R \setminus R'$.

In definition 2.1, a special condition, $\frac{\partial R'_{x,s}}{\partial p} < \alpha$, is applied to remove the calibration parameters that representation is invariant under changes in values of the calibration parameters. The invariance threshold α is useful in classifying the parameters for invariance condition. In this way the calibration is constrained to only the parameters that significantly affect the representation. This way the degree of freedom is lowered. Similarly, the invariance of representations under data measurement errors, input errors, and randomness need to be small.

Definition 2.2:
$$\left\{ R' : \frac{\partial R'_{x,s}}{\partial(\hat{I} - I)} < \beta \,\&\, \frac{\partial R'_{x,s}}{\partial(\hat{x} - x)} < \gamma, \text{where } x \in X' \right\}$$
$$z : \frac{\partial R'_{x,s}}{\partial(z)} < \lambda, \text{where z is the number of random seeds}$$

Until now the representation R has been treated as an abstract set, but the actual operation of measuring the difference between representations of the objects has not been defined.

Distance

Definition 2.3: A dissimilarity space is a pair (Y, d), where Y is the set and d is a distance function $d : Y \times Y \to \mathbb{R}_+^0$, and $d(y_i, y_j)$ *is* the distance between objects $y_i, y_j \in Y$.

Definition 2.4: The distance between Representation sets is then defined as $D(R_{X,S}, R_{X,F}) = \sum d(r_S, r_F) \forall r \in R_X$

In other words, the dissimilarity between representation sets is a cumulative dissimilarity between elements of the set. If $x \in X$ is defined in domain of real-numbers $\mathbb{R}$, then the representation set R, which is a power set of X, can be defined in $\mathbb{R}^n$ domain (n is the cardinality of set X)

One of the possible solutions to the problem of measuring the difference of two representations can be reduced to measuring the difference in two point sets in n-dimensional Euclidean space (see figure 2). In this second level of representation, the object representations are represented in dissimilarity space. Hence the differences are measured in such a metric or non-metric space.

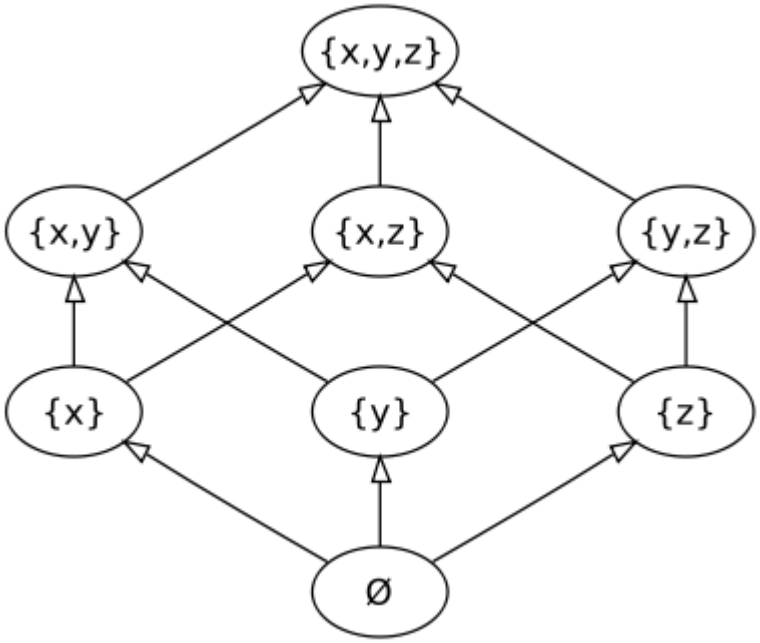

Figure 4.2 A 3-dimensional view of a power set of 3 elements.

Calibration Definition 5

Definition 2.5: Redefining the calibration definition in dissimilarity space, S is partially calibrated or $S \approx F$, iff

$$\exists \overline{P}.\, D\left(R'_{X',S}, R'_{X',F}\right) < \delta \;\; \forall I \mid R' \subset R, X = X_s \cap X_F, X \neq \{\,\}, S\left(P, \hat{I}\right), F(I)$$

Finally, the invariance conditions defined in definitions 2.1 and 2.2 still apply.

$$\overline{P} = P - P' \text{ or } P \setminus P' \text{ and } P' = \left\{ p \in P : \frac{\partial R'_{x,s}}{\partial p} < \alpha \right\},$$

$$\left\{ R' : \frac{\partial R'_{x,s}}{\partial (\hat{I} - I)} < \beta \wedge \frac{\partial R'_{x,s}}{\partial (\hat{x} - x)} < \gamma, \text{where } x \in X' \right\}$$

$$z : \frac{\partial R'_{x,s}}{\partial (z)} < \lambda, \text{where z is the number of random seeds}$$

4.3.2 | FROM CALIBRATION DEFINITION TO PROCEDURE

The calibration definition presented is a formalization of the essence of a calibrated object. However a calibration procedure is different in that it tries to calibrate a model, such that it satisfies the calibration definition. Since it is not possible to test the function for all possible inputs of I, the calibration procedure (or objective) for a simulation model is simplified and changed to two individual steps: estimation and validation.

Estimation:

Find $\overline{P}_c$ such that
$D\left(R'_{X',S}, R'_{X',F}\right) < \delta$ for a given $I_h \neq \{\} \mid R' \subset R, X = X_s \cap X_F, X \neq \{\,\}, S\left(P, \hat{I}\right), F(I)$. The invariance conditions defined in definitions 2.1 and 2.2 still apply.

Validation Definition:

If $D\left(R'_{X',S}, R'_{X',F}\right) < \delta$
for a given $I_k \neq I_h \wedge I_k \neq \{\,\} \mid \overline{P}_c,\; R' \subset R, X = X_s \cap X_F, X \neq \{\,\}, S\left(P, \hat{I}\right), F(I)$

In the first step, the calibration parameter values ($\overline{P}_c$) are estimated for a given input: $I_h \neq \{\}$. In the second step, the simulation model is validated for an input:

$I_k \neq I_h \wedge I_k \neq \{\ \}$. This necessary simplification is based on the assumption that validation is a partial fulfillment of calibration objective.

Mathematically, it is assumed that the dissimilarity measure is invariant of variation in input for a given calibrated parameter values: $\overline{P}_c$. This invariance property again plays an important role in solvability of calibration.

$$\frac{\partial D\left(R'_{X',S}, R'_{X',F}\right)}{\partial\left(I\right)} < \omega \text{ for a given estimated parameter solution (or instance)} : \overline{P}_c$$

In other words, this assumption is necessary to deem the model as calibrated according to the calibration definition. Finally, the $\overline{P}$ calibration set can be represented in a different search space such as binary, gray-coded, discrete, and others. This final representation has much literature in many fields, and is thus not the primary interest of the paper.

4.4 | SUMMARY

In summary, a generic formulation of calibration was presented in this chapter. The generic formulation was based on three distinct levels of representation. Each levels of representation results in certain loss of information, but such representations are nevertheless necessary to solve the complex calibration problem. The generic formulation of calibration definition and accompanying procedures provided a deeper understanding of the nature of the problem.

Representation and invariants were shown to form an important part of the calibration definition. Calibration objective is defined over three levels of representation: traffic, dissimilarity, and search. These three levels of representation succinctly

encompass all of the currently used calibration procedures, while presenting a new generic methodology that improves the quality of calibration by utilizing several traffic flow processes. The representations also provide insight into the flow of information in the calibration process.

The concept of invariance was shown to play an important role in understanding the inner-workings of complex systems. The property of invariance of representation (traffic and dissimilarity) is necessary in accurately solving the calibration objective. The invariance concept improves the calibration process by developing traffic representations that are robust to input or measurement errors and reducing the calibration parameter set to the most important parameters. In the following chapters, a deeper look at each level of representation is presented.

5 | Traffic Representation in Calibration

"Outside of traffic, there is nothing that has held this country back as much as committees."

-Rogers,Will

5.1 | INTRODUCTION

Since the simulation model and the field scenario cannot be compared directly, traffic flow variables are used to represent the simulation model during the calibration process. The assumption being that by reducing the difference between traffic representations, the difference between the simulation and the field objects is simultaneously reduced. Hence, traffic representations are an important part of calibration of simulation models (see figure 5.1). This chapter concerns itself with level-I representation of the simulation and field.

The traffic representations used in calibration methodologies have a great impact on traffic flow aspects of microsimulation models. A calibration procedure based on reducing the difference between a subset of traffic representations does not account for flow process that exist beyond such representations (see definition 1.4). Calibration of microsimulation model involves tweaking a wide variety of parameters. It is important to only expose calibration parameters that significantly affect the traffic variables or representations (see definition 2.1). On the contrary, if there is a parameter that

significantly affects multiple traffic variables, it is important to constraint such a parameter so that it doesn't severely affect the variables that are not being used in the calibration process.

In this chapter, various traffic flow representations are studied by evaluating their suitability for use in a microsimulation calibration procedure. Since there are a vast number of traffic representations, study of all such variables is beyond the scope of this research. Only the most elementary and significant variables are addressed in this research. In addition, the discussions provided in this chapter address the importance of level I representation in terms of traffic engineering and traffic flow processes. Therefore, the discussions about the importance of traffic representations are presented in a non-mathematical fashion, unlike in the previous chapter. The traffic representations ($r \in R$) can be categorized into aggregate-data and disaggregate-data based representations.

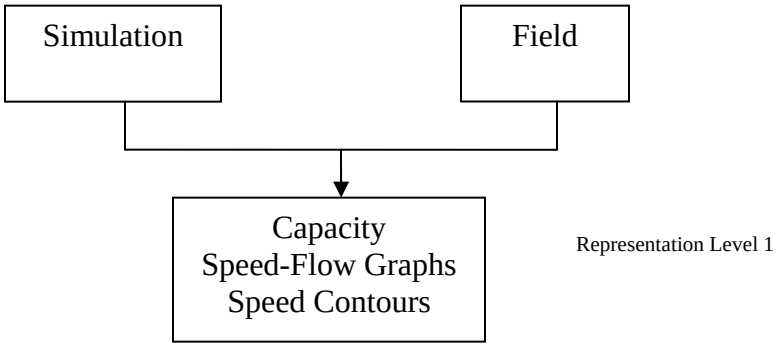

Figure 5.1 Traffic flow representation of simulation and field

5.2 | AGGREGATE DATA BASED REPRESENTATION

This section defines and analyzes different aggregate data-based representations.

5.2.1 | CAPACITY

Capacity is one of the most important variables in traffic flow theory. It is an important variable that is often used by both researchers and practitioners. It is important to study the applicability and suitability of capacity in calibration. As it can be seen in the literature review presented in the previous chapter, capacity is considered as one of the primary variables of interest, and often part of the first level of calibration. As it will be seen through the next few sections that there are some unanswered questions about how capacity should be used in the calibration process. To gain a better understanding, a state-of-the-art literature review on capacity is presented. Discussions have also been presented on tradeoffs of using capacity in microsimulation calibration.

The capacity estimation procedures are important, because calibration of the driver behavior parameters is usually performed by minimizing the difference in simulated and field capacity values. Hence, it is important that the capacity estimation procedures in simulation are consistent with field estimation procedures. However, the problem stems from the different interpretations of HCM's definition of capacity. For example, FHWA microsimulation guidelines for simulation recommend procedures, which are based on the assumption that capacity is the queue discharge flow rate. However, the field estimation procedures are usually based on speed-flow relationships, or the maximum flow rate observed at the facility. Different views exist on definition of capacity, for example, whether capacity is the queue discharge flow rate (QDF) or the pre-queue flow rate (PQF). The standard source of reference on traffic facility operations is the Highway Capacity Manual (HCM), which defines freeway capacity as follows:

> *"The capacity of a facility is the maximum hourly rate at which persons or vehicles reasonably can be expected to traverse a point or a uniform section of a lane or*

roadway during a given time period under prevailing roadway, traffic, and control conditions."

This definition of capacity raises few other questions, which need to be answered for application in simulation and field data; however, further clarifications have been provided in HCM in continuation with the definition (pg.2-2). The first clarification states that capacity is not the absolute maximum flow rate observed at a facility, and that reasonable expectancy is an important part of defining capacity. From the definition it can be inferred that it the value of capacity is selected from a distribution of maximum flow rates observed at a facility over several days. However, there is no guidance provided for selecting a value representing capacity from the distribution. The various possibilities include mean, median, mode, 85th percentile, etc. The concept of reproducibility of capacity is also introduced in this definition.

A slightly different definition is provided for freeway facilities (pg. 13-2). This alternate definition of capacity introduces the concept of sustainability in capacity. The definition also transforms maximum hourly flow rate to 15-min flow rate expressed in cars per hour lane, which introduces passenger car equivalents. But, HCM accepts vehicles-per-hour as an acceptable measure of capacity. The definition also assumes no influence from downstream traffic operations. The definition does not provide guidance on amount of time the flows need to be sustained. It is not clear if maximum sustained 15-min flow rate refers to which of the following:

1. The maximum sustained count-period (i.e., x minutes, x is less than 15 minutes) flow rate over a period of 15 minutes. For instance, capacity is maximum 5 minute flow sustained over a period of 15 minutes.

2. The maximum sustained 15-min flow rate sustained over a period of time. For instance, capacity is maximum 15-min flow sustained for 60 minutes.

In summary, some of the important concepts, in HCM's definition of capacity, which need to be incorporated into capacity estimation procedures, include the following:

1. Reasonable expectancy
2. Reproducibility
3. Sustainability

The Highway Capacity Manual's (HCM) capacity definitions and its various clarifications (HCM, 2000), pg. 2-2, 13-2) could be interpreted in several ways, even though HCM clearly notes some of the important concepts underlying the definition of capacity like reasonable expectancy, reproducibility, and sustainability. All these concepts cannot be easily captured through a single numerical value of capacity. These concepts are important in order to implement the capacity calibration process in the calibration procedure. Capacity is an important parameter that defines a facility and its operational capability. However, defining capacity as a single numerical value results in much loss of information of concepts. A distribution of capacity values has more information than a single numerical value. There have been recent studies which address the stochastic nature of capacity (Brilon et al., 2007). If capacity calibration process is based on a single numerical value, matching the means of capacity distribution does not necessarily match the other important properties of a distribution; for example, spread, shape, and median.

This concept can be extended further to include other traffic parameters like speed. For instance, is it important to match speed at which capacity values are

observed? There are many studies that demonstrate that there are two different types of maximum flows observed in the field, one is queue discharge flow (QDF) and the other is pre-queue flow (PQF) (Banks, 1991). Each of these flows is sustained for a different amount of time. With-respect-to calibration, is QDF or PQF more important to be matched? The author suggests the matching of both values. In summary, it is important to maximize the information used during the calibration process.

5.2.2 | SPEED-FLOW GRAPHS

Speed-flow graphs have been used to describe operational capabilities of highways, and in developing macroscopic relationships for freeways. It is relatively easy to collect speed, flow, and occupancy information due to wide use of instrumentation on freeways. Speed-flow graphs contain much information as described below. It is the intent of this research to use such information available in speed-flow graphs. This methodology is based on matching speed-flow graphs obtained from simulation and field. The HCM (2000) divides speed-flow graphs into three regions: free-flow, congested, and queue discharge. The HCM concepts of capacity are well represented through speed-flow graphs. As a result, capacity information is available in a speed-flow graph. QDF and PQF information can also be derived from speed-flow graphs. In addition, speed-flow graphs also provide information about free-flow and congested regions, which is not present in a single numerical value or distribution of capacities. d

A calibration procedure based on speed-flow graphs, which provides information about all the three regions: free-flow, congested, and queue discharge could replicate the whole range of traffic behavior and not just peak period. One could also just use a

portion of the speed-flow graph instead of the entire graph for calibration such as the queue discharge region.

It is important to recognize that speed-flow graphs lack information about time. However, intensity of points in speed-flow graphs contains partial frequency information. Hence, the concept of sustainability is only partially captured in a speed-flow graph. An alternate graph, maximum flow sustained time graph, based on the concept of maximum flow sustained over different periods of time provides a better picture of the flow sustainability concept in capacity definition. However, due to the stochastic nature of both real and simulated traffic flows, it would not be possible to exactly replicate a volume-over-time curve. Despite the fact that fluctuations and breakdowns will not occur at exactly the same time in the real-world as in simulation, the simulation model is nevertheless correctly calibrated.

The concept of replicating field speed-flow graphs has been used in a number of previous studies. Wiedemann (1974, 1991) used speed-flow graphs to demonstrate closeness of field and simulation model. Fellendorf and Vortisch (2001) demonstrated the ability of a simulation model to replicate speed-flow graphs from real-world freeways. However, there was no literature found that used speed-flow graphs in the microsimulation calibration process. Ngoduy et al. (2004) used an objective function based on speed and flow, which is mathematically close to replicating speed-flow graphs, for calibration of a macroscopic simulation model.

In developing a speed-flow graph, the importance of location for collecting speed-flow graphs has been demonstrated by May (1990). Data can be collected over different locations and multiple days and combined to show a complete speed-flow graph. In

terms of field data, speed and flow information for the section under consideration can be collected for instrumented highways over many locations and different days. The simulation data can be collected by placing detectors at exactly the same locations as detectors in the field. Sample speed-flow graphs developed in the microsimulation model are presented in figure 5.2.

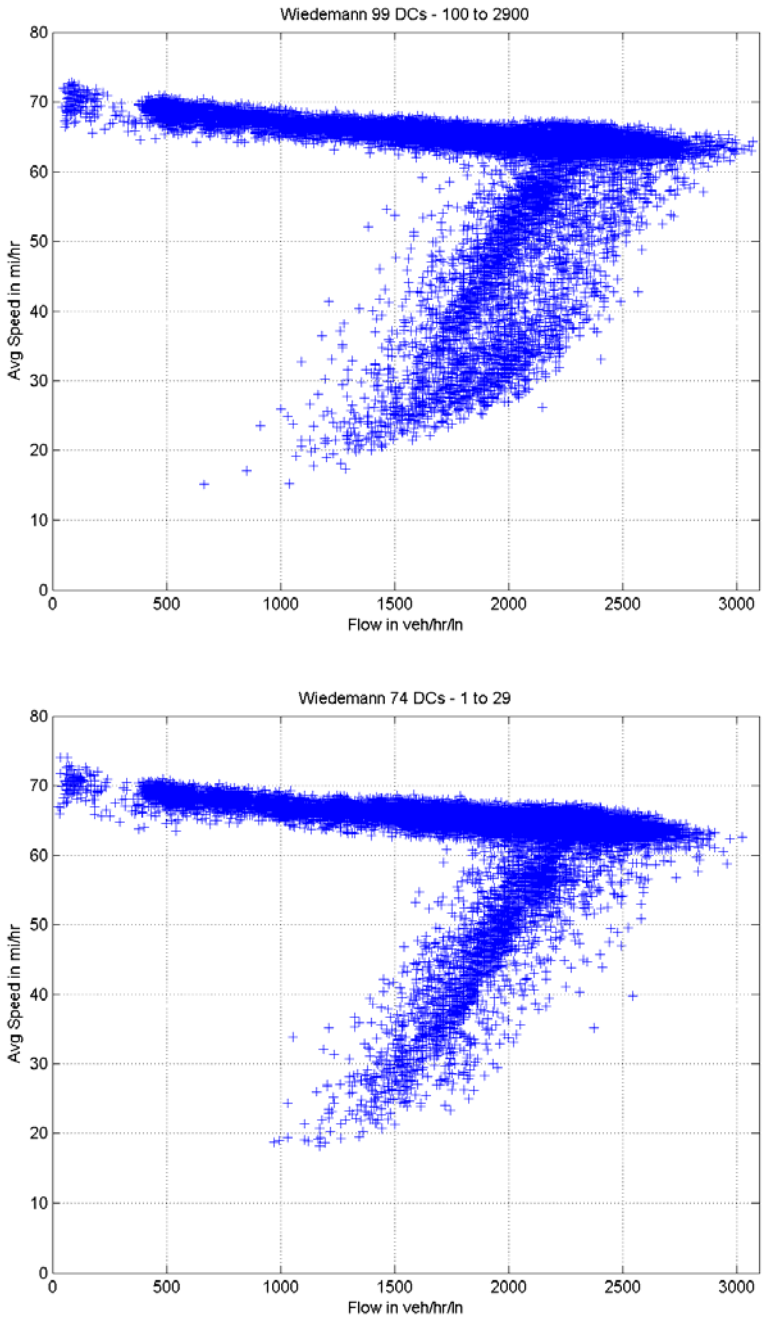

Figure 5.2 Typical VISSIM generated speed-flow graphs

5.2.3 | FLOW-DENSITY, SPEED-DENSITY, AND SPEED-FLOW-DENSITY GRAPHS

In continuation with previous arguments, it can be seen that other relationships that exist between pairs of flow, speed, or density variables can be a valuable source of information. Speed-density or flow-density relationships are similar in nature to speed-

flow graphs. If a calibration procedure is solely based on capacity, there can be resultant changes in calibration parameters that affect the relationships that exist between speed, flow and density. For instance, calibrating a simulation model to achieve a field capacity value might result in different speed-flow graphs for simulation and the field.

This concept can be extended to a three-dimensional speed-flow-density graph, which has information in all three dimensions. An important dimension that is missing in all the relationships between speed, flow, and density is time. Although, partial information of time is available in each of the relationships through intensity (or frequency), it is not complete. Temporal information is important and does relate to the concept of sustainability discussed in the capacity section. To account for time, concept of flow sustained over time is introduced.

One of the important advantages of speed, flow, and density relationships as representations is that they are fairly invariant to errors in input such as OD-data. In cases where acquiring good OD demand data is not possible, these representations are valuable in calibrating the model.

5.2.4 | MAXIMUM SUSTAINED FLOW TIME GRAPHS

Maximum Sustained Flow Time Graphs (or MSFTGs) contain information about maximum sustained flows over varying time periods, and over many days (or runs). Better and more complete information is obtained when MSFTGs are developed over many days or simulation runs. MSFTGs, a new concept developed in this research, can be valuable in describing the concept of sustainability in capacity. A maximum sustained flow time graph is based on a typical min-max function. The graph is built by computing the maximum of the minimum flow that was sustained for a period of time during the

data collection project. By methodology, MSFTG is a non-increasing function over time. A sample example of maximum sustained flow speed time graph is provided in figure 5.3.

However, it can be seen that maximum sustained flows vary by day (or runs) and demand patterns. Also, some empirical evidence exists that higher flows may be sustained for greater amounts of time by metering demand from the ramp (Banks, 1991). It can be seen that MSTFGs are not invariant to errors in input such as OD data. Therefore, calibrating a model with such representation will result in incorrect calibration, since the error propagates from input to the representation. However if good O-D data is available, this method can be used for calibration of the microsimulation model. Since, maximum flow sustained time graphs are dependent on both supply (capacity or speed-flow-density) and demand (O-D).

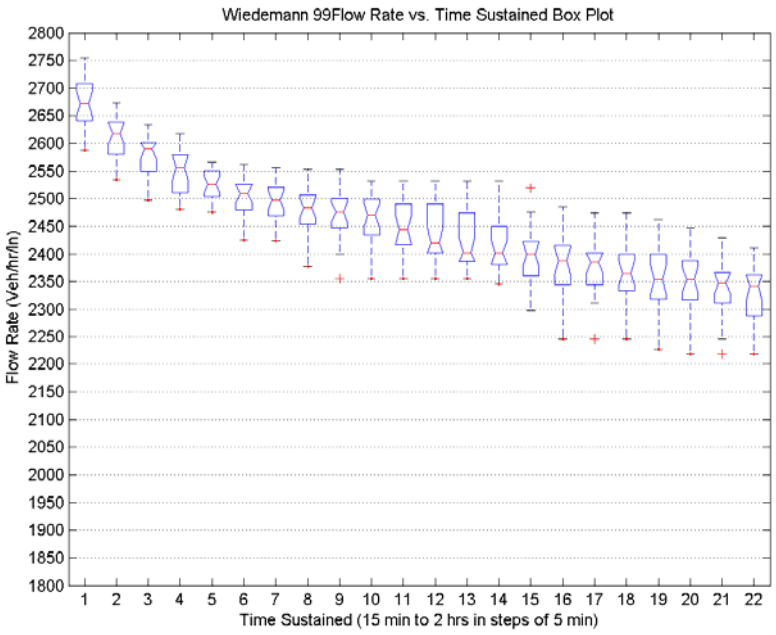

Figure 5.3 Maximum Flow Sustained Time Graph generated using VISSIM (MSFTG)

5.2.5 | SPEED, FLOW, OR DENSITY CONTOURS

Speed, flow, or density contours have been traditionally used in qualitative calibration of microsimulation model (e.g. Gomes et al., 2004). These contour graphs have a wealth of information. Information that can be obtained from contours includes extent (space and time) of congestion, location of bottlenecks, speed, flow, or density information, extent of queues, etc. This kind of information can be valuable in calibration of microsimulation models. Since these contour graphs are a result of supply and demand, logically, there are to be calibrated iteratively with supply and demand parameters, because supply and demand are in a dynamic equilibrium. It is important to only minimally alter the global supply and demand parameters, but concentrate on altering local link specific parameters for calibration. The representation is not invariant to errors in input. So unless good OD data is available, using this representation for calibration will result in erroneous results.

5.2.6 | HISTOGRAMS: FLOW, SPEED, HEADWAY, AND TRAVEL TIME

Histograms also form an important part of the aggregate data based calibration procedures in microsimulation models. Histograms of speed, headway, and travel time have traditionally been used for calibration of microsimulation models. However, travel time histograms can probably be argued to be more important, because several of the measures of performance of traffic flow systems are based on travel time data. Histograms are also fairly invariant to the small errors in input. However, such representations can only provide information about a single traffic variable, but not of relationships that exist between multiple traffic variables. Therefore, histograms are form good representations of traffic variables, but not relationships.

5.2.7 | TIME SERIES: VOLUME, SPEED, AND DENSITY

There have been many studies that adopted a time-series based calibration procedures. Most of these methodologies assumed that good O-D data was available prior to such calibration procedure. Such assumptions are usually not valid in the real-world. Some researchers, e.g. Toledo et al. (2004), suggest using an iterative calibration methodology to simultaneously estimate O-D flows and calibration of driver behavior and route choice parameters, but such procedures can be extensive and time consuming. The maximum sustained flow time graphs are similar in nature to volume time-series, and in that both assume, in most cases, O-D flows as a given.

5.3 | DISAGGREGATE DATA BASED CALIBRATION

This section presents analysis of some of the prominent representations based on disaggregate data.

5.3.1 | VEHICLE TRAJECTORIES

Vehicle trajectories provide detailed information about the car following process, which is central to microsimulation models. Vehicle trajectories can be used to evaluate the stability of car following models. Some researchers have used vehicle trajectories for calibration by minimizing the difference in gaps (or headways) in field and simulated trajectories. Traditionally, in such research, the lead vehicle's trajectory in the field is replicated in the simulation by external control. Thereafter, the car following model parameters are calibrated to minimize the difference in gaps. The microscopic vehicle trajectory data is obtained either from a freeway or a test track. Vehicle trajectories can be valuable in estimating calibration parameters using controlled experiments.

However, calibration methods that are purely based on replicating space-time trajectories have several few shortcomings. First, the microscopic vehicle trajectory data cannot be reasonably be obtained for a range of traffic conditions. Second, test track data usually models a limited number of drivers, thereby only modeling a limited variety of driver behavior. Third, many of the microsimulation models are developed to capture average conditions; modeling specific driver behavior (e.g. replicating vehicle trajectories over time) is beyond the scope of many microsimulation models. Fourth, since many of the microsimulation models are stochastic in nature. A same lead vehicle trajectory might produce a different platoon behavior depending on the random seed.

5.3.2 | RELATIVE DISTANCE VS. RELATIVE VELOCITY

Relative distance vs. relative velocity (dx-dv) graph is also based on microscopic traffic data. The dx-dv graphs were among the popular calibration methodologies used in microsimulation calibration. The dx-dv graphs describe a typical goal-seeking behavior in many car following models. The following car always tries to maintain a safe distance from the lead vehicle, while trying to reduce speed differences. The dx-dv graphs also show a typical oscillation behavior in following condition. Dx-dv graphs form the core of many psycho-physical models like Wiedemann (1974 and 1999), Michaels (1963), Todosiev(1963), etc. In psycho-physical models, the thresholds are mainly modeled in the dx-dv and dv-da phase planes. Therefore, such information can be valuable in calibrating driver behavior thresholds in psycho-physical car following models. The calibration of microsimulation models using dx-dv graphs also suffers from some of the issues described in the previous subsection. However, aggregated threshold information (e,g. action point density) from dx-dv graphs can be a valuable source of information in

calibration. An aggregated behavior can provides insights into average following variation, speed oscillation, minimum following distances, etc. This information is especially valuable in a psycho-physical car following models.

5.4 | SUMMARY

In summary, there are various traffic representations possible for application in microsimulation. The traffic representations presented in this chapter are argued to be of higher fidelity. The representations in the state-of-the-art are based on low fidelity representation, which are susceptible to significant error. Representation of simulation and field based on a single numerical value results in a significant loss of information. The traffic representations presented here contain more information that can help better calibrate the simulation models. Of the representations presented in this section, speed-flow, flow-occupancy, speed-flow-occupancy, and dx-dv graphs are more promising. Some of the representations e.g. speed/flow/density contours, maximum flow sustained time graphs are also promising, but need good OD estimates to be beneficial. In addition, there is a need to quantify the differences in these representations. Traditional parametric or non-parametric statistical methods are not applicable in some of these scenarios. Research was conducted to develop robust measures of degree of closeness for application in calibration. The research on developing such measures is presented in the next chapter.

6 | Dissimilarity Representation in Calibration

"To understand is to perceive patterns"

- Berlin, Isaiah

6.1 | INTRODUCTION

Based on discussions presented in the previous chapter, it can be seen that there are several ways to calibrate a simulation model. Concepts based on relationships between flow, speed, density/occupancy, and time were argued to more information about the traffic flow processes in the model and the field during calibration. It is possible to develop several objectives, each of which is tailored to the nature of the variable, for calibration. But, it is the intent of this study to develop objectives that are generic in nature, so they find application in several areas and require minimal adjustment. In addition, currently there are few existing quantifiable methods available to calibrate simulation models based on new concepts introduced in the previous chapter. After an extensive literature review on methods and tools, it was identified that traditional parametric statistical methods have limited application in calibrating simulation models based on relationships between flow, speed, density, and time. It was also identified that non-parametric statistical methods can only be applied for frequency based distributions;

although, no priori distribution is assumed in such methods. These non-parametric statistical methods can be applied to histograms (speed, headway, flow distributions), but have limited or no application in 2D or 3D graphs, contours, or time-series. However, there are certain statistical and structural pattern recognition methods that are quite well suited to solve such problems.

Traditionally, calibration of simulation models using speed-flow graphs and contours was based on qualitative matching by human-eye matching. In such cases, the researcher usually looks at the graphs from the simulation and the field, and decides how closely the graphs match each other. The human-eye matching technique, although very sophisticated, cannot discern the extent of differences in some close situation. In other words, unless if the differences between two alternatives are significant, the researcher has no way of saying which one is closer to the field graph. This directly impacts the calibration process, since it is not automatable; i.e., the researcher has to be involved in each step of the calibration making decisions about the closeness of the graph, some of which might be wrong.

There are similar problems in other scientific fields where measures of closeness of objects, sets, or data are needed. Pattern recognition is a science with a vast amount of literature that deals with measures of similarity (closeness) or dissimilarity. Pattern recognition has found applications in a variety of fields including database management, digital recognition, data mining, etc. However, pattern recognition has found minimal application in the field of microsimulation calibration. The methods and tools provided by pattern recognition can be invaluable in this field of calibration. In the following section, a general introduction to pattern recognition is presented, followed by definition

of a generic calibration objective. Thereafter, comprehensive research on applications of pattern recognition based dissimilarity measures in calibration is presented.

6.2 | PATTERN RECOGNITION

Pattern recognition is as much a science as it is an art. The science and art of pattern recognition is a source of solution to many a problems in the scientific field. It has made possible some of the most sophisticated production systems to autonomous robots. Human behavior, some argue, is based on recognizing patterns. Humans store a priori information based on perceived patterns of shapes, sounds, smells, behavior, characters, images, events, and data. The science of transforming such ability to recognize and classify objects to help in machine learning is called pattern recognition. Examples of application of patter recognition in the scientific field include automatic sorting of fruit (by quality) in super-fast production lines, modeling learning behavior in autonomous robots, scene analysis, face recognition, biometric security systems, etc.

The concepts of pattern recognition can be borrowed into calibration, almost as if it was the most natural way to solve the calibration problem. For example, one of the fundamental questions in pattern recognition is how to tell the difference between objects. It is inherently an easier task to tell if two objects are different than to say they are the same. Pekalska and Duin (2005) suggest that dissimilarity is more fundamental than similarity, because "…only when the difference has been observed and characterized, similarity starts to play a role." Drawing a correlation, the calibration objective, which is to reduce the difference between two objects (simulation and field), can be stated in pattern recognition terms as reducing the dissimilarity between simulation and field.

A dissimilarity representation provides a value to measure the degree of commonality between objects. For implementation of the calibration objective, there is a need to develop representation at two levels. The first level of representation captures the objects; the second level captures the variables. For instance, in figure 6.1, the objects are represented at level-1 using capacity, speed-flow, etc. The level-2 representation relates to representation of the variables as points, point sets, areas, volumes, distributions, etc. A detailed formulation of the process is provided in the next section by defining a generic calibration objective based on such a concept.

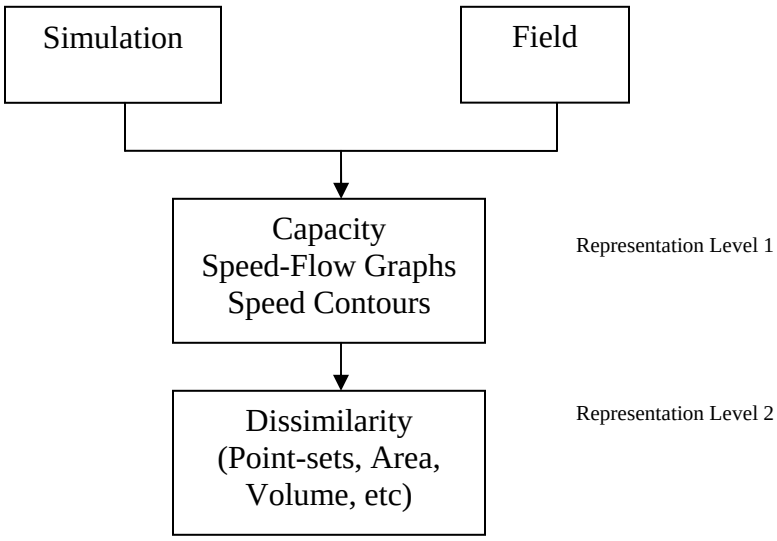

Figure 6.1 Representations in calibration objective problem definition

6.3 | LITERATURE REVIEW ON DISSIMILARITY MEASURES

Dissimilarity measures are relative measures of dissimilarity; the smaller the dissimilarity measure, the more similar the objects. The dissimilarity measures are not always defined for objects, rather for features of the object. This is same as representation level 1 discussed in previous section. These features of objects are also known as variables or

attributes. Dissimilarity measures can be defined for a variety of feature types. Examples of features include points, set of points, images, symbols, text, shapes, etc. There are different dissimilarity measures available depending on feature type. Pekalska and Duin (2005) define five different types of features.

1. Binary
2. Categorical
3. Quantitative
4. Ordinal
5. Symbolic or nominal

There are a variety of measures available for each of the feature types. But, much of the calibration objectives are related to either quantitative or binary data. A brief survey of dissimilarity measures for different types of data is provided in the following section. Much of the literature presented in this section is based on Pekalska and Duin (2005), Duda and Hart(1973), and Fukunaga (2003).

6.3.1 | DISSIMILARITY MEASURES FOR QUANTITATIVE DATA

There are many dissimilarity measures available for quantitative data. The common statistical error measures are also dissimilarity measures. Some of the common statistical error measures include the following:

1. Correlation coefficient
2. Mean squared error or Root mean squared error
3. Percent mean squared error
4. Mean absolute error
5. Root relative squared error

6. Relative absolute error

Mean squared error (MSE), root mean squared error (RMSE), and percent mean squared error are some of the most commonly used error measurement techniques in the field of traffic microsimulation. And if more than one variable is involved, the errors are accrued over several variables. But, there are some other dissimilarity measures available for quantitative data. Some of the popular measures are presented below.

1. Euclidean distance or weighted Euclidean distance
2. Taxicab metric, city block Distance or Manhattan distance
3. Max norm or Chebychevdistance
4. L_p distance or Minkowski distance
5. Canberra Distance
6. Correlation-based

Minkowsky distance is a generic form of Manhattan, Euclidean, and Chebychev distance. All of the distance measures are for point-to-point distances. For a more comprehensive list of dissimilarity measures for quantitative data, the reader is directed to Pekalska and Duin (2005)

6.3.2 | DISSIMILARITY MEASURES FOR BINARY, BOOLEAN OR DICHOTOMOUS DATA

Binary, Boolean, or dichotomous data represents variables that only accept two distinct values. Many of the dissimilarity measures on dichotomous data are based on four different counters:

1. a = the number of properties common to both objects (**i**, **j**)
2. b = the number of properties which **i** has but **j** lacks
3. c = the number of properties which **j** has but **i** lacks

4. d = the number of properties that both objects lack

Most of the similarity measures for dichotomous data are based on these four basic counters. Some of the similarity measures include the following (Pekalska and Duin, 2005):

1. Russel and Rao: $a/(a+b+c+d)$
2. Simple matching: $(a+d)/(a+b+c+d)$
3. Binary Euclidean: $(b+c)^{1/2}$
4. Hamming distance: $b+c$
5. Variance: $(b+c)/4(a+b+c+d)$
6. Binary Pattern Difference: $(bc)/(a+b+c+d)^2$

6.3.3 | DISSIMILARITY MEASURES FOR POPULATIONS

There are a number of parametric and non-parametric methods that are available for measuring dissimilarity between populations. If mean vectors are used to represent populations, then dissimilarity measures for quantitative data can be used. If population is represented as a probability density function (pdf), there are measures available to compute dissimilarity of two distributions. Some of the common dissimilarity measures are

1. Kolmogrov metric
2. Kolmogrov-Smirnov test
3. Mahalanobis distance
4. Chi-square test
5. t-test

6.3.4 | DISSIMILARITY MEASURES FOR SEQUENCES

Dissimilarity measures for sequences such as the ones based on binary data or finite discrete elements are used in pattern recognition and machine learning. There are many problems that can be formulated in terms of sequences, and hence the dissimilarity measures based on such representation are invaluable. Some of the common dissimilarity measures are listed below. Hamming distance measure is based on counting the number of positions in which the sequences differ. It is one of the simplest measures for measuring dissimilarity of sequences. Fuzzy Hamming Distance measures the cost editing one distance using insertion, deletion, and shift. The operations are used to transform one sequence into another, and costs accrued over the operation are used as a dissimilarity measure. Levenshtein Distance measure is one of the most popular edit distance measures. It is based on costs accrued over operations including insertion, deletion, and substitution. If the sequences are not of equal length, then a normalized version of the distance can be used.

6.3.5 | DISSIMILARITY MEASURES FOR SETS

Dissimilarity measures are possible between two sets of points in space. These measures are valuable in several applications where objects can be represented as points in space. This measure is different from dissimilarity measure of quantitative data. For quantitative data, each of the points is a measure of a feature belonging to the object; whereas for sets, sets of points are defined as a feature. Hausdorff distance and its several variations are defined for measuring dissimilarity between point sets. The different dissimilarity measures for point sets are provided below.

Hausdorff distance is defined as the maximum of directed Hausdorff distances between two sets A and B. The directed Hausdorff distance, d_H A->B = $\max_a\{\min_b$ d(a,b)}, is the maximum of collection of minimum distances from each point a in A to b in B. Variants of Hausdorff distance are generalizations of the Hausdorff distances that are more robust against outliners and noise. (Pekalska and Duin, 2005). Modified Hausdorff distance is minor variation of Hausdorff distance wherein a average of minimum is applied instead of maximum of minimum.

6.3.6 | DISSIMILARITY MEASURES FOR IMAGES: TEMPLATE MATCHING

Template matching is a method usually used in the field of scene analysis in pattern recognition, where a template pattern or image is matched to an image closest to itself from a reference set of patterns or images. Template matching utilizes a dissimilarity measure. An image is usually represented as pixel data and the differences in pixel values are measured and accrued over all pixels. The distance between pixel values can be computed by using any of the dissimilarity measures for quantitative data.

6.4 | APPLICATIONS OF DISSIMILARITY MEASURES IN CALIBRATION

In this section various forms of dissimilarity representations are presented for various traffic representations presented in the previous chapter.

6.4.1 | SINGLE NUMERICAL VALUES: $r = \{x\}$ or $\{\bar{x}\}$, OR TIME-SERIES $r = \{x_i, t\}$

Examples: capacity, flow, speed, average travel time etc.

Applicability: single numerical values, mean values, or mean value vectors

If variables are represented as a single numerical value, many standard goodness-of-fit measures may be applied. Some of the dissimilarity measures that can be applied include

many of the statistical measures of error like root mean square error, absolute error, root relative error, etc. But with-respect-to dissimilarity measured based on distance metrics the following can be used:

1. Euclidean distance
2. City block distance
3. Correlation-based distance
4. Any of the L_p distances

In case of time series, the cumulative error of variables over time can be aggregated and represented as dissimilarity measure.

6.4.2 | POPULATION OR DISTRIBUTIONS AND TIME-SERIES $r = \{x_i, f_{x_i}\}$ or $\{x_i, t\}$

Examples: capacity, flow/speed or travel time distributions; flow, speed or density time-series. Applicability: histograms, distributions, time-series

As described earlier, speed and headway distributions are one of the most commonly used calibration methods. Implementations of capacity as a single numerical value can be found in much of the calibration research in the state-of-the-art. After an extensive literature review, applications of calibration based on distribution or population representation of capacity were not found. The dissimilarity measures for populations or distributions are applicable in this case. There are a number of parametric and non-parametric methods that are available for measuring dissimilarity between populations. Some of the dissimilarity measures are listed below.

1. Kolmogrov Metric
2. Kolmogrov-Smirnov test
3. Chi-square test

4. t-test

6.4.3 | N-DIMENSIONAL POINT SETS: $r = \{x_1, x_2 \ldots, x_n\}$

Examples: Speed-flow, flow-density, speed-flow-density graphs.

Applicability: N-dimensional point sets

6.4.3.1 | Point Sets

The dissimilarity representation of speed-flow graphs or other similar graphs can be done in many ways. Much of the discussions provided here is described using speed-flow graphs, but all of the representations presented in this section are equally applicable other graphs of similar nature. If speed-flow graphs are represented as point sets, the dissimilarity measures for point sets can be utilized for measuring the degree of closeness between speed-flow graphs from the simulation and the field. In this case, speed-flow measurements are represented as points in a two-dimensional space. There are three different dissimilarity measures defined as follows.

1. Hausdorff distance
2. Modified Hausdorff distance
3. Variants of Hausdorff distance

The two most popular measures, **Hausdorff distance** and **modified Hausdorff distance**, are presented in this section. But, there are several other Hausdorff variations available. To present mathematical formulation of such measures the following definitions are defined.

A is a set of n_A speed measurements from the simulation, and $a \in A$

B is a set of n_B speed measurements form the field, $b \in B$

$d(a,b)$ is the distance measurement between a and b

Hausdorff Distance, $d_H(A,B)$**,** can be defined as follows:

$d_H(A,B) = \max\{d^{\rightarrow}{}_H(A,B), d^{\rightarrow}{}_H(B,A)\}$, where $d^{\rightarrow}{}_H(A,B)$ is the directed Hausdorff distance defined as, $d^{\rightarrow}{}_H(A,B) = \max_{a\in A} \min_{b\in B} d(a,b)$

Modified Hausdorff Distance, $d_{MH}(A,B)$, can be defined as follows:

$d_{MH}(A,B) = \max\{d^{\rightarrow}{}_{avr}(A,B), d^{\rightarrow}{}_{avr}(B,A)\}$, where $d^{\rightarrow}{}_{MH}(A,B)$ is the directed Hausdorff distance defined as, $d^{\rightarrow}{}_{avr}(A,B) = \frac{1}{n_A}\sum_{a\in A} \min_{b\in B} d(a,b)$.

The distance $d(a,b)$ can be measured in different ways. It can be a Euclidean distance, weighted Euclidean distance, or any of the dissimilarity measures for quantitative data. The concepts presented for dissimilarity measures for speed-flow graphs as point sets, can be extended to cover three dimensional graphs or point sets. The Hausdorff distance defined earlier is still valid in higher dimension. But as the number of dimensions increases, the computational cost increases as well.

6.4.3.2 | Symmetric Difference

If speed-flow graphs are represented as binary images, gray-level, or intensity based images, dissimilarity measures developed using symmetric difference or template matching. Symmetric difference of sets, A and B, is defined as $(A-B)\cup(B-A)$. But, there is a certain loss of information due to the discretization process, due to conversion of vector information to raster information. The continuous speed-flow measurements in a two-dimensional space are transformed into discrete cells, also known as pixels in images. The discretization can be at binary level, where each pixel either represents

existence of data point (1) or no data point (0). The discretization can also be at gray-level or an intensity based measure, where the value of pixel is proportional or equal to the number of data points within the cell or pixel. The image can also be normalized, smoothened, or passed through various transformations in order to make it more representative of the characteristics of the graph. The discretization process, although resulting in some loss of information, possesses some advantages. The discretization smoothens out the data set reducing the "noise" in the traffic data measurement process. Since simulation models are stochastic in nature, there is a lot of noise inherent in the measurement.

If speed-flow graphs are defined as an area, then the measure of symmetric difference can be used as a dissimilarity measure. The mathematical dissimilarity for two graphs is then formulated as follows:

$D(.)$ is the discretization function that converts vector information to raster (or pixel) information.

$D(A) = A(i, j)$ is the speed-flow graph from the simulation obtained by transformation

$D(B) = B(i, j)$ is the speed-flow graph from the field

The dissimilarity measure $d_T\left(A(i, j), B(i, j)\right)$ is defined as follows (Duda and Hart, 1973):

$$d_T\left(A(i, j), B(i, j)\right) = \sum_i \sum_j d\left(a(i, j), b(i, j)\right))$$

Again, various dissimilarity measures can be used for $d(a,b)$. But if Euclidean distance is used, the formulation can then be rewritten as.

$$d_{TE}\left(A(i, j), B(i, j)\right) = \left\{ \sum_i \sum_j \left[a(i, j) - b(i, j)\right]^2 \right\}^{1/2}$$

The concepts of dissimilarity measures for speed-flow graphs as symmetric difference can also be extended to cover three dimensional graphs or point sets. The dissimilarity measure for higher dimension can be rewritten as follows:

$$d_T\left(A(i,\, j,...k), B(i,\, j,...k)\right) = \sum_i \sum_j ... \sum_k d\left(a(i,\, j,...k), b(i,\, j,...k)\right)$$

One recognizable problem with such a definition is that as the number of dimensions increase, the amount of computations require significantly increase, resulting in higher computational cost, but is much lower than cost associated with Hausdoff distance. Dissimilarity measures for speed/flow/density contours can be defined similarly to measures presented in section dissimilarity measures for speed-flow graphs as symmetric difference. The contours can be represented over n-levels and the measures previously proposed can be utilized. In terms of implementation, the levels in the contour are represented in incremental values.

6.4.3.3 | Modified Symmetric Difference

The field speed-flow graphs obtained are usually not complete; for that matter, the speed-flow graphs obtained from simulation are also not complete. Defining dissimilarity measures for partial point sets has not been found in the literature. Since in calibration, the simulation is the one being tweaked. It is logically better to consider differences with-respect-to the field data set. A logical explanation for this is that, to be the best of our knowledge, the information coming from the field is reality; it is the simulation model that needs to be tweaked. A symmetric difference method is not valid for partial point sets; because in such a method, both point sets are considered equally important. Which is not clearly the case with speed-flow graphs, or methods based on calibration. Similar to symmetric difference, this method can be extended to higher dimensions and

also possesses similar advantages as symmetric difference. The dissimilarity measured for partial point sets is defined as follows:

$d(A,B) = B - A \cap B$

6.4.4 | TWO DIMENSIONAL REPRESENTATION: $r = \{x_1, x_2\}$

This representation is similar to binary, gray-level, or intensity images; except that such images are transformed and expressed as a sequence (or vector), rather than a matrix. For instance, let's assume a 4-by-4mage of 16pixels; this can be transformed to a 16 element row or column vector by concatenating the rows or columns. (Figure 6.2)

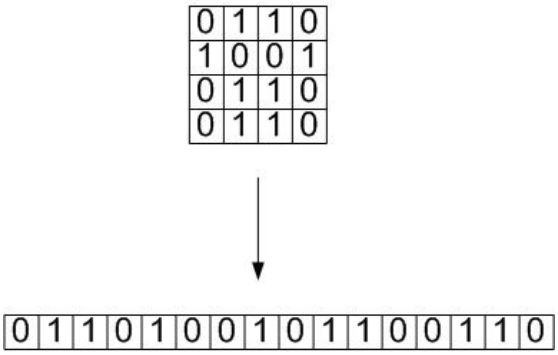

Figure 6.2 Row concatenation representation of a binary image matrix

This process can transform matrix image data to sequences, and dissimilarity measures based on sequences can be used in measuring the degree of closeness.

Some of the measures that can be used are:

1. Hamming distance
2. fuzzy hamming distance
3. Levenshtein distance.

However, this method suffers from a serious flaw; i.e., neighboring cells in the sequences need not be neighbors in space. For example, an 8-by-2 matrix, formed by manipulating the rows in the matrix as [row1 row 2; row3 row4], will be reported as

similar. This representation has several shortcomings and is not a very good dissimilarity representation.

6.5 | SUMMARY

In summary, dissimilarity measures have been proposed for a variety of traffic representation ranging from single numerical values to n-dimensional point sets. The dissimilarity measures provide a way of accurately quantifying the differences between complex relationships such as graphs, contours, histograms, and time-series. The dissimilarity measures also provide automation of the graph matching based on pattern recognition. This provides new way of quantifying the degree-of-closeness of graphs. It solves the various consistency problems that occur in eye-balling techniques previously applied by researchers for qualitatively measuring the difference in graphs, contours, etc.

The automated graph matching concept was shown to be extendable to higher dimensions based on similar principles to n-dimensional point sets. The pattern recognition methods shown are simple, flexible, efficient, extendable and robust. These are some of the important qualities that are required for implementation in the real-world. The simplicity of the measures helps practitioners develop and deploy pattern recognition based calibration that require minimal to no human intervention. The main advantage of dissimilarity measures is that there are no specific assumptions being made about the system, data, population, or the model. The measures are equally applicable in other models in a non-traffic arena. The dissimilarity measures are equally applicable to macroscopic or mesoscopic simulation models, since such systems can also be described using similar traffic representations.

7 | Search Representation in Calibration

"The production of too many useful things results in too many useless people"

Karl Marx

7.1 | INTRODUCTION

Due to the stochastic nature and complexity of microsimulation model, representation of microsimulation as closed-form equation is not usually possible. As a result, traditional calculus based optimization methods cannot be applied. The calibration of simulation models requires the use of other search and optimization methods based on multiple evaluations of the objective function. In chapter 6, various dissimilarity measures were proposed for different traffic representations. The objective all through the development of calibration objective was to produce measures that are based on evaluations of the features of the simulation model. There are many derivative-free optimization methods that can be applied to microsimulation calibration. Most of these methods direct the search path based on multiple evaluations of the objective function. There has been considerable research related to search representation and search based methods. Therefore, it is not the primary focus of this research. However, the integration of the dissimilarity measures with these search methods is very important, and largely dominates the discussions in this chapter.

7.2 | DISSIMILARITY MEASURES AND SEARCH METHODS

For an optimization method that is based on multiple evaluations of the objective function, the performance of the method is dependent on the quality of the objective function. In other words, the search methods are based on how well the function (i.e., the objective function) space is defined. If the function space has a lot disturbance or mis-information, the search method that is based on evaluations represented in such space may invest far greater amount of time in finding accurate solutions. If the objective function can give accurate information about the differences, the optimization method can use such information to better direct the search path.

Also since the amount of information available in an objective function is of utmost importance, higher order traffic representations sets would perform better since they contain more information. For example, if minimization of the difference of numerical capacity values is the objective, there always exists a possibility of optimization method recommending non-optimal parameters, because the degree of freedom is too high. The recommended solution is to expose only the calibration parameters that have a significant effect on the objective function (see definition 2.1 in Chapter 4). However, by using speed-flow graphs, a higher number of parameters can be exposed to the calibration process, resulting in a better fine-tuned simulation model.

A literature review was conducted to establish various optimization methods for use in microsimulation calibration. It was determined that there a variety of optimization methods available for use in calibration. The choice of the method usually depends on a variety of factor including number of variables, performance, run times, availability, etc. But much of the methods can be classified as Direct Search Methods (DSM). There are

some derivative-free optimization methods are also applicable in calibration. Over the years, the terms direct search methods and derivative-free optimization methods have been used synonymously, but there are few researchers who claim differences between these terms (Lewis et al., 2000).

Direct search methods are usually referred to as heuristic methods lacking sound mathematical basis. But, direct search methods are often used for simplicity, flexibility, and reliability (Lewis et al., 2000). Many of the direct search methods are also robust in nature. Some of the direct search methods that can be used in calibration are:

1. Hooke and Jeeve method
2. Nelder-Mead simplex method
3. Pattern Search Methods
4. Box's complex algorithm

The other category of optimization methods are based on natural or evolutionary concepts. Examples of such methods include genetic algorithms, evolutionary algorithms, evolutionary strategies, etc.

Evolutionary algorithms have been chosen for implementation of calibration objective in this research. For the past few years, Evolutionary Algorithms (EA) has been successfully applied in traffic microsimulation calibration (Ma and Abdhulai, 2002; Kim and Rillet, 2001; Schultz and Rillet, 2004)). They have found acceptability in the field of calibration of traffic simulation models. The Evolutionary Algorithms favorably lend themselves to the nature of the calibration problem and the concepts described in this research. Application of dissimilarity measures in well-recognized search algorithms such as evolutionary algorithms will demonstrate the suitability of such measures to the

traffic engineering community. However, tt is not the intent of this study to comment or test the performance differences in different optimization methods. In the following sections, description and implementation framework of evolutionary algorithms are presented.

7.3 | EVOLUTIONARY ALGORITHMS

Evolutionary algorithm (EA) is a search method wherein some of the mechanisms are based on concepts of natural selection and evolution. These algorithms work on a population of solutions, rather than on a single point. EA is one of the many algorithms based on principles of natural selection and can be considered as an extension to a simple or a canonical genetic algorithm over types of representation, crossover, mutation, and selection. Genetic algorithm (GA) was introduced by Holland (1975), and later developed by DeJong (1975). The algorithms developed by Holland (1975) are usually referred to as canonical genetic algorithm. Genetic algorithms are different from traditional optimization methods in that they work on a representation (or coding) and operate on probabilistic transition rules (Goldberg, 1989).

Encoding (or representation): defines the way the parameters are represented. Some of the popular representations include:

1. Binary strings
2. Gray-coded string
3. Real-value

In canonical genetic algorithms, the parameters are encoded as strings, and various operators are defined on strings. A simple genetic algorithm consists of three operators: Reproduction, Crossover, and Mutation.

Reproduction (or selection): Is the process of copying strings, based on fitness values (measure of performance). The process of selection involves two steps. In the first step, the objective evaluations of individual members are transformed using a fitness assignment. There are various ways of assigning fitness values. Some of the methods include:

1. Proportional
2. Linear
3. Rank-based

In the second step, the actual selection process is implemented based on fitness assignment. Some of the selection methods include:

1. Roulette-wheel
2. Stochastic uniform
3. Tournament
4. Remainder

Crossover (or recombination): Is the process of selecting a pair of string and swapping string bits to form two new strings. The process of recombination depends on representation or encoding. Some of the methods in recombination include:

1. Single point
2. Two point
3. Scattered
4. Arithmetic

Mutation: Is random alteration of bits in a string, often with a very small probability. The type of mutation applied usually depends on encoding. Some of mutation methods include

1. Gaussian
2. Uniform
3. Adaptive feasible

A prototypical flow chart of the evolutionary algorithm search procedure is shown in figure 7.1.

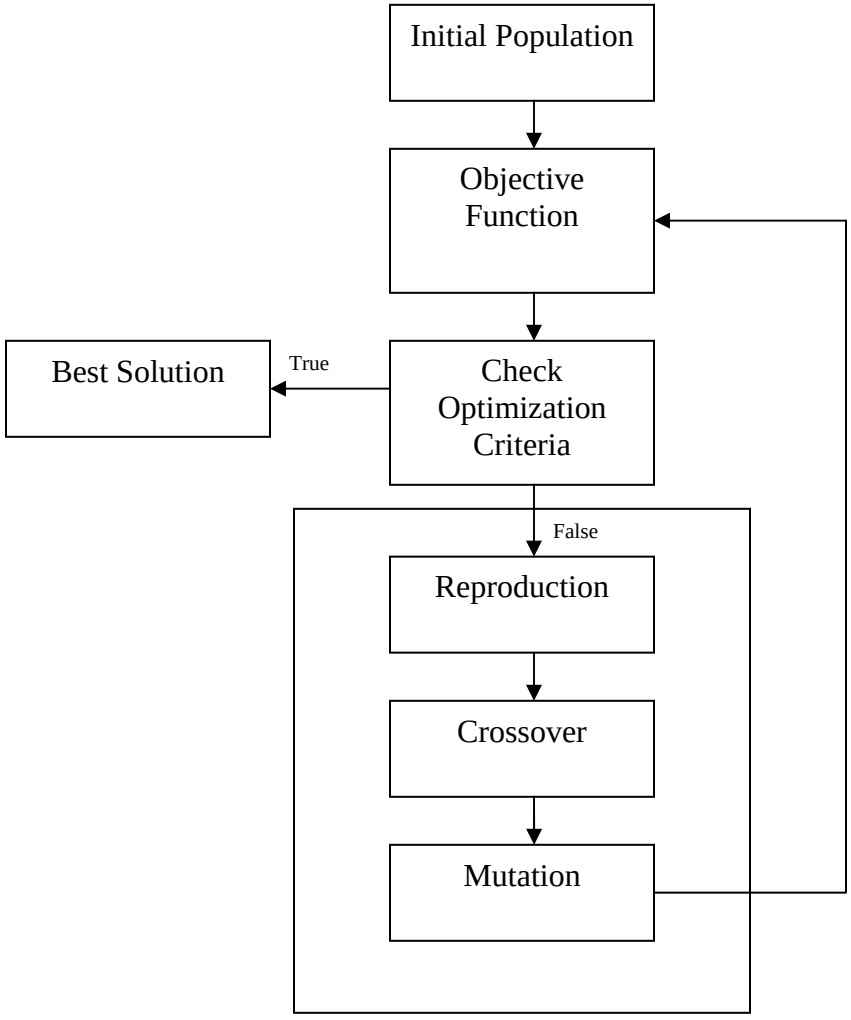

Figure 7.1 A prototypical evolutionary algorithm implementation

7.4 | EA TOOL IN MATLAB

An EA tool in MATLAB, a scientific programming tool, was selected for use in the project. The EA tool in MATLAB allows for implementation of various operations involved in evolutionary algorithms. Some of the features of EA Tool in MATLAB are as follows:

1. Fitness scaling
2. Selection
3. Reproduction (including elite individual, crossover fraction)
4. Mutation
5. Crossover
6. Migration
7. Algorithm settings (penalty settings)
8. Hybrid function (e.g. pattern search)
9. Stopping criteria (tolerance, maximum number of generations, etc)
10. Real-valued, binary, or custom encoding

The EA tool also poses built-in plotting functionality. The tool allows for both unconstrained and constrained minimization, with linear or non-linear constraints, and bounds.

7.5 | EA IMPLEMENTATION FOR CALIBRATION

The pseudo code of the evolutionary algorithm implementation used in this research is presented below.

```
Pseudo-Code for the Evolutionary Algorithm
BEGIN
     INITIALIZE population with random candidate solutions
     EVALUATE individual candidates
     REPEAT UNTIL (TERMINATION CONDITION is satisfied) DO
          SELECT parents
          RECOMBINE pairs of parents
          MUTATE the resulting offspring
          CHECK if candidates are already evaluated
          EVALUATE candidates not previously evaluated
          STORE fitness values
          SAVE elite individual
          SELECT elite individual and remaining individuals
     for the next generation
     END
END
```

EA performs the optimization process based on multiple evaluations of the objective function. The candidates for the next generation are selected based on fitness values. However, the elite individual (best fitness seen yet) is sent to the next generation without mutation. The EA can be implemented using different representations like real-number, binary, gray-coded, etc. The EA was tested for each of the representations, and real-number representation performed slightly better than binary and gray-coded representations. The recombination, mutation, and selection were chosen to improve diversity, which is paramount to achieving a global optimum. Proportional scaling of fitness values and roulette wheel method was employed for selection. Gaussian methodology was used for mutation. It is possible to choose more than one elite individual to send to the next generation, but increasing the number of elite individuals usually results in a premature convergence due to decreased diversity.

The EA based optimization can be thought of as the third level of representation in the calibration process. In this research, there are three defined levels of representation in microsimulation calibration: traffic flow, dissimilarity, and EA. Figure 7.2 describes the three levels of representation.

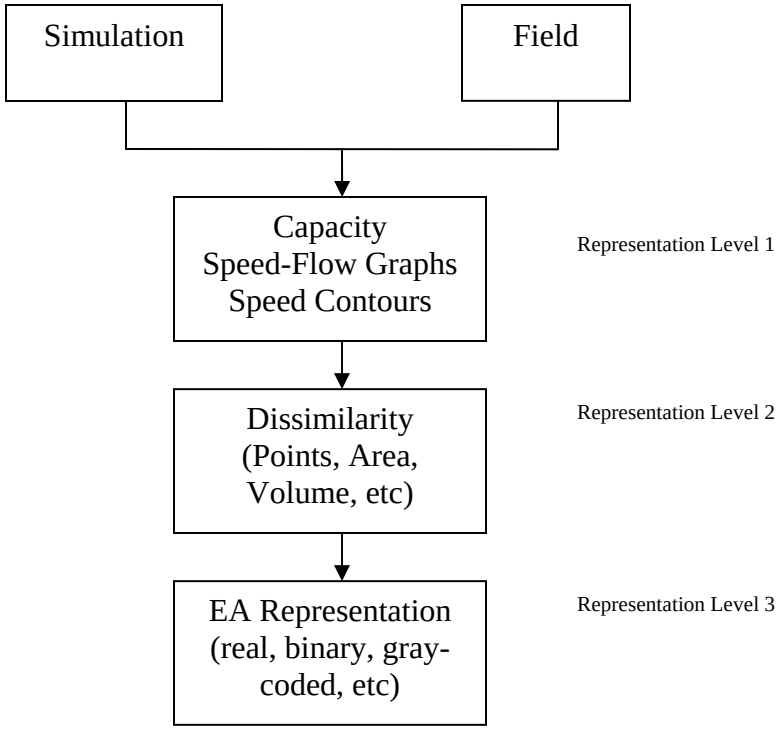

Figure 7.2 Three levels of representation in microsimulation calibration

8 | Generalized Hierarchical Calibration Methodology

"The Learning and Knowledge that we have, is, at the most, but little compared with that of which we are ignorant"

-Plato

8.1 | INTRODUCTION

The methods presented in previous chapters 6 and 7 were integrated, wherein the traffic flow representations in chapter 5 are represented in dissimilarity space in chapter 6. In chapter 7, the search representation was presented. An evolutionary algorithm was introduced as a search-based optimization tool for microsimulation calibration in this research. There are many other search-based optimization tools available for use in microsimulation calibration, and the dissimilarity representation can be applied in most of the methods. However, evolutionary algorithm is an attractive tool that is flexible and powerful enough to be applied in a whole range of problems. Evolutionary algorithms, unlike some traditional search-based algorithms, are capable of being used in nonlinearly constrained multi-objective optimization. In summary, chapters 5, 6, and 7 can be provided the three levels of representation of calibration. In this chapter, the higher level calibration methodology is provided. This methodology integrates the other aspects of

calibration like selection of parameters, sensitivity analysis, range definition, data analysis, etc based on lesson from previous three chapters.

8.2 | SENSITIVITY ANALYSIS MODEL

This is one of the first steps in a calibration process. After a preliminary list of calibration parameters is selected for the simulation model, the sensitivity of each of the parameter to the objective at hand is analyzed. A detailed description of the model is provided in figure 8.1. In this process, sensitivity analysis is conducted at two levels: aggregate and disaggregate. Two test networks were created to assist in the sensitivity analysis process. For disaggregate data, a two mile one-lane circular track was created. A circular track was created to ensure constant global density during the data collection process, since many of the traffic flow processes are dependent on density. For aggregate data, a 6-mile two-lane freeway network with two on-ramps, one at 2-mile and other at 4-mile marker, was created. This network was created after significant testing. Initially, a test network without ramps was created, but such a network was not capable of producing a wide variety of traffic conditions. Testing followed first with one ramp and then with two ramps, and network with two ramps created the variety needed for sensitivity analysis.

For assisting in the evaluation process, data analysis module was created using MATLAB. The program description and source code are available in the appendix. In addition, a VC++ COM module was created to automate the communication with VISSIM.

The sensitivity analysis was performed on disaggregate data (headways, relative distance vs. relative velocity) and aggregate data (capacity, speed-flow, flow-occupancy,

etc). In addition, sensitivity analysis included other traffic flow processes like shockwaves. Statistical analysis module was used to quantify the process, but was not very comprehensive due to various reasons. Statistical analysis was not performed to test for sensitivity of two or more parameters together. The statistical analysis process usually requires a large number of runs that require a significant amount of time, which was not feasible given the high simulation times. In these cases, the researcher intervenes and makes a qualitative judgment about the sensitivity of the parameter. In addition, the researcher also provides a theoretical background to the whole process.

The final result of sensitivity analysis is categorization of selected parameters to accepted, declined (i.e., the representations are invariant to these parameters), and external control parameters. The declined parameters are removed from the calibration process as suggested in chapter 4. The accepted parameters and external control parameters continue on to the next step in the calibration process.

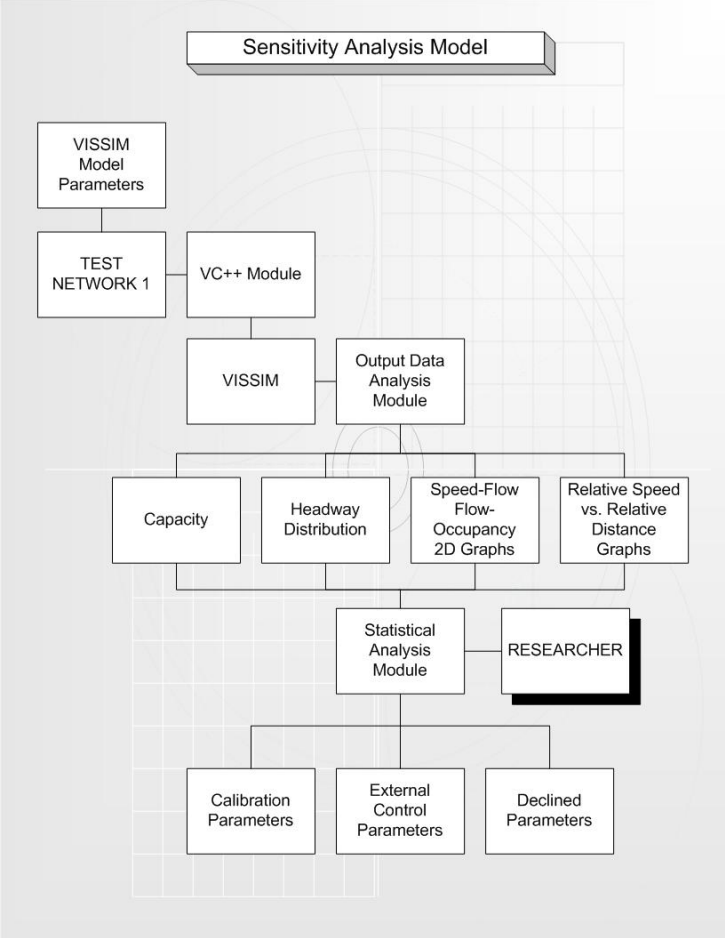

Figure 8.1 Sensitivity analysis model

8.3 | RANGE DEFINITION MODEL

The second model utilized in the calibration process is the range definition model. In this model, the accepted and external control parameters are processed further to obtain range information for each of the parameters. For range definition, the test networks similar to the ones used in sensitivity analysis model can be applied; or otherwise, test networks can be created to analyze specific parameters. Similar to the sensitivity analysis model, disaggregate and aggregate data is utilized. No specific statistical model is utilized here, and much of the decision making is again left to the researcher, who utilizes a variety of data obtained from the simulation model. In addition to the tests performed on

simulation models, real-world aggregate and disaggregate data described in section 3.4 of chapter 3 is utilized. In addition, a thorough theoretical analysis of the simulation model is performed. Mathematical and physical deductions based on the theoretical framework are used in range definition process. This process uses both real-world and simulated data to develop range definitions for calibration parameters. A flow-chart description of the model is presented in figure 8.2.

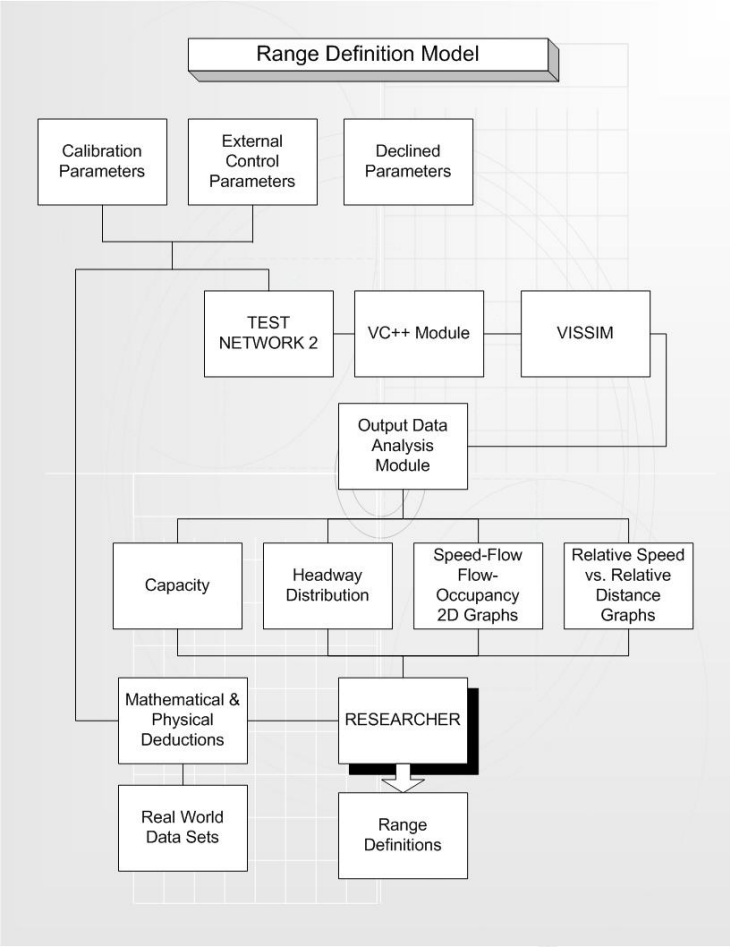

Figure 8.2 Range definition model

8.4 | GENERALIZED CALIBRATION MODEL

In this low-level calibration process, the range definitions for calibration parameters and external control parameters are fed into the simulation model and the evolutionary

algorithm. The evolutionary algorithm described in chapter 7 is used as a search-based optimization tool to calibrate the parameters. The external parameters are not fed into the evolutionary algorithm. An objective function based on pattern recognition was developed using MATLAB. The program description and the source code are available in the appendix section. The calibration process is usually based on aggregate data (speed-flow, capacity, headway distribution). Disaggregate data is rarely applied in this process, since such information is not valuable when dealing with average conditions. However, disaggregate data based calibration can be valuable for some of the parameters, as seen in a later chapter. This low-level calibration methodology requires much traffic data, and is not always suitable for practitioners. The data needed in this process is usually only available in certain locations. However, this process is very useful, since many of the parameters values from low-level calibration can be used, instead of default parameters, for a different location (assuming no significant change in driver behavior). In addition, many more parameters can be calibrated using low-level calibration due to more degree of freedom in the calibration procedure. A flow-chart description of the model is presented in figure 8.3.

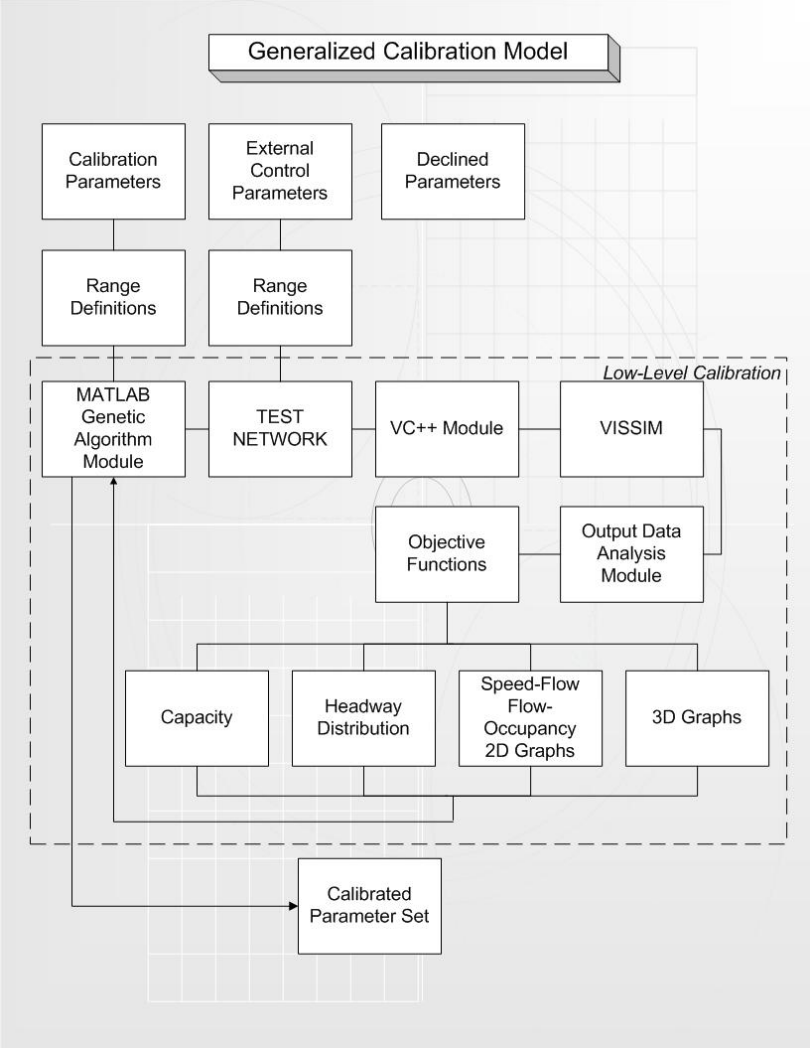

Figure 8.3 Generalized calibration model

8.5 | GENERALIZED HIERARCHICAL CALIBRATION MODEL

A generalized hierarchical calibration methodology is proposed to assist practitioners. In this process, there are two-levels of calibration. First, a low-level calibration is performed on a larger calibration parameter set. Second, a high-level calibration is performed on a smaller calibration parameter set. In the low-level calibration much of the parameters are calibrated and categorized into two categories. Calibration parameters that need further calibration to match conditions at a different location are stored in the

new calibration set. Calibration parameters that do not require further calibration are used as external control parameters. The process of iterative evolutionary algorithm based high-level calibration is similar to the low-level calibration; however, typically, a lower fidelity objective function is employed due to unavailability of a sophisticated data set. A flow-chart description of the generalized hierarchical calibration process is provided in figure 8.4.

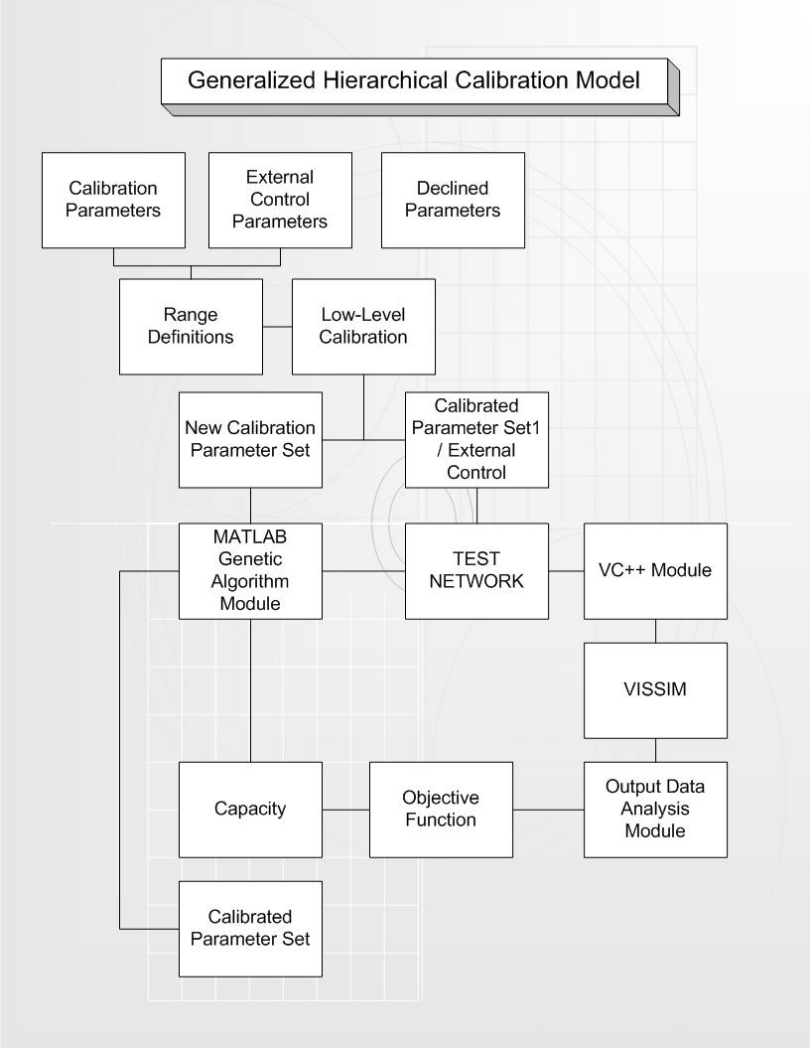

Figure 8.4 Generalized hierarchical calibration model

8.6 | SUMMARY

This chapter defines and completes the methodology for accurate calibration of simulation models based on a variety of concepts. This chapter proposes a generalized calibration methodology that integrates methods for parameter selection, sensitivity analysis, range definition, and calibrations based on three levels of representation. The generalized hierarchical methodology was presented to assist practitioners in efficiently calibrating their models, while reducing the amount of time invested in such a procedure. The methodologies presented in this chapter are demonstrated through two case studies conducted on a freeway in California. The case studies are presented in chapter 9 and 10.

9 | Microsimulation Calibration using Speed-Flow Relationships

"If you torture data sufficiently, it will confess to almost anything"

-Menger, Fred

9.1 | CASE STUDY: US 101 SAN MATEO, CA

To demonstrate the usefulness of the proposed methodology and to provide results of comparison with current calibration procedures, a real-world freeway was simulated and calibrated using the described methodology. The case study network is a 5-mile 4-lane section on US101 Northbound in San Mateo, CA. A picture describing the extent of the simulation model and detector locations is provided in Figure 9.1. The data source is the California PeMS database (PeMS Group, 2007). Data was collected over four detectors numbered 401199, 400935, 400007, and 400420; and from January 2, 2007 to January 4, 2007 from 5AM to 10PM over each day. It was verified that all detectors were in good health and reporting throughout the data collection period.

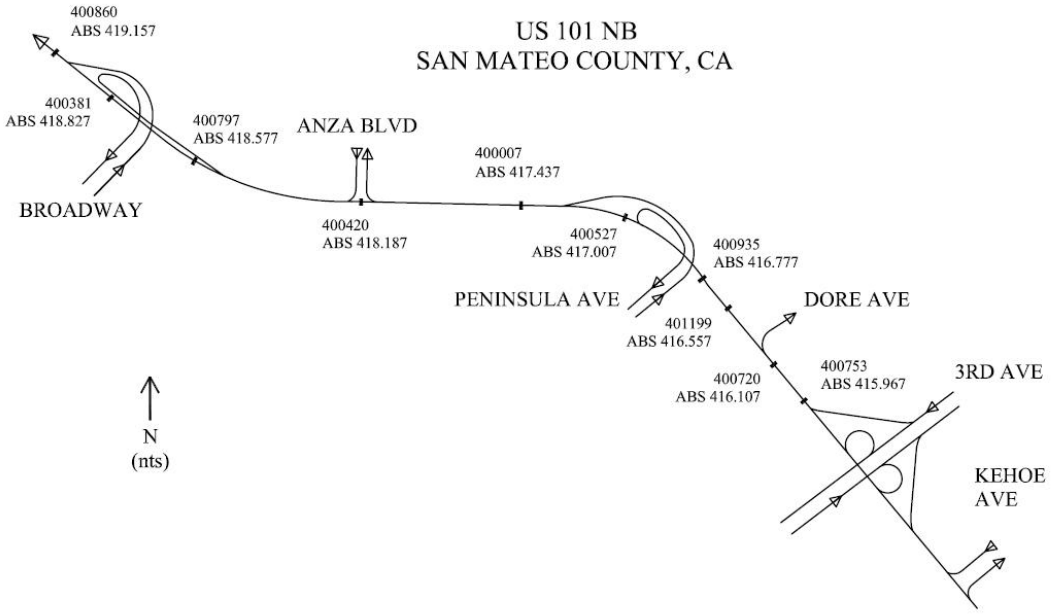

Figure 9.1 Extent of simulation for US101 NB, San Mateo, CA.

9.2 | VISSIM MODEL

VISSIM 4.30 microsimulation software was used to develop and test the calibration procedure. VISSIM is based on a psycho-physical car-following model (see chapter 2: Wiedemann Car Following Models) and uses perception thresholds to model drivers (Wiedemann, 1974 and 1999). The model was coded for the extent provided in Figure 9.2 and detectors were place at exactly the same position as reported by California PeMS database (PeMS Group, 2007). Speeds and flows are aggregated and averaged over lanes over a 5 minute interval. This aggregation over time and space follows the procedures published by PeMS Group (2007). In addition, a test network similar to one illustrated in a consecutive section was developed to test the applicability of test networks to assist in calibration of simulation models.

VISSIM Driver Behavior Calibration Parameters

The following five calibration parameters were used in the calibration procedure.

1. CC1: The headway time (in seconds) that the driver wants to keep between vehicles.
2. CC2: Following variation - controls longitudinal oscillation in the car-following process.
3. CC3: Threshold for entering car-following - controls the start of the deceleration process, i.e. when a driver recognizes a preceding slower vehicle.
4. CC4: Following threshold - controls the speed differences during closing in following process.
5. CC5: Following threshold - controls the speed differences during opening in following process.

For a more detailed explanation of VISSIM microsimulation and the calibration parameters, please refer to Chapter 2 and the VISSIM 4.30 user manual (PTV AG, 2007).

9.3 | PATTERN RECOGNITION BASED OBJECTIVE

The objective function used in calibration is based on the concept of reducing the difference between speed-flow graphs obtained from field and simulation (see chapter 5: speed-flow representations). For comparing speed-flow graphs, researchers have traditionally tested the closeness of the graphs by visually matching the simulated and field graphs. A fitness function for measuring closeness of simulated and field speed-flow graphs is needed (see chapter 6). In addition, the fitness function should be automated and consistent across multiple evaluations. The development of an automated comparison method to replace manual eyeballing has the following benefits:

1. Multiple simulation runs can be compared without human intervention.
2. Maintains consistency across multiple comparisons.
3. Produces a quantitative value for the objective function.

In order to formulate a fitness function to measure the dissimilarity of speed-flow graphs, a closer look at important properties like shape, scatter, extent, and intensity is necessary. Since the speed and flow measurements are stochastic in nature, it is also required to account for such a noise created in the speed-flow graphs. Based on the discussions provided in chapter 6 about dissimilarity measures for various traffic flow representations, modified symmetric difference was utilized in measuring the difference in speed-flow graphs.. In other words, the dissimilarity of two graphs is measured by calculating the amount of area that is not covered by the other. Since speed and flow measurements are represented as point sets, discretization to convert point information to area is necessary. As mentioned in chapter 6, the discretization also has the effect of smoothing thus reducing noise in speed and flow measurements for matching purposes. Since the information coming from the field and simulation is often just partial and not a complete speed-flow graph, the comparison is only made over the space occupied by the field graph. The objective function, Z, for the calibration process of the field is as follows:

Min. Z = Sum of all the speed-flow area in the field data that is not covered by the simulated data.

```
Pseudo-code for fitness function evaluation
BEGIN
     CONVERT field and simulation vector data to raster data
at a certain resolution
     FOR every cell in field data
          CHECK IF the same cell has a value in simulation
data
          IF
TRUE continue
FALSE increment the objective function by a certain value
          END
     RETURN the final objective function value
END
```

This objective function does not capture the frequency of occurrence of speeds and flows. This information is purposely left out for reasons mentioned in an earlier section. The objective function is consistent over different evaluations, because the number of speed-flow points developed by the simulation model across each evaluation is constant. In order to compare the described methodology with existing methodologies two additional objective functions are used. These two objective functions are

1. Minimize the difference between maximum 5 min. flows observed in the field and simulation.
2. Minimize the difference between maximum 5 min. flow sustained over 15 min. observed in field and simulation.

There are ramifications related to the use of different aggregation period for speed and flow data. If speed and flow information is collected and aggregated over a five minute interval, the simulation model might need to be run for long periods of time and over many random seeds to develop a reasonable sample of points. For example, if data is aggregated over five minute intervals, it would require about 16 simulation-hours to produce 500 points on the speed-flow graph. The amount of time required to run 16 simulation-hours depends on the size of the microsimulation model. In addition, most of

the optimization methods available are based on multiple evaluations of the microsimulation model.

9.4 | EVOLUTIONARY ALGORITHM

The evolutionary algorithm presented in chapter 7 was used for calibrating the simulation model. Each simulation model was run for 3 simulation-hours and for five different random seeds. The evolutionary algorithm used 10 members per population and 5 runs per member. Since there is possibility that some of the individuals might be repeated in future generations, the fitness values for individuals were stored in a database to reduce computation times. The total run times varied for the evolutionary algorithms ranged from 12 to 30 hours based on the objective function.

9.5 | A PRACTITIONER ORIENTED SIMULATION MODEL

In order to keep the amount of time required to produce a reasonable number of sample points to a minimum, it might be advantageous to use a test network, instead of an actual network, to assist in optimization of calibration parameters by producing speed-flow graphs. Test network is a small-scale network developed to produce the widest range of speed and flows over the least amount of time (Figure 9.2). However, the use of test network for calibration is only valid under the assumption that speed-flow graphs from a test network are equivalent to the graphs produced by an actual network Test network also provides other advantageous in calibration process. A simple test network was developed to replicate different flow conditions and a complete speed-flow graph. It is important to produce different range of operations to develop complete speed-flow graphs.

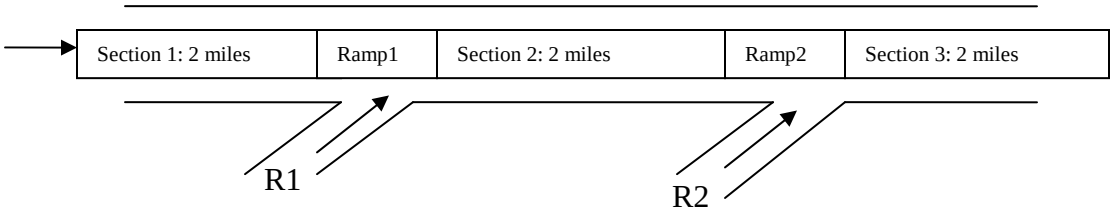

Figure 9.2 Illustration of the test network.

Figure 9.2 shows an example of a test network that consists of a mainline and two ramps. The main line is approximately 6 miles long, and two ramps are placed at 2 miles apart. The mainline has the same number of lanes as the actual network. Detectors are placed every ¼ mile and no detectors are placed near the influence area of on-ramps to avoid distorted results. A total of 9 detectors (3 in each section) are placed on the mainline. An artificial demand pattern is created to force demands above capacity in order to produce breakdown conditions on the freeway. The demands are gradually increased, sustained, and dropped over time. It is not possible to replicate a complete speed-flow graph without ramps. This test network was intended to represent the mainline freeway segment as specified in the Highway Capacity Manual, but two ramps had to be introduced in order to create the diversity in range of operations that would lead to a complete speed-flow graph.

9.6 | RESULTS

In this section the results from three different applications of the methodology are presented.

1. Calibration of test network to the objective functions

2. Calibration of US101NB to the objective functions

Application of test-network-calibrated parameter values to US101NB

The first application is on the test network shown in Figure 9.3 and the second and third application on the US101 freeway network shown in Figure 9.4. For each scenario, 5 runs were performed, each run being 3 simulation-hours. Five minute speed and flow data were collected from the mainline detectors. The data from multiple runs were aggregated and the speed-flow graphs were produced. The three objective functions consisted of comparisons between the field and simulated data for:

1. Maximum five minute flows (Maximum Flow)
2. Maximum five minute flows sustained over 15 minutes (Sustained Flow)
3. Matching speed-flow graphs (Speed-Flow)

9.6.1 | TEST-NETWORK

Figures 9.3.a-9.3.c show the results of the comparisons. The visual inspection of these three figures shows that the speed-flow objective resulted in the best match between field and simulated data. This is as expected since the objective function itself involves the minimization of non-overlapping speed-flow points. Figure 9.3.a shows that the maximum flow objective focuses solely on the highest flow values thus missing badly the congested regions of the speed-flow graph. Figure 9.3.b shows that while the sustained flow objective captures the congested region better than maximum flow, it does not produce the realistic scatter of data in the congested region as shown in Figure 9.3.c. Consequently, the matching of the shape of the speed-flow graph results in the most complete and realistic coverage of the speed-flow graph. Theoretically, this means that the simulation based on shape matching can better represent traffic during longer periods

of time and not just the top five or fifteen minutes of the day. The practical implication is that the use of the new methodology would better capture the entirety of the peak period which typically lasts several hours in most metropolitan areas.

Table 9.1 Calibration Parameters for Test Network

Objective	CC1 (s)	CC2 (m)	CC3 (s)	CC4	CC5
Default Values	0.9	4	-8	-0.35	0.35
Speed-flow	1.28	8.11	-10.92	-0.45	1.06
Sustained flow	1.06	7.79	-5.66	-2.50	2.32
Maximum flow	0.83	12.02	-14.19	-1.42	2.31

Table 9.1 shows the calibration values that resulted from the test network. The default values are provided in the first row to draw a comparison with the optimization suggested values. The CC1 column shows that speed-flow matching produces the longest CC1 value. This is expected since speed-flow matching involves the whole range of traffic conditions and not just the capacity or short headway conditions. CC2 and CC3 show similar trends in that the maximum flow produces the highest value while highest sustained flow produces the smallest value. Speed-flow is between those two values. For CC4 and CC5, the speed-flow results in a driver that is much more sensitive to speed differences between the leader and follower than capacity (rows 3 and 4). Table 9.1 shows that parameters calibrated using speed-flow graphs are significantly different from those calibrated using capacity.

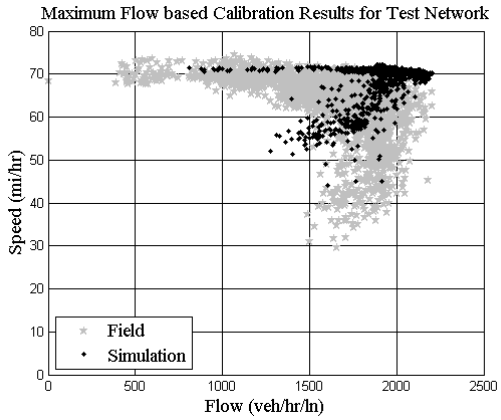

(a)

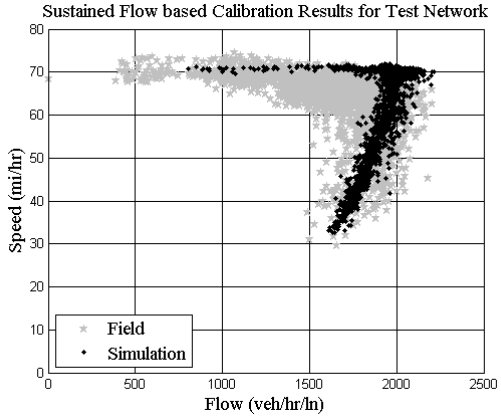

(b)

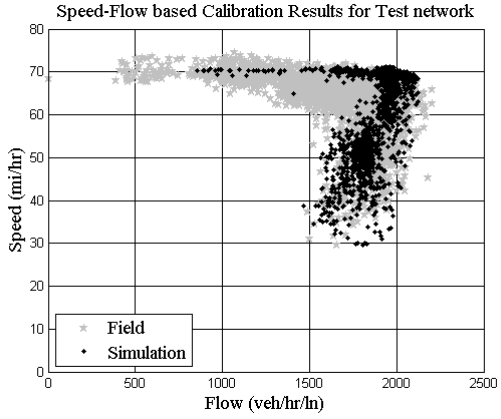

(c)

Figure 9.3 Test network speed-flow graph comparisons for different objective functions.

9.6.2 | US101 NB NETWORK

Analogous to the test network cases, the same three objective functions were also applied to the US101 network. Figures 9.4.a-9.4.c show the results of the comparisons. Compared with the test network, the simulated US101 network produces a much more

scattered pattern right before the pre-queue flow area. This might be explained due to existence of more varied traffic conditions for US101 NB than the test network. Once again the objective based on the matching of the speed-flow graphs produces the simulated speed-flow graph that matches the field data the most closely. Figure 9.4.a shows that maximum flow objective results in a speed-flow graph that is shifted to the left, so flows in the congested region are underestimated significantly. On the other extreme, the sustained flow objective results (Figure 9.4.b) in a graph shifted to the right so flows are overestimated. It is only the third objective function that produces the closest match for all traffic regions of the speed-flow graph (Figure 9.4.c).

Table 9.2 Calibration Parameters for US101 NB

Objective	CC1 (s)	CC2 (m)	CC3 (s)	CC4	CC5
Default Values	0.9	4	-8	-0.35	0.35
Speed-flow	1.09	10.59	-7.91	-2.50	0.64
Sustained flow	1.12	2.98	-5.5	-2.59	2.46
Maximum flow	0.83	12.12	-7.7	-2.20	1.17

Table 9.2 shows the calibration values that resulted from the simulated US101 network. The first column, CC1, shows that maximum flow produces the smallest value of headway which means overly aggressive driving. The second column, CC2, show that sustained flow produces fairly insensitive behavior to longitudinal oscillation that is unrealistic. The third column, CC3, shows that sustained flow produces a smaller value for the car-following threshold. The other interesting observation is that CC3 values suggested by both test network and US101 were close to the default values suggested by VISSIM.

CC4 and CC5 are speed thresholds in following for closing and opening process. For example, in VISSIM, when a car is in following condition the driver tries to hold the

acceleration values to a minimum. The driver reacts when one of the following speed thresholds in broken. In addition, CC2 also control the oscillation and also results in driver reaction during following process. Therefore, in a closing condition, if speed differences exceed absolute value of CC4, the driver reacts by braking. Analogously, if CC5 is broken, the driver reacts in an opening condition by accelerating. Intuitively speaking, CC4 and CC5 should exhibit an asymmetrical behavior since drivers are more sensitive when closing than when opening. The speed-flow objective values for CC4/CC5 were not in compliance with this and the values suggested by speed-flow objective are very different from the default values in VISSIM. However, the results of the test network are in compliance with this effect.

In order to truly understand the reason behind non-compliance of CC4 and CC5 values, vehicle trajectory data from Next Generation Simulation (NGSIM) (NGSIM, 2007) is needed. Since the thresholds defined by CC4 and CC5 are not speed dependent, the values are average values used for all speed levels. Throughout all the parameters, the values derived from shape matching results in the most reasonable values according to traffic flow theory.

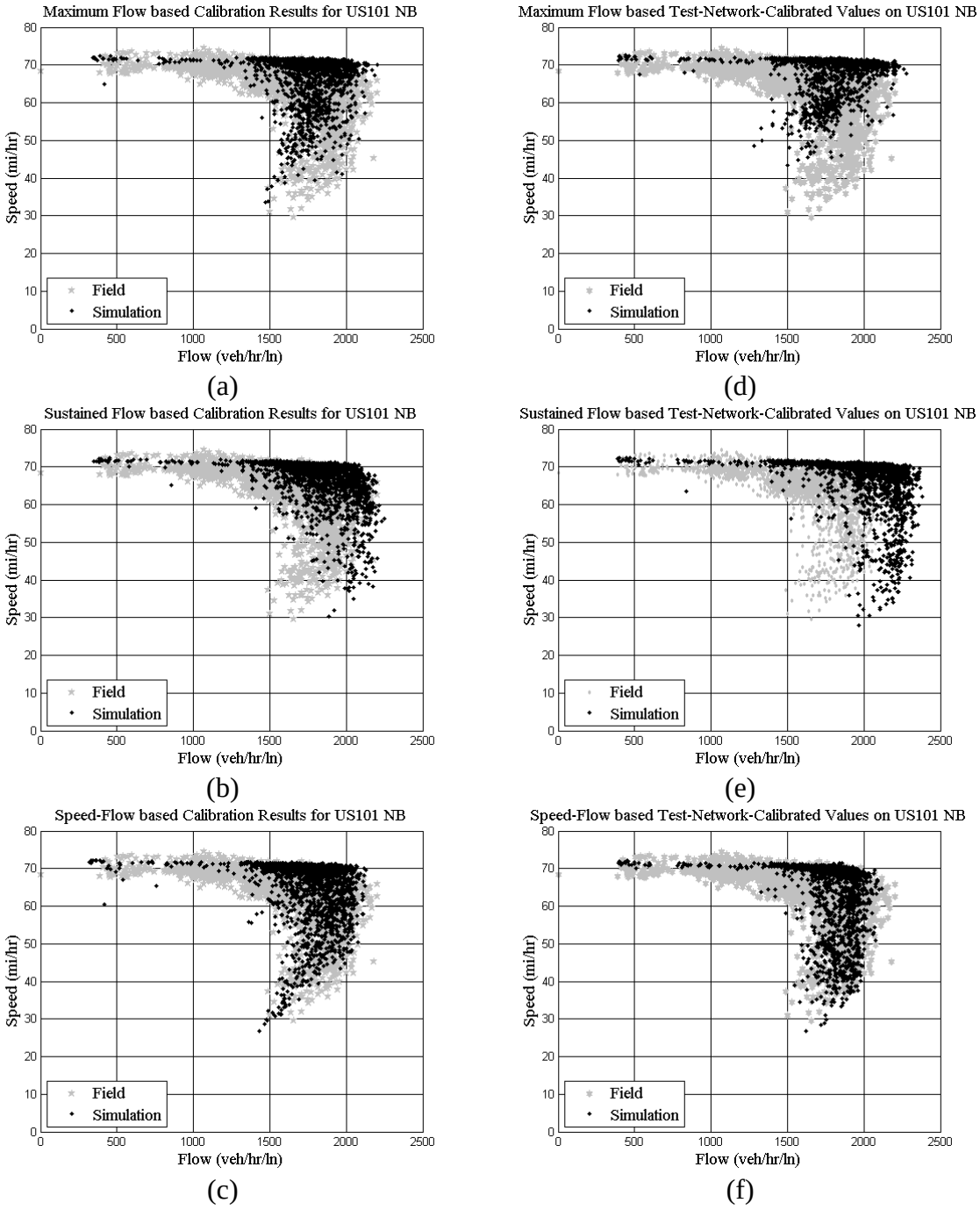

Figure 9.4 Speed-flow graph comparisons for US101 NB using different objective functions.

9.6.3 | TEST-CALIBRATED-VALUES APPLIED TO US101 NB

In order to evaluate the applicability of using test network to calibrate an actual network, the test-network-calibrated values for each of the objective functions is fed into the

US101 NB simulation model. The results of such a comparison are provided in Figures 9.4.d-9.4.f. Table 9.3 shows the speed-flow objective evaluations on each of the graphs in Figure 9.4. Speed-flow objective give a sense of dissimilarity of graphs. The lower the value of objective the better the match is between the graphs. The comparison amongst these values is fair, because the speed-flow measurements are made over the same simulation model (US101 NB) resulting in equal number of observations. The comparison amongst graphs produced from test network and US101 NB is not fair, because the number of observations on test network is not equal to US101 NB. Figures 9.4.c and 9.4.f are fairly similar to each other. The speed-flow objective evaluation for these graphs (Table 9.3) shows a 10% variation in objective function value for speed-flow based calibration. A much higher variation is observed for the other objective functions. However, the graph achieved using test-network-calibrated values for speed-flow objective is quite comparable to the ones achieved using US101 NB. In addition, the test network can take advantage of time again when applied to large scale simulation models.

Table 9.3 Speed-Flow Objective Evaluations for US101 NB Speed-Flow Graphs

Objective	**Speed-Flow Objective Fitness Values**	
	Calibration using US101 NB	**Test-Network-Calibrated values on US101 NB**
Speed-flow	193	210
Sustained flow	244	317
Maximum flow	237	293

9.7 | CONCLUSIONS

A new methodology for calibrating microsimulation was presented. This new methodology introduced the use of speed-flow graphs as a calibration objective, defined a fitness function for point sets, and included an automated technique for optimization

based on Evolutionary Algorithm. Encouraging results were obtained from the application on the US101 freeway in California. The results from speed-flow objective function have been shown to perform better than the objective function based on maximum 5-min. flow and maximum 5-min. flow sustained for 15 minutes. The calibration parameter values from the speed-flow calibration are shown to perform well in all three regions of the speed-flow graph: free-flow, congested, and discharge. The speed-flow objective calibrated parameter values resulted in a scatter in speed-flow graphs similar to the field graphs. This accounts for the stochastic nature of speed and flow observations on the field. The results suggested by the Evolutionary Algorithm based on speed-flow objective are plausible and sometimes even close to default values. The evolutionary algorithm suggested calibration parameter values resulted in speed-flow graphs similar to the one noticed in the field. The objective function can be expected to perform similarly even if a different search and optimization method was employed. But the comparative efficiencies of the search and optimization methods are beyond the scope of this study. It can also be seen that test networks can be employed to assist in calibration of parameter values when the simulation networks are large. However, the degree-of-freedom of the speed flow objective with respect to the calibration parameters was high, resulting in multiple plausible solutions to the objective. The CC4 and CC5 values suggested by the algorithm were not in accordance with the intuitive asymmetry of speed thresholds. In order to understand the true nature of these variables, an extensive microscopic data analysis was performed using NGSIM freeway data sets. The results of such analysis resulted in an integrated calibration methodology is presented in the next chapter.

10 | Integrated Micro-Macro Calibration for Psycho-Physical Car Following Models

Reality continues to ruin my life.

Calvin

10.1 | INTRODUCTION

In previous chapter a calibration based on matching speed-flow graphs was presented The pattern recognition based objective function was applied to calibrate a 5-mile 4-lane section on Northbound US101 in San Mateo, CA. The simulation model was calibrated by reducing the difference between simulation and field speed flow graphs using an evolutionary algorithm. The dissimilarity between simulation and field was measured by calculating the amount of area that was not covered by the other. Since speed and flow measurements were represented as point sets, discretization to convert point information to area was necessary. The discretization also had the effect of smoothing and reducing noise in speed and flow measurements for matching purposes. Since the field and simulation data were often partial speed-flow graphs, the comparison was only made over the space occupied by the field graph. The objective function (Z) for the speed-flow graph calibration of simulation (S) to field (F) was:

Z = Sum of all the speed-flow area in the field data that was not covered by the simulated data.

$$= F - F \cap S$$

The result of the calibration process, for convenience, is presented again in Figure 10.1. The calibration was achieved by modifying CC1, CC2, CC3, CC4 and CC5. The suggested values are CC1 = 1.28 s; CC2 = 8.11 m; CC3 = -10.92 s; CC4 = -0.45; and CC5 = 1.06 .

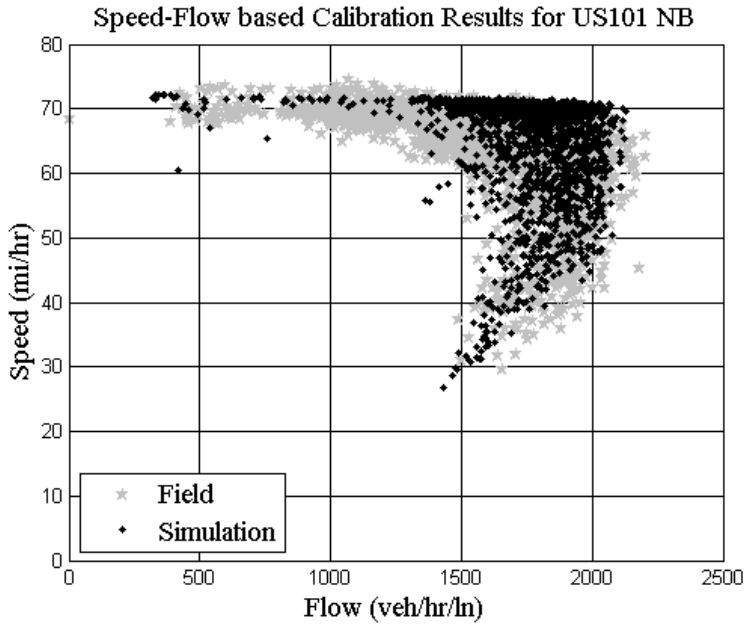

Figure 10.1 Speed Flow based calibration results for US 101 NB.

However, as expected, the speed flow graph based macroscopic calibration resulted in multiple plausible solutions. There was a need to understand the degree-of-freedom of the speed-flow based objective to reduce the number of plausible solutions. In addition, further analysis is required to understand the validity of the suggested values. For instance, in a closing condition, if speed differences exceed absolute value of CC4, the driver reacts by braking. Similarly if CC5 is broken, the driver reacts in an opening

condition by accelerating. Intuitively speaking, CC4 and CC5 should exhibit an asymmetrical behavior since drivers are more sensitive when closing than when opening. The calibrated values for CC4/CC5 were not in compliance with driver behavior and were different from the default values in VISSIM. In order to improve upon the previous calibration, research into supplementing macroscopic calibration with microscopic was undertaken. .

10.2 | METHODOLOGY

The integrated calibration is based upon using both microscopic and macroscopic data to calibrate a psycho-physical car following model such as the Wiedemann car following model. A first step in the integrated calibration approach is to perform microscopic calibration (see chapter 8: generalized calibration methodology). This served to fix the values and ranges for certain parameters so that the macroscopic calibration could be performed on a reduced set of parameters. Microscopic data from Next Generation Simulation (NGSIM) data collection effort (NGSIM, 2004) was utilized in range definition (see chapter 8: Range Definition Model) of calibration parameters and qualitative calibration of the Wiedemann car following model. The calibration methodology in a simplified version is presented in Figure 10.2. The macroscopic calibration is again based on dissimilarity measures for speed flow graphs.

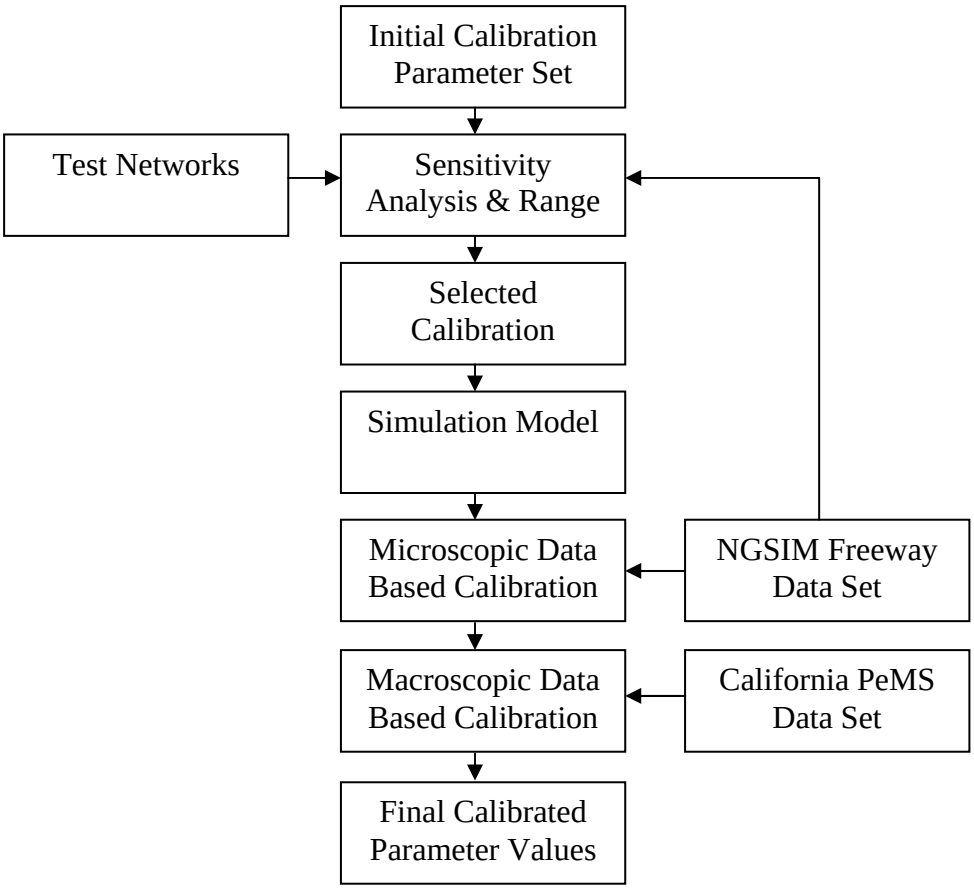

Figure 10.2 Integrated calibration.

10.3 | MICROSCOPIC DATA BASED CALIBRATION

The vehicle trajectory data provided by the Federal Highway Administration (FHWA) via the World Wide Web through its Next Generation Simulation (NGSIM) community effort served as the source for microscopic data. The data consisted of sub-second vehicle trajectory information from two freeways in California: US101 and I80. Although microscopic data provided detailed information of the traffic flow processes, it has some disadvantages (see chapter 6: Disaggregate Data). For instance, in many cases, microscopic data was collected over a small period of time covering a small local geometric region. Thus the applicability of such local information to other temporal and spatial situations could be questioned – unless if an invariance under temporal and spatial

transformation can be proved. Despite the aforementioned caveat, microscopic data could still provide valuable information about calibration parameters used in car following models. This is especially true in psycho-physical car following models where calibration parameters are physical perception thresholds and not just purely mathematical parameters. It is more likely that the perception thresholds population of drivers is invariant to location within a geographic region.

As mentioned, many of the Wiedemann car-following model thresholds can be represented on relative distance vs. relative velocity (dx-dv) graphs (see chapter 2: Wiedemann Car Following Models). For this reason, much of the effort was dedicated to developing these graphs by analyzing vehicle trajectories of pairs of leading and following vehicles. A typical relative distance vs. relative velocity graph consists of longitudinal and speed oscillation in a following process. Since many of the Wiedemann thresholds are velocity dependent, accurate representation of these thresholds required an additional speed dimension. However, a full calibration or analysis of thresholds over a 3-dimensional graph is a daunting task. Therefore, analyzing thresholds over particular speed levels or intervals is a much more efficient solution.

To develop oscillation loops, relative distance vs. relative velocity graphs are plotted for different leader-follower pairs. An oscillation process is defined by a leader-follower pair starting at a point on the dx-dv graph and approximately returning to the same location over the entire period of oscillation. A typical oscillation process and the terms used in data analysis are shown in Figure 10.4. In this study, researchers analyzed over 300 different oscillation processes from NGSIM data with samples equally distributed among US101 and I80 data sets.

In order to extract usable information that can be related to these four parameters, the researchers extracted speed/distance oscillation loops from the graph. For example in figure 10.3, three distinct oscillation loops: red, blue, and green were obtained and studied. The oscillation loop is selected based on the vehicle starting at a point on the graph and approximately returning to that point over time, thus completing a single oscillation process.

For instance, the red loop from figure 10.3 is presented in isolation in figure 10.4. Figure 10.4 describes data collected from these isolated loops.

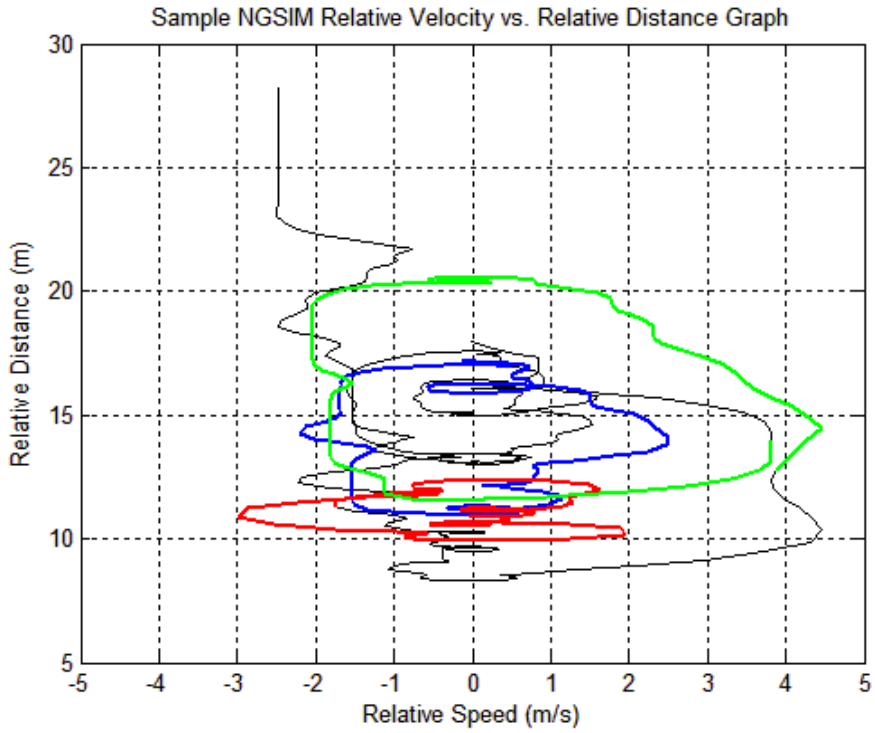

Figure 10.3 Sample NGSIM relative velocity vs. relative distance graph

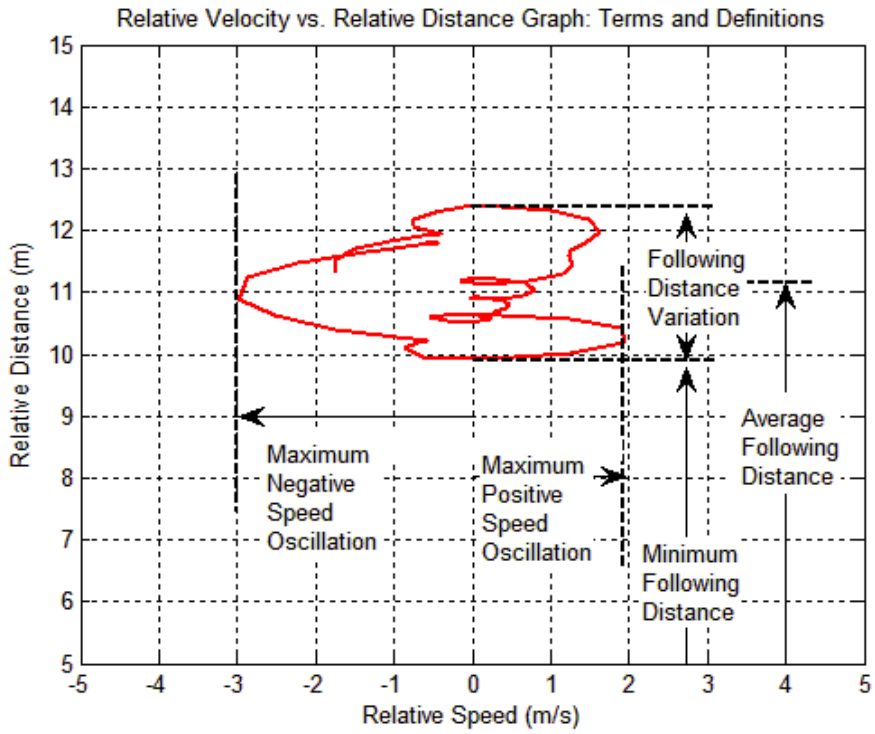

Figure 10.4 Relative velocity vs. relative distance graph: terms and definitions.

Six different types of data were collected from analysis of the oscillation process.

1. Minimum following distance during oscillation
2. Following distance variation during oscillation
3. Average following distance during oscillation
4. Maximum absolute positive speed oscillation
5. Maximum absolute negative speed oscillation
6. Average following speed during oscillation

The aforementioned six data types are not in definition same as the driver behavior parameters in VISSIM such as CC2, CC4, and CC5. However, such data can be used in qualitative calibration of these parameters. As an example, the following distance variation and CC2 are considered. These two values are not identical because the following threshold was defined by both a dx_safe term and CC2, where

$dx\_safe = L_{n-1} + CC0 + CC1 * v$; L_{n-1} = length of the leader; v = speed of the vehicle

While CC2 is a speed independent term, dx_safe is a speed dependent term. Similarly, maximum positive and negative speed oscillations are not same as CC4 and CC5. One reason is that CC6 also plays a role in defining speed thresholds, and other reason is that observed oscillations in car following are not same as thresholds. A more detailed discussion about these "action" points is presented in the following section. However, maximum speed oscillations are still good representatives of speed oscillation thresholds as well as their symmetry or asymmetry.

10.4 | MICROSCOPIC CALIBRATION RESULTS

The relative distance vs. relative velocity graphs produced from NGSIM vehicle trajectories are used for microscopic calibration. First, the following variation in an oscillation process was analyzed for US101 and I80 to obtain a better understanding of CC2. The histograms from both datasets were presented in Figure 10.5. The average following variation for I80 and US101 are 5.5 m and 5 m. Both histograms showed a monotonically decreasing frequency for higher values of following variation. The dependence of following variation on following distance was also analyzed for both data sets and was presented in Figure 10.6. The following variation seems to be fairly invariant of following distance with many of the values below 10 m at all speed levels, except for some outliers. In summary, the following variation is consistent with the Wiedemann car following model and is fairly constant across various average following-speed levels and following distances.

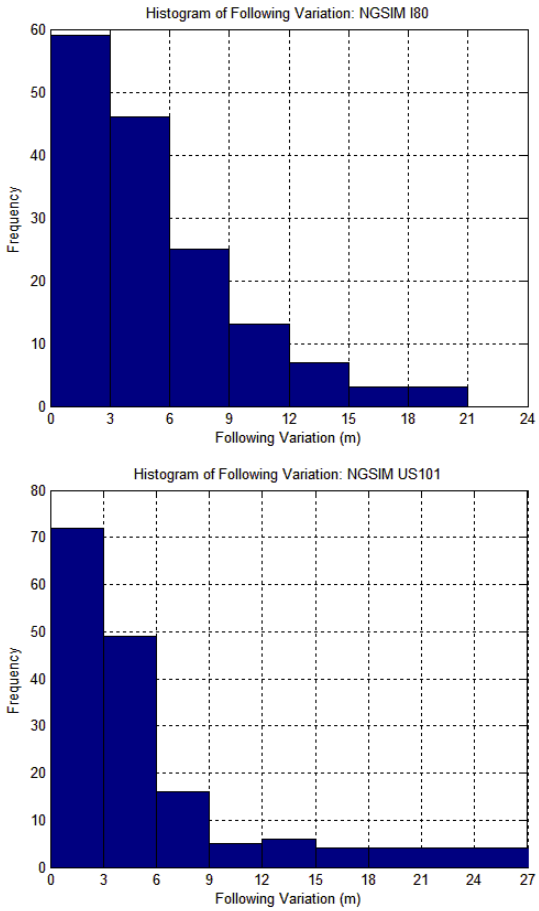

Figure 10.5 Histograms of following variation for I80 and US101 data sets.

The maximum positive and negative speed oscillations were obtained to obtain a better understanding of speed thresholds (CC4, CC5) in a following process. The maximum positive and negative speed oscillations from each complete oscillation process were plotted on a relative distance vs. relative velocity graph and are presented in Figure 10.7. The main observation from these graphs is the symmetry in positive and negative speed oscillations. The symmetry is counter-intuitive, since one would expect the drivers to be more sensitive to a closing process than an opening process. The graphs from US101 and I80 also show amazing similarity, which might mean an underlying similarity in traffic behavior invariant of the location. This is expected since the driver perception thresholds

of a population of driver within reasonable geographic regions do not change by much. Both freeways show a maximum of -1 m/s for negative speeds and minimum of 1 m/s for positive speeds for the maximum speed oscillations. The graphs also show an increasing magnitude of maximum speed oscillation with increasing distance, which is modeled by CC6 parameter in the Wiedemann car following model.

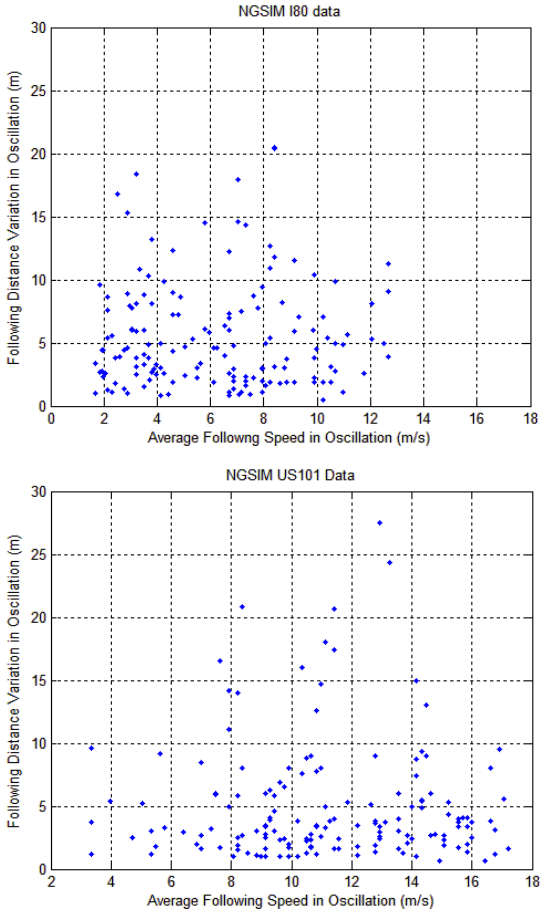

Figure 10.6 Average following speed vs. following distance variation.

The relative distance vs. relative velocity graphs were also developed to determine action points on these graphs. Action points represent changes in direction of slope of an oscillation trajectory on a relative distance vs. relative velocity graph. In other words, it represents the following driver either applying relative acceleration to

avoid moving away from a leading vehicle or applying relative deceleration to avoid moving closer to a leading vehicle; i.e., driver was changing relative acceleration from positive to negative value or vice versa. Action points were first used by Todosiev (Todosiev, 1963) to calibrate car following thresholds in a close following mode. The graphs from US101 and I80 from different time periods are shown in Figure 10.7. The graphs showed remarkable similarity in distribution over both data sets. These graphs are fairly uniform across positive and negative relative speeds indicating a symmetric behavior. These graphs do not show an increasing speed oscillation over increasing following distances. However in Figure 10.8, the maximum speed oscillations show an increasing magnitude of speed oscillation over increasing distances.

The action points for US101 and I80, figures 10.7 and 10.8, data also showed a symmetric speed oscillation, and thus the calibration effort was narrowed to symmetric speed thresholds (CC4 and CC5). It is important to note that action points are not identical to perception thresholds. In perception or threshold based model such as the Wiedemann car following model, drivers reactions are modeled based on thresholds. The driver continues to be in the current driving ("inertia") state until a threshold was "broken". In a discrete time-step simulation model, computations of vehicle states and thresholds are not continuous. Thus the discrete computation will also have resulted in action points being different from the threshold. Hence, simulation resolution also plays an important role in the analysis of action points and perception thresholds. In figure 10.8, it is seen that the minimum of maximum-magnitude "action" points, in other words minimum of max-speed-oscillation, from both data sets are -1 and 1 m/s. Therefore, it is more likely that the speed thresholds are lower than -1 and 1 m/s.

NGSIM I80 Data	NGSIM US101 Data
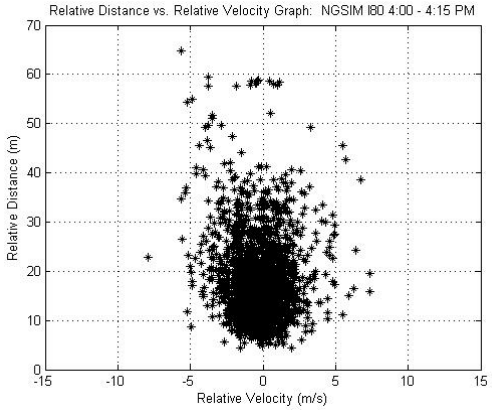	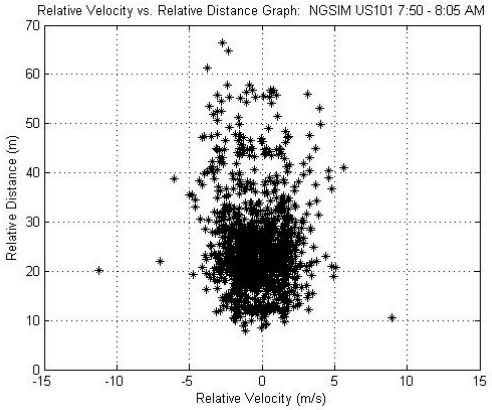
(a)	(d)
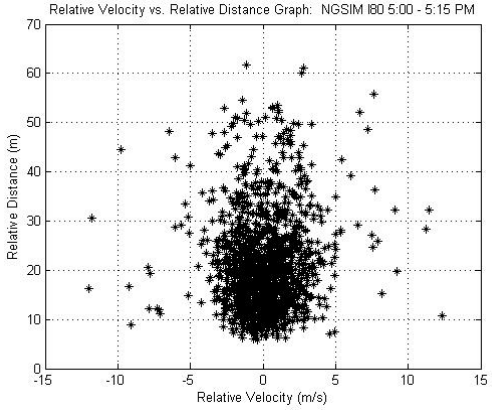	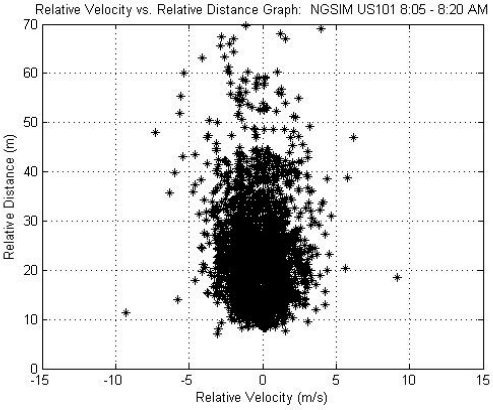
(b)	(e)
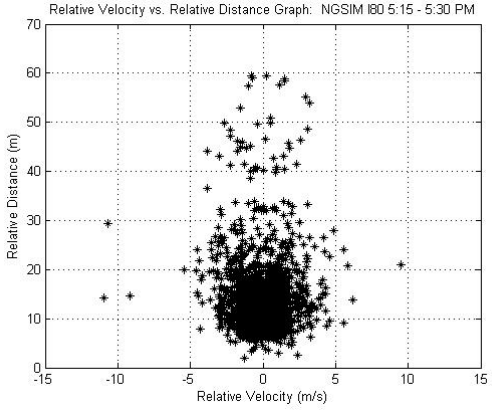	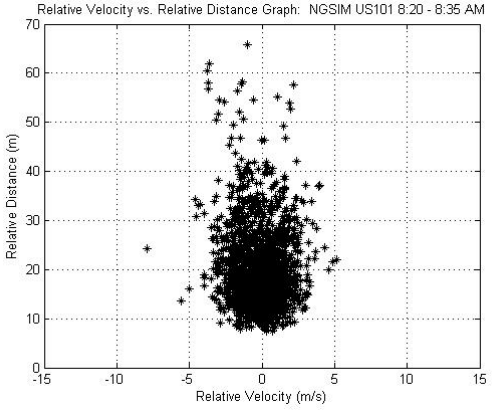
(c)	(f)

Figure 10.7 Action points in relative velocity vs. relative distance graphs for US101 and I80 datasets.

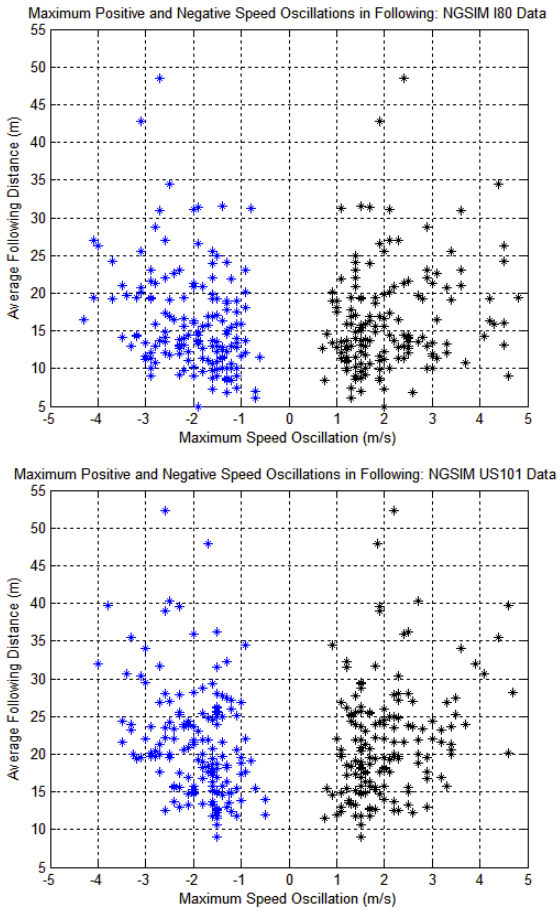

Figure 10.8 Maximum positive and negative speed oscillation vs. average following distance.

10.5 | INTEGRATED MACRO/MICROSCOPIC CALIBRATION

An integrated process was developed to utilize both microscopic and macroscopic data in accurately calibrating the model. In this process, several parameters were exposed to the process and the best fitness function values from each calibration were noted. The final parameter values and best fitness values are shown in Table 10.1. This process also helped in determining the degree of freedom of the objective function. In the first calibration run, all of the five parameters CC1, CC2, CC3, CC4, and CC5 are exposed; the resulting speed-flow graph provided good coverage over the field speed flow graph. However, the CC4 and CC5 values do not conform to the observations from the

microscopic calibration. A CC4 value of -2.50 m/s resulted in an approximate shockwave speed of 20 mi/hr, which is much higher than real-world values of approximately 12 mi/hr (Lu and Skabardonis, 2007). Tests were then conducted to determine CC4 values that resulted in shockwaves speed that were closer to real-world values. The possible solutions for CC4 values that matched shockwave speed values of 12 mi//hr ranged from -0.35 to -0.70 m/s. A second calibration run was conducted with four calibration parameters [CC1, CC2, CC3, and CC5], the resulting CC5 value was close to 2 m/s, which did not conform to symmetric speed oscillation observed in microscopic calibration. The resultant CC1 value was similar to the first calibration run. The final fitness function value was actually slightly lower than the first calibration run. The speed flow graph from the calibration process is shown in Figure 10.9(a).

In the third calibration run, the significance of CC3 parameter on the fitness function was tested. The CC3 threshold represents approaching process and represents the transition from free flow to approaching process. A calibration run was conducted using three parameters [CC1, CC2, and CC5]. The resulting parameter values are shown in Table 10.1 and the speed flow graph is shown in Figure 10.9 (b). There was no reduction in the final fitness function value. However, slightly lower CC1 value and slightly higher CC2 values resulted. This can be better explained by the fact that average following distances in a following condition lie between dx_safe and $dx\_safe + CC2$. Similar following distance can be achieved by slightly increasing CC1 and decreasing CC2 or vice versa. Therefore, this could be due to the combination effect among the parameters, i.e. the non-uniqueness of multi-parameter optimization. In addition, CC5 value suggested by the calibration was still high at 2.30 m/s.

In the fourth calibration run, CC4 and CC5 values from microscopic calibration were employed. Only two parameters CC1 and CC2 were calibrated. The resultant CC1 and CC2 values were close to the values suggested in previous runs. However, the final fitness value increased by 5% from previous runs. The final speed flow graph after calibration is shown in Figure 10.9(c). Although the final fitness function value increased by 5%, this resulted in better combined microscopic and macroscopic objective. A fifth calibration run using two parameters CC1 and CC2 was conducted at CC4 = -0.35 and CC5 = 0.35. There was no change in the final fitness value, but higher CC1 and lower CC2 values resulted. In this case, narrowing the dv-range of the oscillation, assuming the applied acceleration values were unchanged, will result in a narrower dx-range as well, which was reflected by the smaller CC2 value. But since CC1 is the lower bound of following distance, it must increase to get the same observed average following distances. This was again consistent with the car following model behavior. The final speed flow graph after calibration was shown in Figure 10.9(d). As a result of the integrated macroscopic/microscopic calibration runs, it was determined that CC1 and CC2 parameters along with CC4 and CC5 values of [-0.70 and 0.70] or [-0.35 and 0.35] resulted in a good balance in calibration objectives. In other words, CC4 and CC5 values achieved consistency with microscopic calibration while the overall fitness values attained optimality through macroscopic calibration.

Table 10.1 Speed Flow Based Calibration with Varying Number of Parameters

	Calibration Parameters					Fitness	Fixed Parameters		
	CC1	CC2	CC3	CC4	CC5	Value	CC4	CC5	Others
Default	0.9	4	-8	-0.35	0.35	-	-	-	-
1	1.09	10.59	-7.91	-2.50	0.64	193	-	-	default
2	1.1	7.97	-12.3	-	2	192	-0.7	-	default
3	1.04	9.01	-	-	2.31	193	-0.7	-	default
4	1.16	9.9	-	-	-	204	-0.7	0.7	default
5	1.29	5.65	-	-	-	204	-0.35	0.35	default

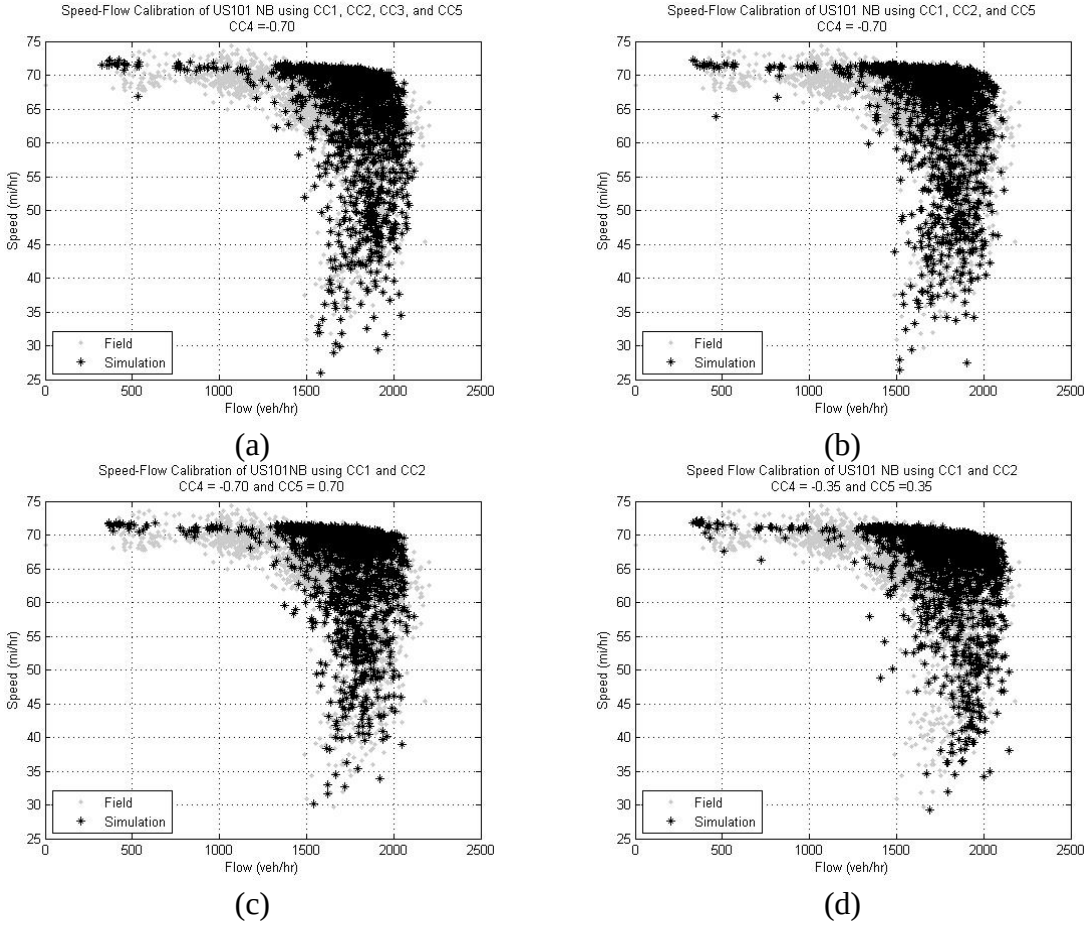

Figure 10.9 Speed flow based calibration of US101 NB with varying numbers of parameters.

10.6 | SIMPLIFIED CALIBRATION METHOD FOR PRACTITIONERS

Because the integrated macroscopic/microscopic calibration was so elaborate, a simplified methodology was developed for practitioners. Flow contours were developed

at different CC1 and CC2 values so that parameters could be calibrated to achieve field capacities. CC4/CC5 values were not parameters in the flow contours since their calibration was arguably the most labor intensive portion of the integrated calibration process. The flow contours were developed for two sets of CC4/CC5 values: [1] CC4 = -0.70 and CC5 = 0.70 and [2] CC4 = -0.35 and CC5 = 0.35. The graphs for option 1 are shown in Figures 10.10(a)-(d). The graphs were developed for 0% trucks and free flow speed of 70 mi/hr for values of capacity that were sustained for 5, 15, 30, and 60 minutes. Thus the user could easily determine the plausible set of parameters using sustained flows from different time periods. Users with partial information could still benefit from these solutions, even though the solutions might not be unique.

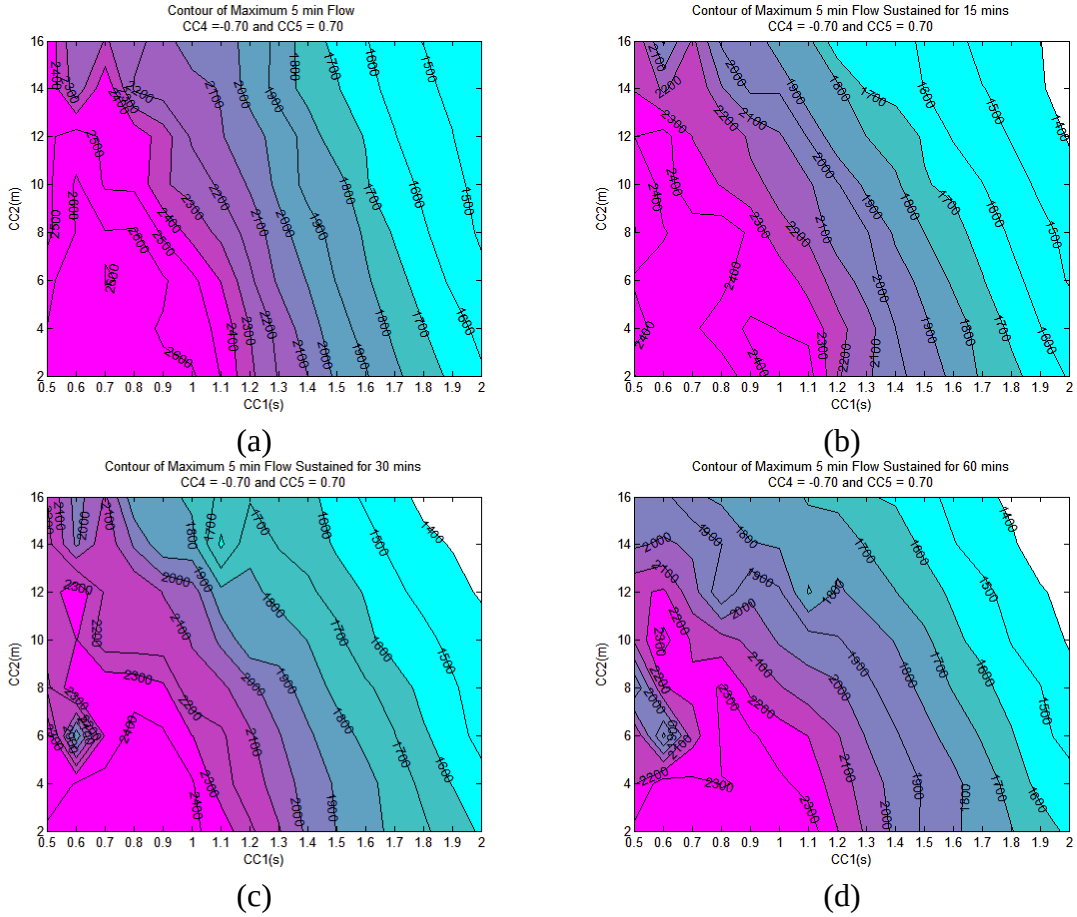

(a) (b)

(c) (d)

Figure 10.10 Flow Contours of maximum 5 min flows sustained for varying amounts of time. [CC4 = -0.70 and CC5 = 0.70]

10.7 | CONCLUSIONS

In this chapter, a new calibration based on integrated use of microscopic and macroscopic data was presented. The research built upon macroscopic based calibration of microsimulation models using speed-flow graphs presented in the previous chapter. The addition of detailed analysis of oscillation processes using microscopic vehicle trajectories from NGSIM data provided valuable information in qualitative calibration of the microsimulation model. From analysis of vehicle trajectories, speed thresholds in closing and opening process in car following (CC4, CC5) were found to be symmetric for US conditions. Macroscopic calibration using multiple calibration parameter sets was helpful in identifying the degree-of-freedom of the speed-flow based objective function. Using this procedure, the set of calibration parameters for speed-flow based macroscopic calibration was reduced to the most important parameters: CC1 and CC2. By identifying the degree-of-freedom of the objective function, the number of plausible solutions in search terms was reduced. The microscopic data was also valuable in reducing the number of plausible solutions; for instance, CC4 and CC5 parameter combinations were reduced to symmetric combinations.

The maximum positive and negative speed oscillation vs. following distance graphs, Figure 10.7, showed similarity between US101 and I80 data sets. Similarly, histograms from average following variations, Figure 10.5, also showed similarity between data sets in terms of mean and shape of the distribution. The scatter and distribution of action points on relative distance vs. relative velocity graphs, figures 10.7 and 10.8, also showed inherent similarity in driving behavior between two different locations. It was helpful to identify similarity in traffic behavior invariant of locations,

since such information is valuable in calibration of simulation models from different locations. The research also raised some questions that still needed to be answered. For example, the action points were analyzed for different time periods and locations, but it would be interesting to analyze such data in higher detail. It would also be interesting to replicate action point density curves at various speed levels that were first used by Todosiev(1963) in calibrating thresholds in close following conditions. In addition, it would also be important to address the level of applicability of microsimulation data in calibrating simulation models that were at a different location.

The integrated microscopic/macroscopic data based calibration achieved a balance in calibration objectives at both microscopic and macroscopic levels. In addition to the comprehensive calibration, a simplified methodology based on the final parameter set, CC1 and CC2, was also developed. The simplified solution included flow contours graphs of sustained five minute flows over different period of time (15, 30, and 60 minutes) over the CC1/CC2 parameter plane. The simplified solution enables practitioners to easily calibrate to field capacity values.

11 | Conclusions

"Our greatest glory is not in never falling, but in rising every time we fall."

Confucius

A generalized formulation of calibration of traffic simulation models based on representations and invariants was developed in this research. The formulation defines a formal definition of calibration that partly fills the void in the current state-of-the art. The generic formulation of calibration definition and accompanying procedures provided a deeper understanding of the nature of the problem. Representation and invariants were shown to form an important part of the calibration definition. Calibration objective is defined over three levels of representation: traffic, dissimilarity, and search. These three levels of representation succinctly encompass all of the currently used calibration procedures, while presenting a new generic methodology that improves the quality of calibration by utilizing several traffic flow processes. Each of these three levels of representation results in certain loss of information, but such representations are ultimately necessary in solving the complex problem of calibration. The representations also provide insight into the flow of information in the calibration process. The concept of Invariance was shown to play an important role in understanding the inner-workings of

complex systems. The property of invariance of representation (traffic and dissimilarity) is necessary in accurately solving the calibration objective. The invariance concept improved the calibration process by developing traffic representations that are robust to input or measurement errors and reducing the calibration parameter set to the most important parameters.

The lessons learned from the theoretical formulation of calibration were utilized in improving the calibration process. In the first level, several traffic representations were evaluated for use in calibration. In the second level, pattern recognition based dissimilarity measures were seamlessly applied to measure the dissimilarity of traffic representations. These methods were then utilized in calibration microsimulation model of a real-world freeway network in California, it was demonstrated that a calibration method based on speed-flow graphs performed better than a calibration method based on capacity or sustained flow. The case study also demonstrated the usefulness of a pattern recognition based dissimilarity representation for automated measuring the degree-of-closeness of graphs. The automated pattern recognition based objective provided great benefit for evolutionary algorithm based search of calibration parameters.

The automation of the graph matching using pattern recognition provides new way of quantifying the degree-of-closeness of graphs. It solves various consistency problems that occur in eye-balling techniques previously applied by researchers. The automated graph matching concept can be extended to higher dimensions based on similar principles to n-dimensional point sets. The pattern recognition methods applied in the case study were simple, flexible, efficient, extendable and robust. These are some of the important qualities that are required for implementation in the real-world. The

simplicity of the model helps practitioners develop and deploy pattern recognition based calibration that require minimal to no human intervention.

The main advantage of dissimilarity measures is that there are no specific assumptions being made about the system, data, population, or the model. The measures are equally applicable in other models in a non-traffic arena. The dissimilarity measures can also be applied to macroscopic or mesoscopic simulation models, without any major modifications.

Results from the calibration based on macroscopic traffic representation – speed-flow graphs - in California revealed the speed-flow representation showed a higher degree of freedom with respect to the calibration parameters; thereby, expectedly resulting in multiple plausible solutions. It was identified that the speed-flow graphs were partially invariant to some of the calibration parameters. In order to accurately calibrate the model, microscopic traffic representations based on leader-follower car-following processes was utilized in calibrating the parameters. Several leader-follower vehicle pairs from NGSIM vehicle trajectories were analyzed to obtain "action points", which are representative of speed perception thresholds in psycho-physical car following models. The data was utilized to calibrate the speed-thresholds in an iterative method along with macroscopic calibration. The integrated methodology allowed for accurate calibration of parameters based on concepts of representation and invariants.

Finally, all of the methodologies developed in this research will help practitioners reach better calibrated modeled more efficiently. Both the case studies demonstrated simpler methods that will help practitioners calibrate their simulation models accurately and efficiently. The first case study proposed alternate traffic networks capable of

reproducing a variety of traffic conditions for calibrating using speed-flow graphs to improve the algorithm run times. In the second case study, a very detailed calibration was followed by a simpler methodology based on parameter search over capacity contour, which further increased the simplicity of calibration.

The research raised several questions; some of the questions were answered during the study, but some other interesting questions remain unanswered. Especially, related to representations and invariants. One of the most interesting questions raised during the research was of existence of invariant traffic representations. For instance: are there any traffic representations that are invariant of local driving behavior; i.e., do any traffic representations exist that are applicable to all drivers? This important property is essential in developing accurate base simulation models that are applicable in different countries or states within a country. Since such relationships are invariant of local driver behavior change, all simulation models must satisfy such a condition. To answer these questions one suggested way is to research the various transformations that are valuable and find traffic representations, relationships, or flow processes that are invariant under such transformations. This study will inherently lead to a deeper understanding of the traffic flow processes and relationships.

12 | References

1. Abdulhai, B., J. B. Sheu, and W. Recker. (1999) Simulation of ITS on the Irvine FOT Area Using 'PARMICS 1.5' Scalable Microscopic Traffic Simulator: Phase I: Model Calibration and Validation. UCB-ITS-PR-99. California PATH Research Report.
2. Alperen, B., and M. C. Gersten. (1987). Use of the FREQ8PL Model To Evaluate an Exclusive Bus-High-Occupancy-Vehicle Lane on New Jersey Route 495. In *Transportation Research Record: Journal of the Transportation Research Board, No. 1132,* TRB, National Research Council, Washington, D.C., pp. 42–52.
3. Aycin, M. F., and B. F. Benekohal. (1998). Linear Acceleration Car-Following Model Development and Validation. In *Transportation Research Record: Journal of the Transportation Research Board, No. 1644,* TRB, National Research Council, Washington, D.C., pp. 10-19.
4. Banks, J. H. (1991). The Two-Capacity Phenomenon: Some Theoretical Issues. In *Transportation Research Record: Journal of the transportation Research Board, No. 1320, TRB. National Research Council,* Washington D. C., pp. 234-241.
5. Bayarri, M. J., J. O. Berger, G. Molina, N. M. Rouphail, and J.Sacks. (2004). Assessing Uncertainties in Traffic Simulation: A Key Component in Model Calibration and Validation. In *Transportation Research Record: Journal of the Transportation Research Board, No. 1876,* TRB, National Research Council, Washington, D.C., 2004, pp. 32–40.
6. Benekohal, R. F., and J. Treiterer. (1988). CARSIM: Car-Following Model for Simulation of Traffic in Normal and Stop-and-Go Conditions. In *Transportation Research Record: Journal of the Transportation Research Board, No. 1194,* TRB, National Research Council, Washington, D.C., pp. 99–111.
7. Brockfeld, E., R.D. Kühne, and P. Wagner. (2004). Calibration and Validation of Microscopic Traffic Flow Models. In *Transportation Research Record: Journal of the Transportation Research Board No. 1876,* TRB, National Research Council, Washington, D.C., 2004, pp. 62–70.
8. Brilon, W., J. Geistefeldt, and H. Zurlinden. Implementing the Concept of Reliability for Highway Capacity Analysis. Presented at 87th Annual Meeting of the Transportation Research Board, Washington, D.C., 2007.
9. Cheu, R. L., W. W. Recker, and S. G. Ritchie. (1994). Calibration of INTRAS for Simulation of 30-sec Loop Detector Output. In *Transportation Research Record: Journal of the Transportation Research Board, No.1457,* TRB, National Research Council, Washington, D.C., pp. 208–215.
10. Cheu, R. L., X. Jin, K. C. Ng, Y. L. Ng, and D. Srinivasan. (1998). Calibration of FRESIM for Singapore Expressway Using Genetic Algorithm. In Journal of Transportation Engineering, Vol. 124, No. 6, Nov-Dec 1998.
11. Dixon, P. M. (1997). Calibrating and validating TRAF-NETSIM Model of Single-Point Urban Interchange. . In *Transportation Research Record: Journal of the Transportation Research Board, No. 1591,* TRB, National Research Council, Washington, D.C., pp. 38-44.

12. Dowling, R., A. Skabardonis, J. Halkias, G. McHale, and G. Zammit. (2004). Guidelines for Calibration of Microsimulation Models: Framework and Applications. In *Transportation Research Record: Journal of the Transportation Research Board, No. 1876*, TRB, National Research Council, Washington, D.C., pp. 1–9.
13. Duda, R. O., and P. E. Hart. (1973). Pattern Classification and Scene Analysis. A Wiley-Interscience Publication, John Wiley and Sons, New York.
14. Drew, D. R. (1968). *Traffic Flow Theory and Control*. McGraw-Hill Book Company, New York.
15. Federal Highway Administration. (2004). Traffic Analysis Toolbox Volume III: Guidelines for Applying Traffic Microsimulation Software. FHWA-HRT-04-040. Washington D.C.
16. Fellendorf, M. and P. Vortisch. (2001). Validation of the Microscopic Traffic Flow Model VISSIM in Different Real-World Situations. Presented at 80th Annual Meeting of the Transportation Research Board, Washington, D.C.
17. Gardes, Y., A.D. May, J. Dahlgren, and A. Skarbardonis. (2002). Bay Area Simulation and Ramp Metering Study. UCB-ITS-PRR_2002-6, California PATH Research Report.
18. Gazis, D. C., R. Herman, and R. B. Potts (1959). *Car Following Theory of Steady State Traffic Flow*. Operations Research 7(4), pp. 499-505.
19. Gazis, D. C., R. Herman, and R. W. Rothery (1961). *Non-Linear Follow the Leader Models of Traffic Flow*.Operations Research, 9, pp. 545-567.
20. Gazis, D. C., R. Herman, and R. W. Rothery (1963). *Analytical Methods in Transportation: Mathematical Car-Following* Bonn, Germany. *Theory of Traffic Flow*. Journal of the Engineering Mechanics Division, ASCE Proc. Paper 3724 89(Paper 372), pp. 29-46.
21. Gerlough, D. L., and M. J. Huber. (1975). *Traffic Flow Theory: A Monograph.* Special Report 165, TRB, National Research Council, Washington D.C.
22. Gomes, G., A. May, and R. Horowitz. (2004). Congested Freeway Microsimulation Model Using VISSIM. In *Transportation Research Record: Journal of the Transportation Research Board, No. 1876*, TRB, National Research Council, Washington, D.C., pp. 71–81.
23. FHWA (2005) Traffic Flow Theory http://www.tfhrc.gov/its/tft/tft.htm. Accessed June, 2007.
24. *Highway Capacity Manual*. (2000). TRB, National research Council, Washington, D. C.
25. Hourdakis, J., P. G. Michalopoulos, and J. Kottommannil. (2003). Practical Procedure for Calibrating Microscopic Traffic Simulation Models. In *Transportation Research Record: Journal of the Transportation Research Board, No. 1852*, TRB, National Research Council, Washington, D.C., pp. 130–139.
26. Jha, M., G. Gopalan, A. Garms, B. P. Mahanti, T. Toledo, and M.E. Ben-Akiva. (2004). Development and Calibration of a Large-Scale Microscopic Traffic Simulation Model. In *Transportation Research Record: Journal of the Transportation Research Board, No. 1876*, TRB, National Research Council, Washington, D.C., 2004, pp. 121–131.
27. Kim, K., and L. R. Rilett. Genetic-Algorithm-Based Approach for Calibrating Microscopic Simulation Models. *Proc., IEEE Intelligent Transportation Systems Conference*, IEEE, Oakland, Calif., 2001, pp. 698–704.
28. Kim, S. J., W. Kim, and L. R. Rilett. (2005). Calibration of Microsimulation Models Using Nonparametric Statistical Techniques. In *Transportation Research Record: Journal of the Transportation Research Board, No. 1935*, Transportation Research Board of the National Academies, Washington, D.C., 2005, pp. 111–119.
29. Khasnabis, S, R. R> Karnati, R. K. Rudraraju. (1996). NETSIM-Based Approach to Evaluation of Bus Preemption Strategies. In *Transportation Research Record: Journal of the Transportation Research Board, No. 1554*, TRB, National Research Council, Washington, D.C., pp. 80-89.
30. Kometani, E. and T. Suzaki (1958). *On the Stability of Traffic Flow.* J. Operations Research, Japan 2, pp. 11-26.

31. Liebermann E., and A. K. Rathi. (2005). Traffic Simulation. In *Revised Monograph on Traffic Flow Theory* (N. H. gartner, C.J. Messer, and A. K. Rathi, ed.). Ma, T., and B. Abdulhai. (2002). Genetic Algorithm-Based Optimization Approach and Generic Tool for Calibrating Traffic Microscopic Simulation Parameters. In *Transportation Research Record: Journal of the Transportation Research Board, No. 1800*, TRB, National Research Council, Washington, D.C., pp. 6–15.
32. Lu, X., and A. Skabardonis. Freeway Traffic Shockwave Analysis: Exploring NGSIM Trajectory Data. Presented at 86th Annual Meeting of the Transportation Research Board, Washington, D.C., 2007.
33. Ma, T., and B. Abdulbai. (2002). Genetic Algorithm-Based Optimization Approach and Generic Tool For Calibrating Traffic Microsimulation Parameters. In *Transportation Research Record: Journal of the Transportation Research Board, No. 1800*, TRB, National Research Council, Washington, D.C., pp.6-16.
34. May, A. D. (1990). *Traffic Flow Fundamentals*, Prentice-Hall Inc., New Jersey.
35. Michales, R. M. (1965). Perceptual Factors in Car Following. Proceedings of 2nd Intrernational Symposium on Theory of Traffic Flow.
36. NGSIM. (2007). Home of the Next Generation Simulation Community. Federal Highway Administration. Washington D.C., http://www.ngsim.fhwa.dot.gov/. Accessed June, 2007.
37. Ngoduy, D., S. P. Hoogendoorn, and H. J. V. Zuylen. (2004). Comparison of Numerical Schemes for Macroscopic Traffic Flow Models. In *Transportation Research Record: Journal of the Transportation Research Board, No. 1876*, TRB, National Research Council, Washington, D.C., pp. 52–61.
38. Park, B. and H. Qi. (2005). Development and Evaluation of a Procedure for the Calibration of Simulation Models. In *Transportation Research Record: Journal of the Transportation Research Board, No. 1934*, Transportation Research Board of the National Academies, Washington, D.C., 2005, pp. 208–217.
39. Payne, H. J., S. Thompson, G-L. C. Chang, and W. Ge. (1997). Calibration of FRESIM to Achieve Desired capacities. In *Transportation Research Record: Journal of the Transportation Research Board, No. 1591*, TRB, National Research Council, Washington, D.C., pp. 23-30.
40. PeMS. (2007) *Freeway Performance Measurement System*. California Partners for Advanced Transit and Highways. University of California Berkeley and California Department of Transportation. http://PeMS.EECS.Berkeley.EDU. Accessed June, 2007.
41. Pekalska, E., and R. P. W. Duin.(2005). *The Dissimilarity Representation for Pattern Recognition.* World Scientific Publishing Co. Pte. Ltd., Singapore.
42. *PTV*. (2007). *Vissim User Manual—V.4.30.* Planung Transport Verkehr AG, Karlsruhe, Germany, March 2007.
43. Radwan, A. E., F. Naguib, and J. Upcurch. (1991). Assessment of the Traffic Experimental and Analysis Simulation Computer Model Using Field Data. In *Transportation Research Record: Journal of the Transportation Research Board, No. 1320*, TRB, National Research Council, Washington, D.C., pp. 216-226.
44. Rakha, H., M. Van Arde, L. Bollberg, and X. Huang. (1998). Construction and calibration of a Large-scale Microsimulation Model of the Salt Lake Area. In *Transportation Research Record: Journal of the Transportation Research Board, No. 1644*, TRB, National Research Council, Washington, D.C., pp. 93-102.
45. Rakha H., and B. Crowther. (2002). Comparison of Greenshields, Pipes, and Van Aerde Car-Following and Traffic Stream Models. In *Transportation Research Record: Journal of the Transportation Research Board, No. 1802*, TRB, National Research Council, Washington, D.C., pp. 248-253.
46. Ranjitkar, P., T.Nakatsuji, and M. Asano. (2004). Performance Evaluation of Microscopic Traffic Flow Models with Test Track Data. In *Transportation Research Record: Journal of*

the Transportation Research Board, No. 1876, TRB, National Research Council, Washington, D.C., 2004, pp. 90–100.
47. Reuschel, A. (1950). Fahrzeugbewegungen in der Kolonne Beigleichformig beschleunigtem oder vertzogerten Leitfahrzeub, Zeit. D. Oster. Ing. U. Architekt Vereines Ed. (Vehicle Movements in a Platoon with Uniform Acceleration or Deceleration of the Lead Vehicle), pp. 50-62 and 73-77.
48. Rillet, L. R., K. O. Kim, and B. raney. (2001). Comparison of Low-Fidelity TRANSIMS and High-Fidelity CORSIM Highway Simulation Models with Intelligent Transportation Systems Data. In *Transportation Research Record: Journal of the Transportation Research Board, No. 1739,* TRB, National Research Council, Washington, D.C., pp. 1-8.
49. Schultz, G. G., and L. R. Rilett. (2004) Analysis of Distribution and Calibration of Car-Following Sensitivity Parameters in Microscopic Traffic Simulation Models. In *Transportation Research Record: Journal of the Transportation Research Board, No. 1876,* TRB, National Research Council, Washington, D.C., pp. 41–51.
50. Skabardonis, A. (2002). Simulation of Freeway Weaving Areas. In *Transportation Research Record: Journal of the Transportation Research Board, No. 1802,* TRB, National Research Council, Washington, D.C., pp. 115-125.
51. Stokes, R. W. and J. M. Mounce. (1984). Computer Simulation to Compare Freeway Improvements (Abridgement). In *Transportation Research Record: Journal of the Transportation Research Board, No. 971,* TRB, National Research Council, Washington, D.C., pp. 45–49.
52. Todosiev, E. P. (1963). The action-point model of the driver-vehicle-system. The Ohio State University, Report 202 A-3.
53. Toledo, T. M. E. Ben-Akiva, D. Darda, M. Jha, and H. N. Koutsopoulos. (2004). Calibration of Microscopic Traffic Simulation Models with Aggregate Data. In *Transportation Research Record: Journal of the Transportation Research Board, No. 1876,* TRB, National Research Council, Washington, D.C., pp. 10–19.
54. Toledo, T., H. N. Koutsopoulos, A. Davol, M. E. Ben-Akiva, W. Burghout, I. Andréasson, T. Johansson, and C. Lundin. (2004). Calibration and validation of Microscopic Traffic Simulation Tools: Stockholm Case Study. In *Transportation Research Record: Journal of the Transportation Research Board, No. 1831,* TRB, National Research Council, Washington, D.C., pp. 65-76.
55. Wiedemann, R.(1974). *Simulation des Straßenverkehrsflusses* (in German). Schtiftenreihe des Instituts fur Verkehrswesen der Universitat Karlsruhe, Heft 8, Germany.
56. Wiedemann, R. (1991). Modelling of RTI-Elements on Multi-Lane Roads. In *Advanced Telematics in Road Transport,* Vol. II, Elsevier, Amsterdam, Holland, pp. 1001–1019.
57. Wohl, M., and B. V. Martin. (1967). *Traffic Systems Analysis for Engineers and Planners,* McGraw-Hill Book Company, New York, pp. 496-536.
58. Zarean, M., and Z. A. Nemeth. (1988). WEAVSIM: A Microscopic Simulation Model of Freeway Weaving Sections. In *Transportation Research Record: Journal of the Transportation Research Board, No. 1194,* TRB, National Research Council, Washington, D.C., pp. 48–54.

13 | Appendix A

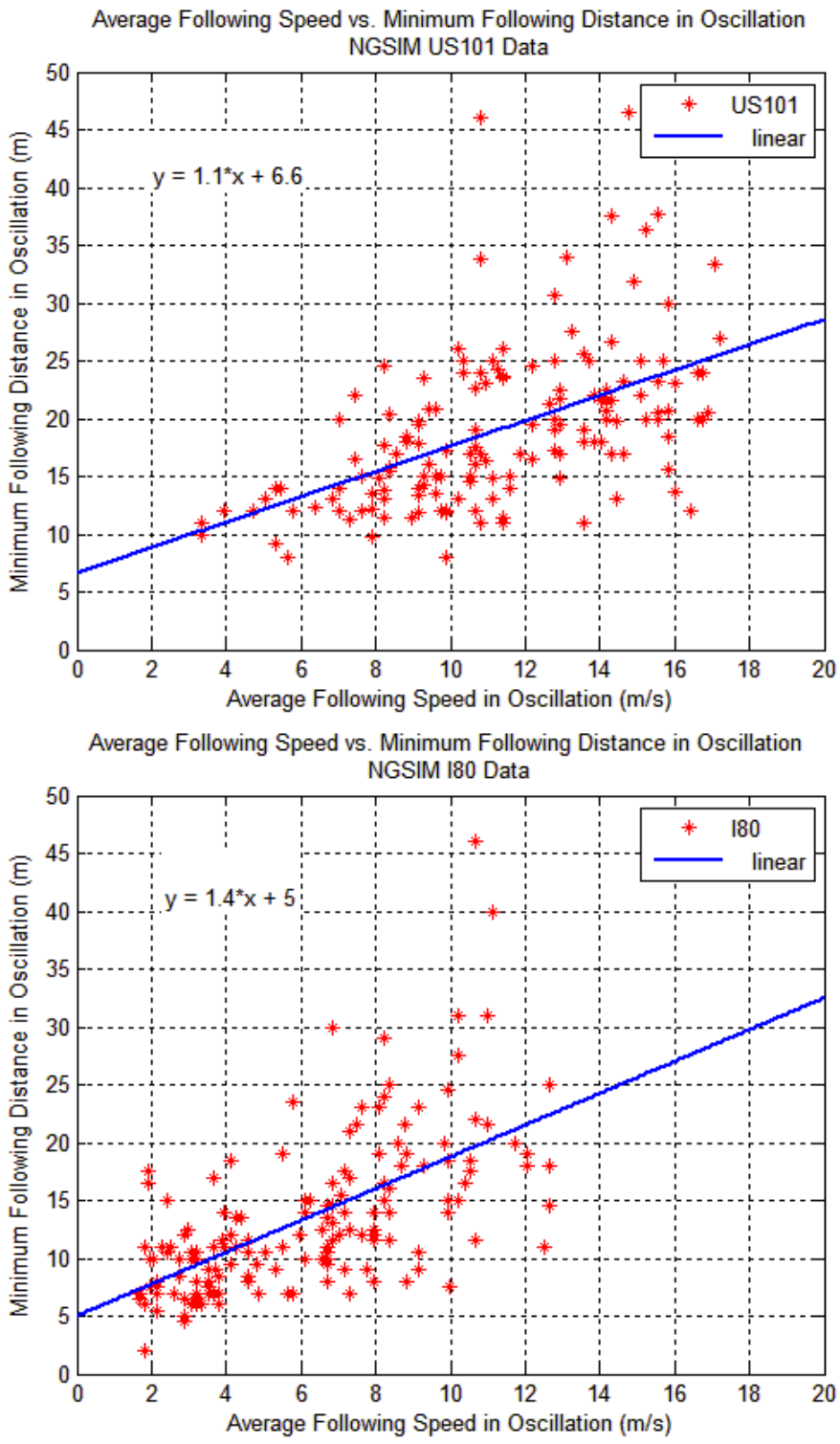

Figure 13.1 Average following speed vs. minimum following distance

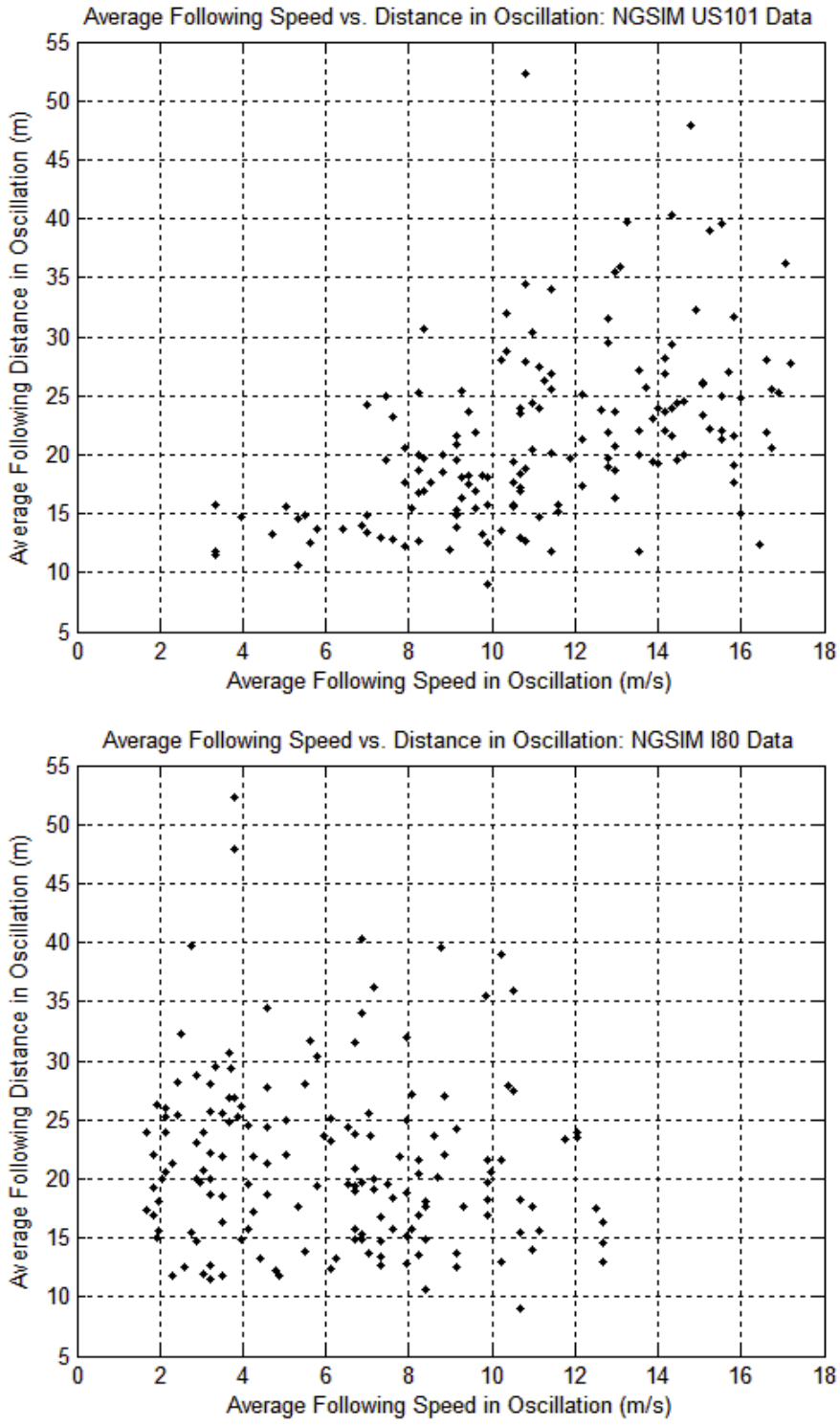

Figure 13.2 Average following speed vs. average following-distance

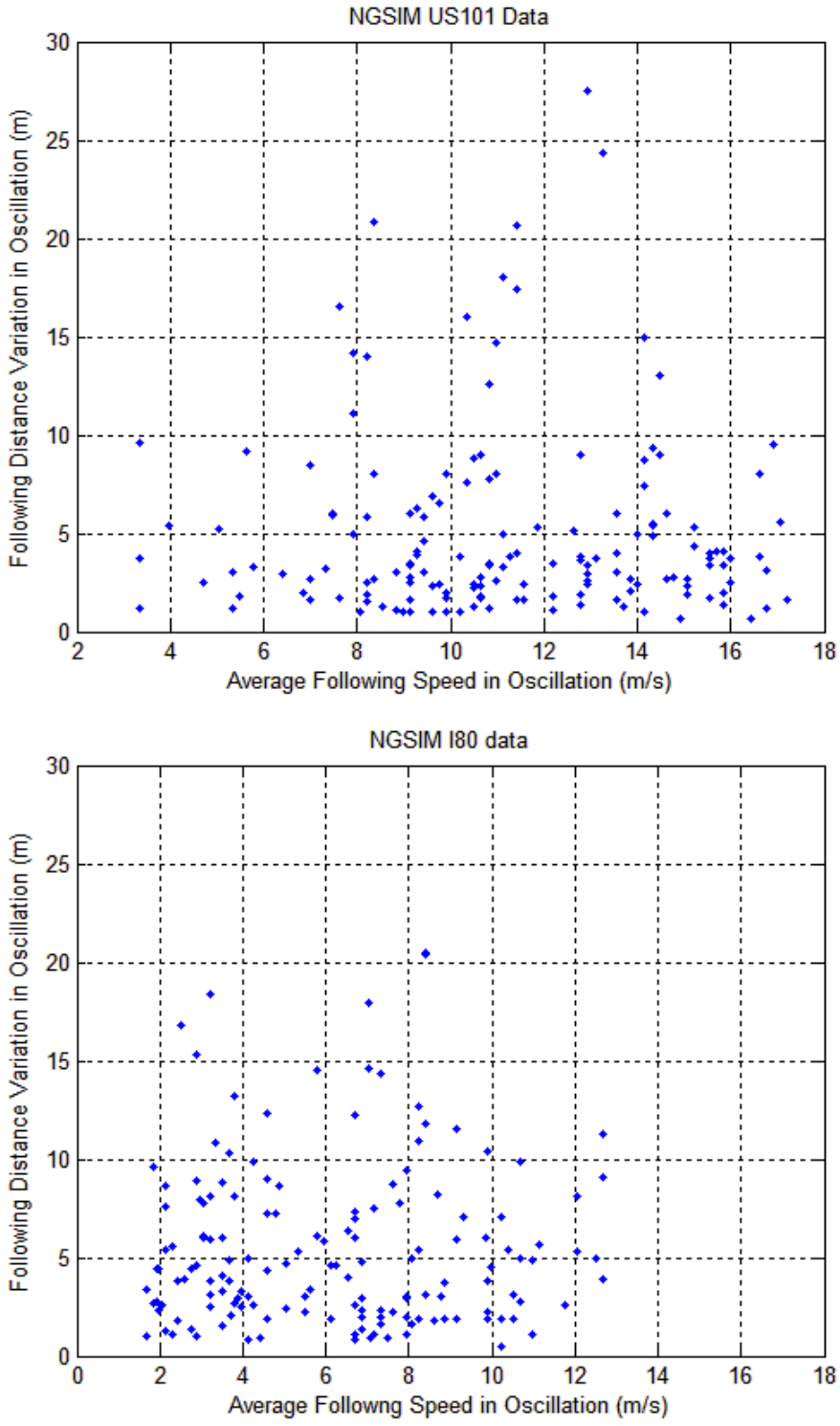

Figure 13.3 Average following speed vs. following distance variation

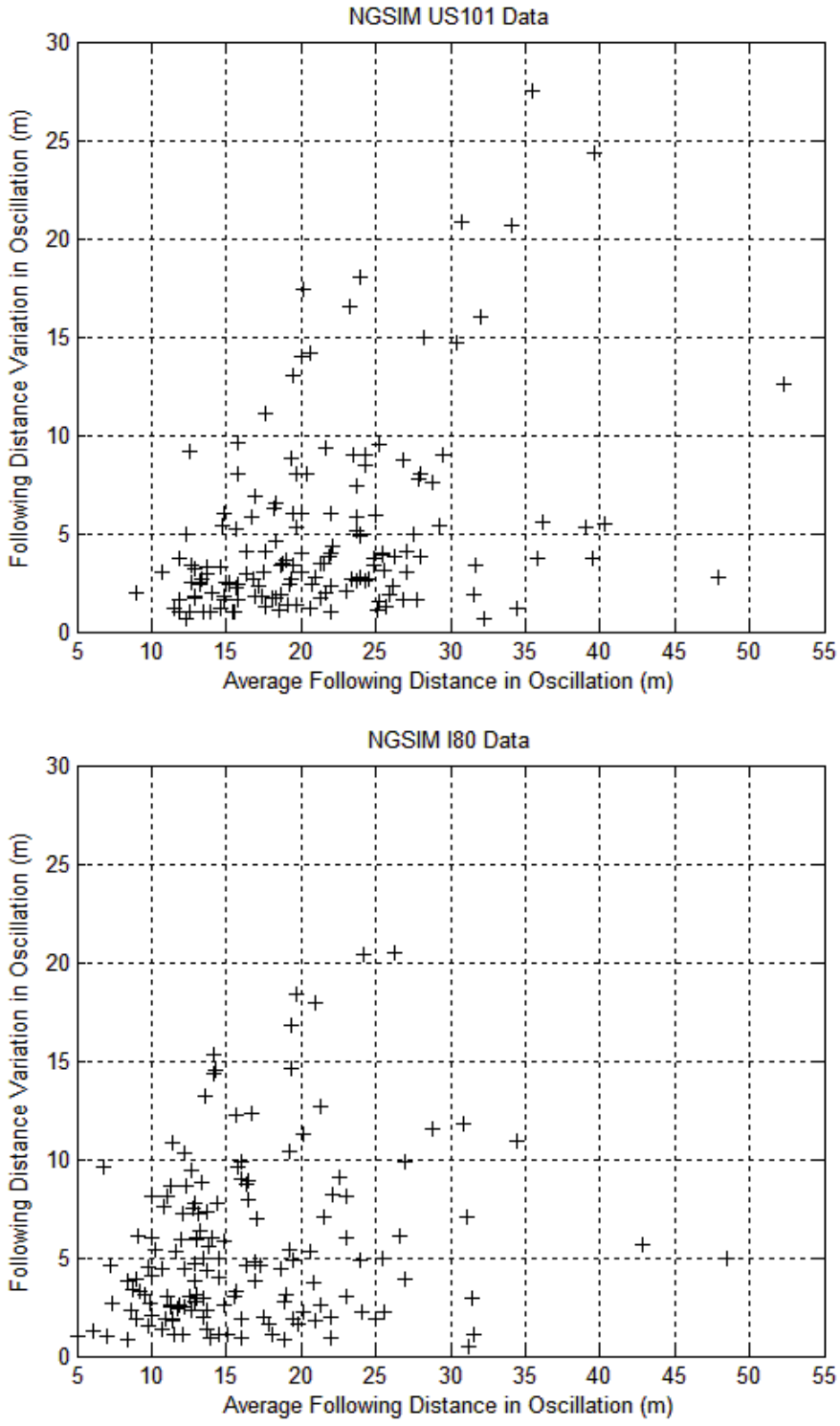

Figure 13.4 Average following distance vs. following distance variation.

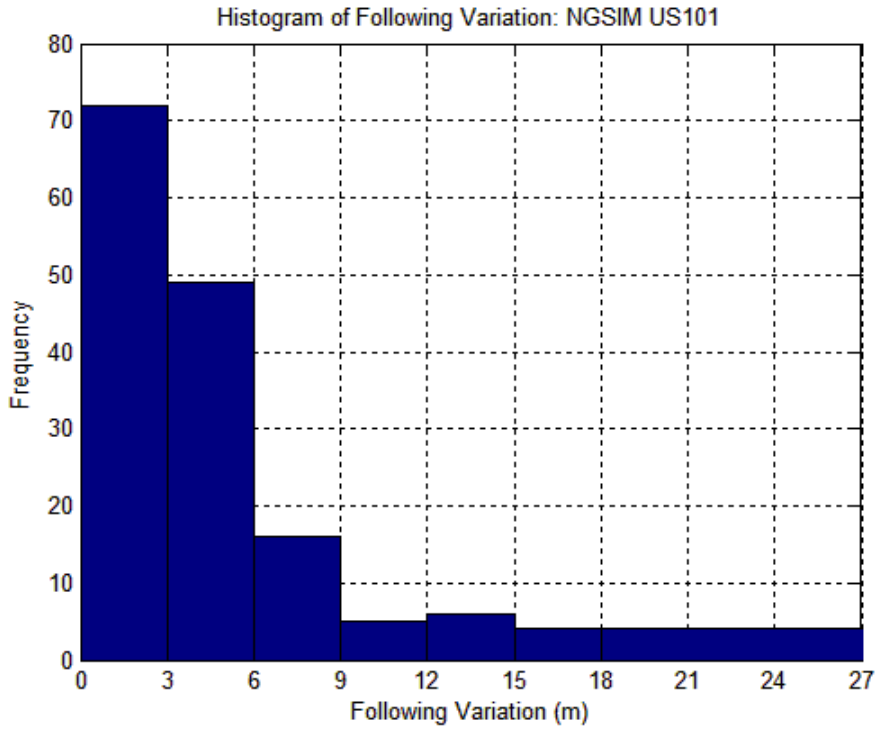

Figure 13.5 Histogram of following variation on US101

Table 13.1 Descriptive Statistics of Following Distance Variation: US101

Following Distance Variation Statistics NGSIM US101	
Mean	4.966987
Standard Error	0.378934
Median	3.4
Mode	1
Standard Deviation	4.732879
Sample Variance	22.40015
Kurtosis	5.766431
Skewness	2.26217
Range	26.8
Minimum	0.7
Maximum	27.5
Sum	774.85
Count	156
Largest(1)	27.5
Smallest(1)	0.7
Confidence Level(95.0%)	0.748541

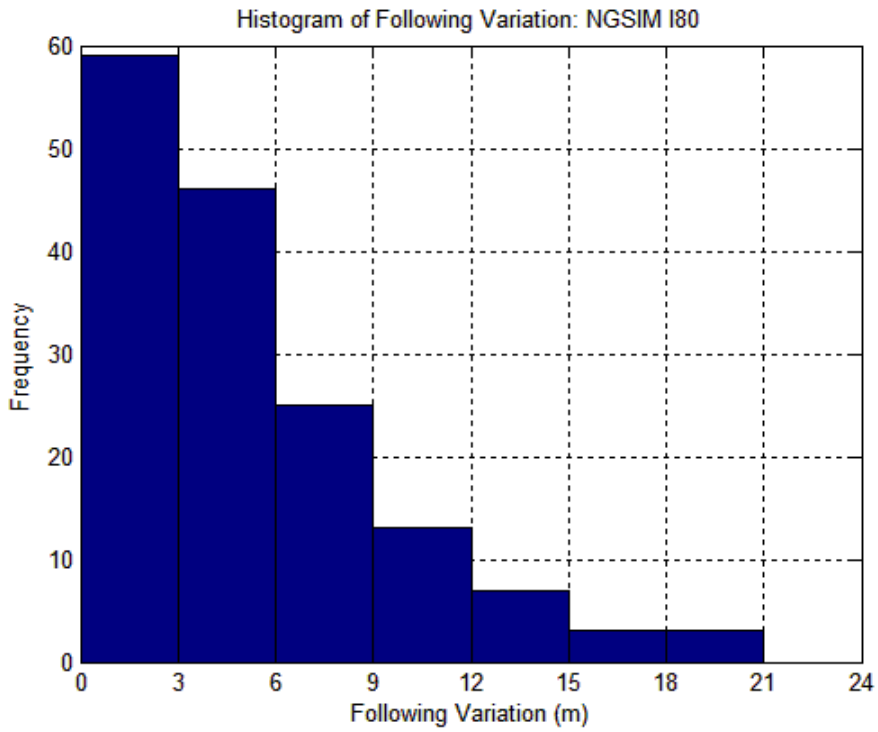

Figure 13.6 Histogram of following variation on I80

Table 13.2 Descriptive Statistics of Following Distance Variation: I80

Following Distance Variation Statistics NGSIM I80	
Mean	5.494872
Standard Error	0.336752
Median	4.4
Mode	1.9
Standard Deviation	4.206029
Sample Variance	17.69068
Kurtosis	1.837483
Skewness	1.374309
Range	20
Minimum	0.5
Maximum	20.5
Sum	857.2
Count	156
Largest(1)	20.5
Smallest(1)	0.5
Confidence Level(95.0%)	0.665215

14 | VITA

Sandeep Menneni was born in Hyderabad, India. After completing high school at Atomic Energy Central School III, Hyderabad, India, he entered the Indian Institute of Technology Madras, receiving the degrees of Bachelors of Technology and Masters of Technology in Civil Engineering. He entered the Graduate School at University of Missouri Columbia in August of 2004 to pursue the degree of Doctor of Philosophy in Civil Engineering.